146p.

AERONUTRONIC DIVISION

63-241
[redacted]

Ford Motor Company
AERONUTRONIC DIVISION

Publication No. U-2189

N64 12070*

ENGINEERING

0166009 Aeronutronic, Newport Beach, Calif.

FINAL REPORT

DEVELOPMENT AND FABRICATION OF OMNI-DIRECTIONAL ACCELEROMETERS

Prepared for: Jet Propulsion Laboratory
California Institute of Technology
Pasadena, California

Under Contract: This work was performed for the Jet Propulsion Laboratory, California Institute of Technology, sponsored by the National Aeronautics and Space Administration under Contract NAS7-100.

Prepared by: C. F. Husen, ~~Mechanical Engineering~~ and
R. G. McClellan ~~Test Engineering~~

Approved by: R. S. Kraemer
R. S. Kraemer
Program Engineer

19 July 1963 146 p + refs

OTS PRICE
XEROX $ 11.00 pb
MICROFILM $ 4.58 mf

(NASA ~~Contract~~ NAS7-100)
(NASA CR-55091; Publ. U-2189)

Index as U-2189

CONTENTS

ILLUSTRATIONS

ILLUSTRATIONS (Continued)

ILLUSTRATIONS (Continued)

SECTION 1

SUMMARY

12070

Design and development effort on the hydrostatic omni-directional accelerometer (Figure 1) was performed under Task 2A of JPL Contract 950267. Ten accelerometers were fabricated and calibrated, with seven of the ten delivered to JPL as specified in the contract. Calibration data on all ten accelerometers are contained in this report.

Design objectives of acceleration range, overload capacity, thermal compensation, sterilization capability, and maximum dimensions were basically met or exceeded. The omni-directional accelerometers quite closely duplicated the acceleration traces of the reference Endevco uni-directional accelerometer in drop tests at up to 2000 g's. The accelerometers were very closely reproducible under each particular test condition and good linearity was realized in both static pressure calibration and shock testing up to 2000 g's, but there was generally some off-set between static and dynamic test data. Eight of the accelerometers have an accuracy of approximately $\pm$ 10 percent of full range under all conditions tested. One of the two discrepant units, Serial No. AA 6, gives evidence of having too high a fill pressure, while the other, AA 12, developed a large void bubble as an indirect result of sterilization baking. It is believed that these two units could be readily upgraded through reassembly and refill.

Further improvement effort on the accelerometers should include a redesign of the Invar thermal compensator sphere to provide more direct access of the fluid pressure to the face of the transducer, and an investigation into the thermal drift characteristics of the transducer.

AUTHOR

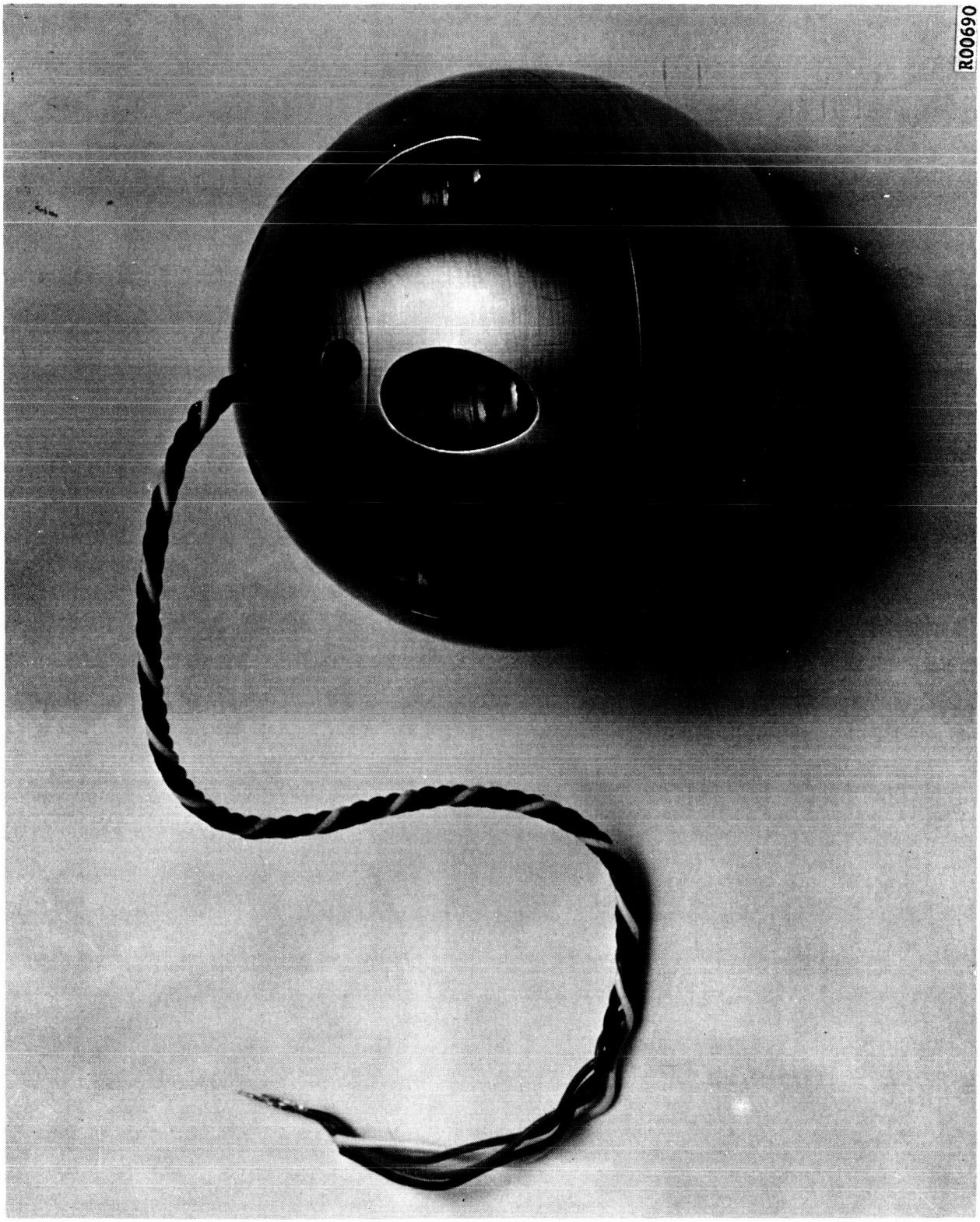

FIGURE 1. OMNI-DIRECTIONAL ACCELEROMETER, ASSEMBLED

Seven accelerometers numbered AA-3, -4, -5, -7, -8, -9, and -11 were delivered to JPL on 28 June 1963. The remaining three units, AA-6, -10 and -12 are at Aeronutronic awaiting further disposition.

SECTION 2

INTRODUCTION

Feasibility effort was initiated at Aeronutronic in the fall of 1961 on an omni-directional accelerometer for the Lunar Surface Measurement Capsule (SURMEC). This proposed Ranger capsule would eject small spheres onto the lunar surface in a dispersed pattern and record the acceleration versus time traces during their impacts as a measure of surface hardness. The simple omni-directional accelerometer devised for this application measures the hydrostatic pressure at the center of a small mercury-filled spherical cavity. This center pressure is linearly proportional to the magnitude of the acceleration, independent of the direction of the acceleration.

In March 1962 the Jet Propulsion Laboratory authorized Aeronutronic to experimentally investigate the feasibility of the accelerometer concept under Task 2 of JPL Contract 950267. That effort was successfully concluded in July 1962 (Reference 1) with the test model in all respects exceeding the SURMEC design specifications. Directional sensitivity was less than 2 percent and peak amplitude error was within the accuracy of the instrumentation calibration from 100 percent down to 2.5 percent of full range. Response frequency range was from 0 to 7500 cps and the natural frequency was 25,000 cps. Thermal compensation was excellent over the tested range from 32° to 155°F. This test model featured an Invar sphere mounted in the mercury cavity to balance the system in thermal expansion, and had two diametrically-opposed pressure transducers mounted on the outer periphery of the cavity so that an average of their readings represented the pressure at the center of the cavity. While the performance was excellent, it was recommended that an attempt be made to redesign for only a single transducer to simplify the signal circuitry and eliminate the close balancing requirement.

In October 1962 JPL authorized Aeronutronic under Task 2A of JPL Contract 950267 to design and develop a pre-prototype model of the accelerometer, utilizing only a single transducer mounted in the center of the cavity, and to fabricate and calibrate ten accelerometer units. Design objectives were as follows:

(1)	Acceleration Range:	5g to 2000 g in any direction
(2)	Accuracy:	$\pm$ (2.5 g plus 10 percent of measured value)
(3)	Overload Capability:	to withstand 50 percent overload (3000 g) without injury
(4)	Frequency Response:	d.c. to a minimum of 2000 cps
(5)	Thermal Compensation:	compensated for a temperature range of 20°F to 125°F. Capable of surviving sterilization heating at 257°F for 24 hours
(6)	Case Dimensions	spherical, 2 inch diameter maximum.

This report describes the effort and results accomplished under this Task 2A.

SECTION 3

DESIGN

The design of a single-transducer omni-directional accelerometer follows basic criteria determined in the earlier advanced development of a dual-transducer accelerometer. The single-transducer installation eliminates complicated power division and output summing circuits which would be installed in the case of the dual-transducer configuration. In addition, the single-transducer configuration does away with output errors caused by subtractive interaction of the two transducer diaphragms during some impact conditions.

The device operates on the principle that pressure at the center of a liquid filled spherical cavity varies in proportion to the acceleration imposed on it and is independent of the direction of acceleration. The final configuration consists of four major components which are the outer spherical case, the mercury hydrostatic fluid, an Invar temperature compensator and transducer housing, and the pressure transducer (see Figures 2 and 3).

The pressure transducer is mounted so that the diaphragm is at the center of the mercury cavity. Solid-state strain elements are bonded to the back of the pressure sensing diaphragm and are wired in a full bridge circuit to convert the pressure induced stress to high voltage output. The diaphragm has a very high natural frequency which eliminates problems associated with its use as the sensing element in an accelerometer. A heavy integral flange permits installation with minimum case distortion. In order to measure accelerations of 2000 g with a hydrostatic height of 1/2 inch, a 0-500 psia range transducer was selected (Micro Systems Model PO 3BA4-500 modified). This transducer can withstand an overpressure of 150 percent, permitting acceleration measurements up to 3000 g, and has a minimum bursting pressure of 300 percent.

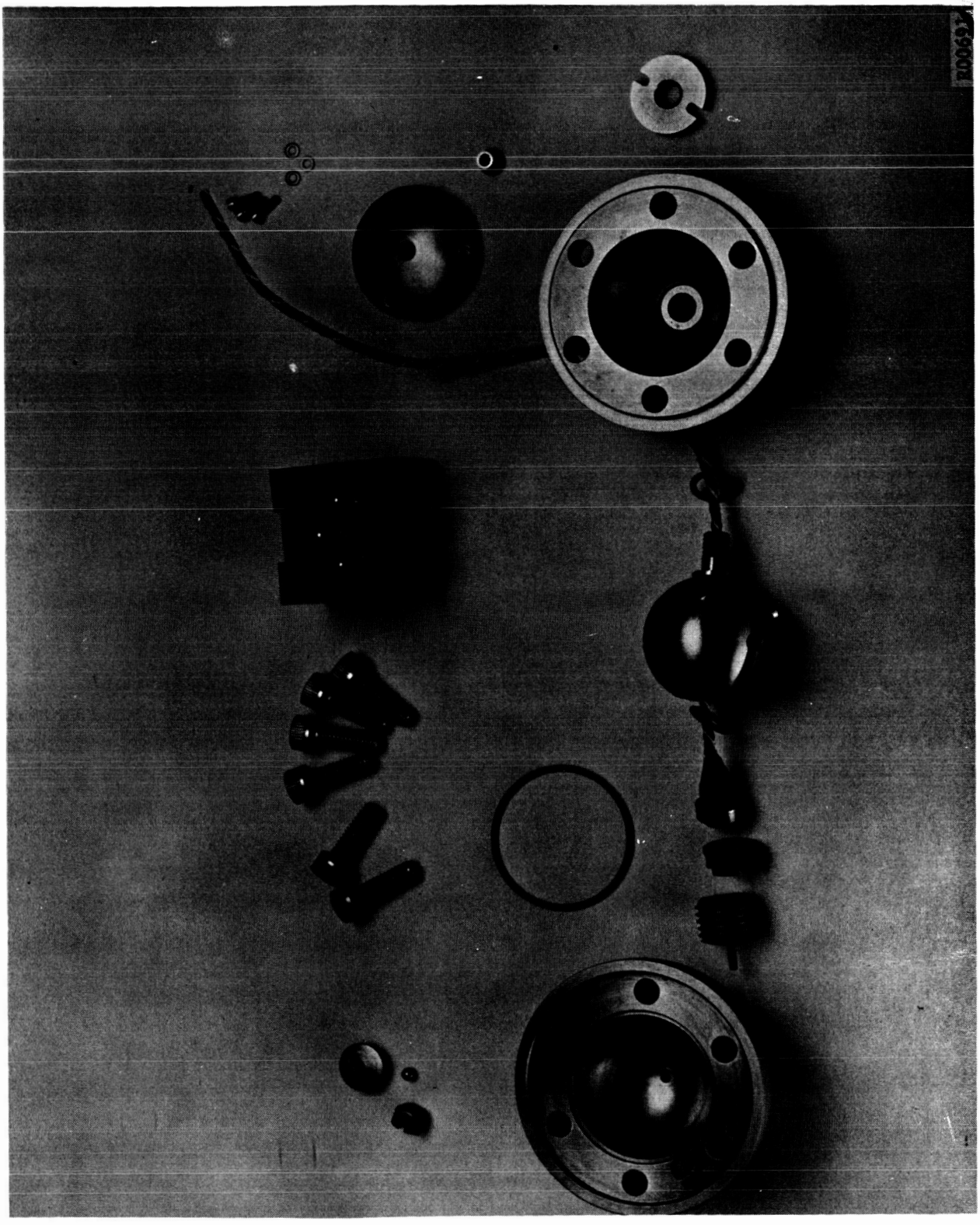

FIGURE 2. OMNI-DIRECTIONAL ACCELEROMETER, UNASSEMBLED

Ford Motor Company
AERONUTRONIC DIVISION

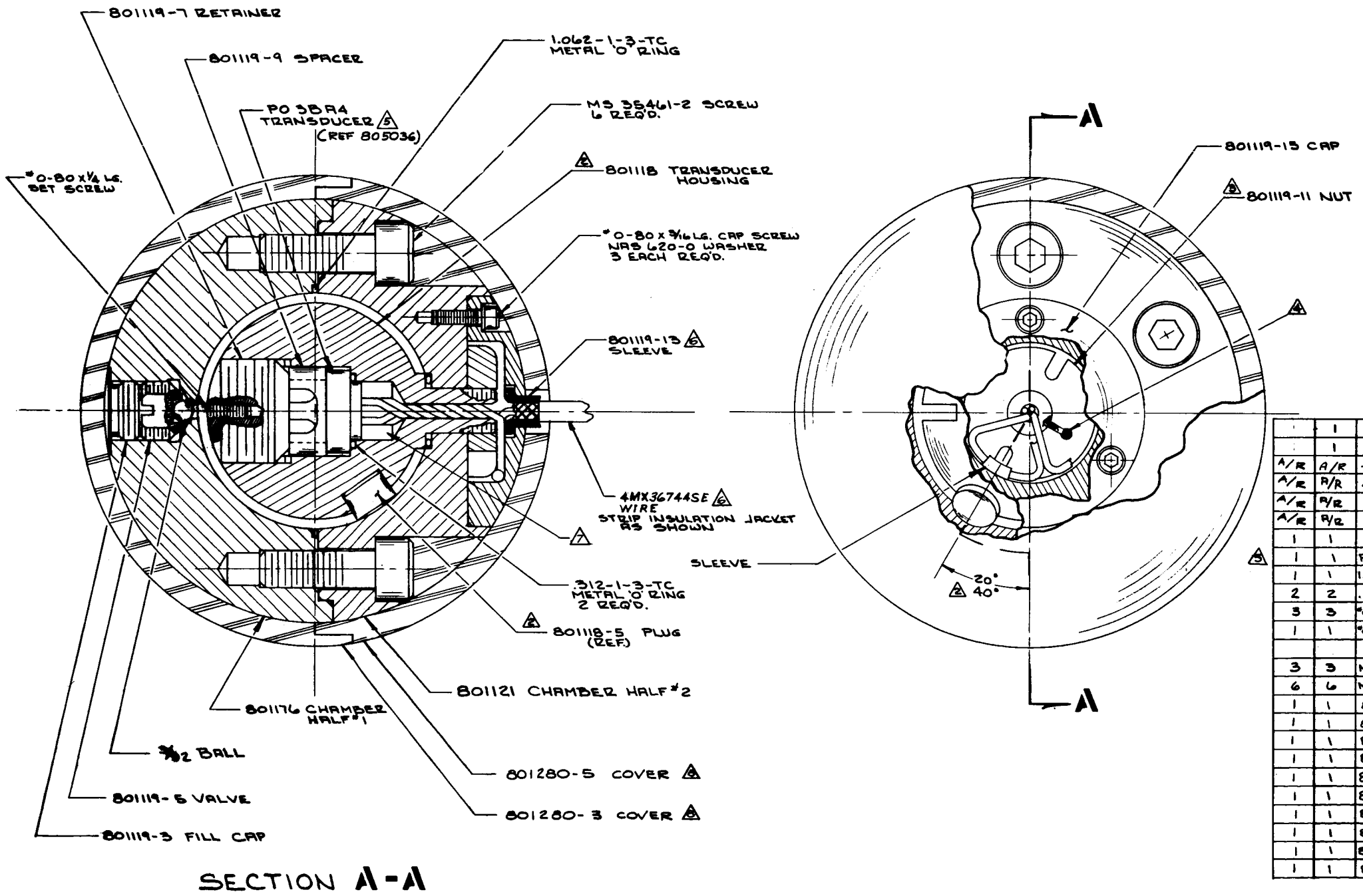

SECTION A-A

NOTE: UNLESS OTHERWISE SPECIFIED
1. IDENTIFY BY TRG & DRG PER AMPS 12.15
2. INSTALL 801118 HOUSING WITH 801118-5 PLUG LOCATED AS SHOWN.
3. RADIAL LOCATION OF SLOTS OPTIONAL
4. SOLDER SHIELD TO 801119-11 NUT, USING MELA PROVIDED, PER AMPS 2.5
5. SOURCE CONTROL DWG 805036
6. BOND 801119-13 SLEEVE TO 4MX36744SE WIRE JACKET PER AMPS 02.8.3.14
   FILL INSIDE OF WIRE SHIELD & BOND 4 WIRES TO A DEPTH OF APPROX .10 FROM EDGE OF SLEEVE
7. FILL WITH RTV-11 SILICONE RUBBER
8. BOND PER PROCESS SPEC. #AS 800349 OMNI-DIRECTIONAL ACCELEROMETER PROTECTIVE COATING
9. ASSEMBLE PER AS 800197

	1	801280-5	COVER	4
	1	801280-3	COVER	4
A/R	A/R	RTV-11 THERMOLITE 12	SILICONE RUBBER CATALYST	GENERAL ELECTRIC DOWNEY CALIF
A/R	A/R	4MX36744SE	WIRE	HITEMP WIRE CO.; MONROVIA, CALIF.
A/R	A/R		MERCURY	
A/R	A/R	SIZE 24	SLEEVE	THERMOFIT RNF RAYCLAD TUBES INC. [illegible]
1	1	3/32 DIA.	BALL	M-10 W.S. STL. OR EQUIV.
1	1	PO 3BR4	TRANSDUCER	5
1	1	1.062-1-3-TC	METAL 'O' RING	ADVANCED PRODUCTS CO. NORTH HAVEN, CONN.
2	2	.312-1-3-TC	METAL 'O' RING	ADVANCED PRODUCTS CO. NORTH HAVEN, CONN.
3	3	*0-80-NF-3A x 3/16 LG	SOCKET HEAD CAP SCREW	STAINLESS STL.
1	1	*0-80-NF-3A x 1/4 LG.	SOCKET SET SCREW	STAINLESS STL.
3	3	NAS 620-0	WASHER	
6	6	MS 35461-2	SCREW	
1	1	801176	CHAMBER HALF	
1	1	801121	CHAMBER HALF	
1	1	801119-15	CAP	
1	1	801119-13	SLEEVE	
1	1	801119-11	NUT	
1	1	801119-9	SPACER	
1	1	801119-7	RETAINER	
1	1	801119-5	VALVE	
1	1	801119-3	FILL CAP	
1	1	801118	TRANSDUCER HOUSING	

R00762

FIGURE 3. OMNI-DIRECTIONAL ACCELEROMETER

Mercury was chosen as the hydrostatic fluid because of its high density and the fact that it had the lowest coefficient of expansion of the liquids surveyed. The coefficient of expansion, however, is still larger than that of any case material. Compensation for the differential rate of expansion must be provided for in order to protect the transducer diaphragm and to hold temperature-pressure effects to within the design specifications. Compensation is provided by a low expansion material, Invar, in the form of a sphere which is firmly fixed in position in the mercury chamber. The Invar volume is very closely controlled so that the expansion of the remaining mercury when added to the low volume expansion of the Invar exactly equals the volume expansion of the case.

The Invar compensator is held in position in the mercury cavity by three stainless steel support plugs and a stem on the Invar sphere, as shown in Figure 3. The stem is inserted in a hole in the case and is held in position by a special nut threaded on the stem from the outside of the case. To prevent movement of the sphere away from the support plugs due to a bouyancy force created by the mercury on impact of the accelerometer, the nut is tightened with a minimum torque of 12 inch-pounds. This produces a tensile preload in the Invar stem. The stainless support plugs are spaced 120 degrees apart around the axis of the stem and are angled approximately 57 degrees from the axis of the stem in order to prevent movement of the plugs on the inside surface of the case due to differential expansions or contractions caused by temperature changes.

The Invar compensator doubles as a housing for the pressure transducer. A cavity in the compensator permits installation of the pressure sensitive diaphragms of the transducer at the center of the mercury chamber. The transducer leads are lead through a control hole in the compensator stem to a connection on the outside of the accelerometer case. An Invar retainer screwed into the end of the compensator is used to hold the transducer in place. A spacer between the retainer and transducer flange provides an interior plenum chamber at the face of the transducer. Three holes spaced 120 degrees apart and parallel to the plane of the transducer diaphragm connect the annular space between the accelerometer case and compensator with the plenum chamber at the transducer diaphragm. A slot cut into the outer surface of the compensator across the end of each hole and parallel to the axis of the compensator stem is used to reduce the distance from various points in the mercury chamber to the transducer diaphragms.

The accelerometer case consists of two hemispherical stainless steel shells. These are joined by six machine screws. The half into

which the transducer housing is inserted also supplies the means to terminate the transducer leads and to provide a stronger connection with the external cable.

Leads from the transducer are terminated outside of the nut holding the compensator-transducer housing unit in place in the chamber half. At this point a four-conductor, shielded, teflon-coated external cable is attached to the transducer leads. The cable is bonded to a sleeve which fits into a recess on the under side of a cover plate. A rubber nipple over the lead is used on the outside of the cover plate to eliminate strain caused by sharp bends at the point the lead leaves the cover. The cover plate is used to hold the complete external cable assembly and transducer lead connection firmly in place in the accelerometer case. The cover also completes the spherical outer surface of the case.

A fill hole in the other chamber half is used to vacuum fill the accelerometer with mercury. This hole is threaded for most of its depth. The bottom of the hole reduces to 1/16 inch diameter before entering the mercury cavity. The accelerometer is sealed by a valve screwed down on a 3/32 inch diameter steel ball which seats against a ledge at the bottom of the fill hole. This arrangement permits sealing of the accelerometer after vacuum filling while the internal pressure is at 1 to 2 inches of mercury pressure. A cap, screwed in over the valve, completes the outer spherical surface.

Three seals are required. These are located between the transducer housing and the case at the point the compensator stem is inserted into the chamber half, under the transducer flange in the transducer housing, and at the main joint between the two case hemispheres. The first two locations were designed to use the same size seal. For the final configuration, the seal used for these two locations is a neoprene O-ring. The main seal consists of a crushable soft copper O-ring in combination with Permatex sealing compound.

Since bubbles, or voids, in the mercury have a marked effect on the response of the accelerometer, all interior surfaces are gold plated before assembly, in order to cause the mercury to wet the interior surfaces in sharp corners and channels.

A transducer driver supplied with the transducer is attached to the end of the external cable. The driver permits remote operation from an unregulated 28 volt D.C. supply without sacrificing transducer performance. The driver is also used to help compensate the transducer throughout its operating temperature range. This unit completes the accelerometer assembly.

SECTION 4

DEVELOPMENT

The engineering development of the single-transducer omnidirectional accelerometer may best be described by considering various areas of development separately. It should be noted, however, that while each area will be discussed separately, there was very close inter-relationship of the development effort for one area to that of another area.

4.1 ASSEMBLY

The assembly of the omnidirectional accelerometer can be considered to be made up of five basic steps as follows:

(1) Initial mechanical assembly

(2) Pressure check and calibration of the pressure transducer

(3) Vacuum fill of the accelerometer with mercury

(4) Temperature compensation check and cavity volume correction, if required

(5) Final mechanical assembly

The initial mechanical assembly consists of the assembly of the internal components in one chamber half of the accelerometer case followed by joining of the two parts of the case. The accelerometer at this point is capable of holding pressure and is ready to be filled. During assembly

of the first units, several changes in assembly procedure were necessary. A preload of about 240 pounds in tension in the stem of the Invar compensator is required to prevent movement of the compensator from its supports under a 3000 g shock loading. The torque required to tighten the nut on the stem was estimated to be about 15 inch-pounds. This torque was found to be insufficient to properly seat the metal O-ring seal initially used between the compensator and the case. It was found that a load of 500 pounds/inch of seal was required. The applied torque had to be increased to 22 inch-pounds to crush the metal ring. (see Figure 4)

A similar situation was encountered with the seals under the flange of the pressure transducer and at the joint between case halves. The torque on the retainer was increased from 20 inch-pounds to 40 inch-pounds while the torque on the six screws joining the two case halves was increased from 15 to 20 inch-pounds. In addition, a revised tightening procedure was instituted in order to pull the main joint seal down evenly.

As a result of difficulties encountered with the seals and described in more detail in Section 4.2, the metal O-rings between the compensator and case and between the transducer flange and compensator were replaced with rubber O-rings. This permitted the torque applied to the nut on the compensator stem and to the transducer retainer to be reduced to the original values. The main seal was replaced with a special copper ring and Permatex sealing compound. The torque on the six screws joining the case halves required to crush the seal properly was found to be about the same as that required for the teflon coated metal ring.

Before assembly of the internal components, measurements were made of several basic dimensions in order to determine the tolerance build-up in the parts caused by maching tolerances. To compensate for any increased volume of Invar the retainer was shortened in length according to the dimensional changes noted.

Several internal modifications are found to be necessary. These consisted of cutting small channels in the sides of the compensator supports to allow mercury to flow into the small cavity under each support. A similar channel was cut in the side of the spacer to permit mercury to flow into the space between the transducer flange and compensator wall. In addition, all interior parts were plated with gold in order to reduce mercury surface tension effects. The reason for this is described more fully in Section 4.5.

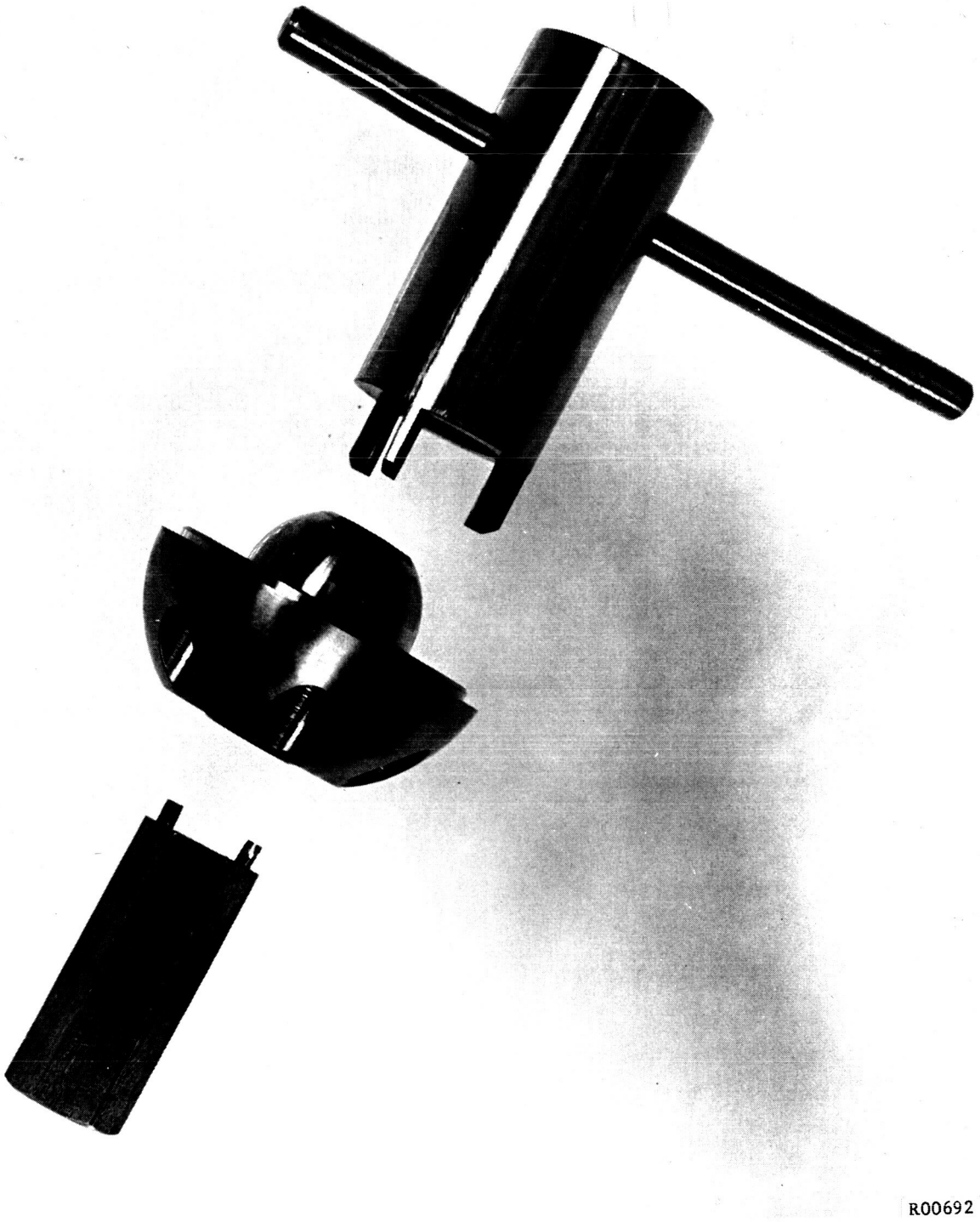

FIGURE 4. TORQUING TOOLS

After completion of the initial assembly, the accelerometer is leak checked with a helium leak detector. This is a modification of the initial assembly procedure made necessary by problems encountered with the seals. A pressure calibration of the transducer follows the leak check. The vacuum filling operation and temperature compensation are discussed in Sections 4.3 and 4.4.

Final assembly consists of attaching the external leads and filling the screw holes in the case. The leads from the transducer are cut off within about 1/2 inch of the point they leave the compensator stem. The external leads are attached at this point and are firmly attached to the accelerometer by means of a stainless steel cap. The external cable is bonded to a sleeve which fits into a seat on the under side of the cap and the assembly is held to the accelerometer case with three 0-80 socket head cap screws. A rubber grommet was added at the point the external cable leaves the cap in order to provide additional stiffness and strain relief. A hard-setting epoxy, Hysol, is used to fill the screw holes and is smoothed to the contour of the outer surface, completing the assembly.

4.2 SEALING

One of the major problem areas encountered was in obtaining a satisfactory seal at all three seal locations. Because of a threshold pressure effect, the accelerometer must be sealed with an internal pressure of approximately 1 psi. The seals, therefore, must seal against an external pressure differential of approximately 14 psi and also be capable of withstanding an internal pressure of 750 psi when undergoing a 3000 g acceleration, all for a temperature range from 20°F to 125°F.

The single-transducer design originally called for the use of metal O-ring seals. These seals consisted of crushable stainless steel tubing formed into a ring and then coated with a thin layer of teflon. Metal rings were selected in order to reduce flexibility effects noted during the development of the dual-transducer model. Results of initial helium leak checks using these seals indicated that poor sealing was obtained. In the case of the small rings under the transducer and between the transducer housing and the accelerometer case, this was traced to insufficient crushing of the seals. It was found that about 500 pound per inch of seal was required to properly crush these seals. A substantial increase in the torques applied to the nut on the compensator stem and to the retainer which holds the transducer in place appeared to solve the leakage problem at these two points.

The more difficult seal problem to solve was at the main seal between case halves. It was found that the metal O-rings tended to pull inward into the mercury cavity and away from the outside wall of the seal seat. A thin layer of teflon primer was deposited on the seal seat in an effort to improve sealing. A successful seal was achieved at room temperature when the material was built-up on the edges of the seat. This helped to push the seal against the outer wall of the seat and also provided somewhat of a bond between the teflon of the ring and the seal seat. It was found, however, that under temperature extremes and some operating conditions the seal could not be relied upon to hold an internal pressure of less than 2 psi. It appears that the teflon coated rings are not sufficiently flexible to respond to quick changes in temperature and flexure of the case.

Several rubber O-rings made of viton or neoprene were selected to replace the metal O-rings. While successful sealing was obtained with the small O-rings under the transducer and between the compensator and case, the rubber rings for the main joint were a disappointment. Part of the failure of the rubber rings to provide a good seal was due to the fact that a replacement seal of the proper size could not be found. The rings had to be expanded on a mandrel to the proper inside diameter. In addition, seal flexibility was a problem since the seal groove was closed on only three sides permitting the seal to move inward toward the center of the case. Several neoprene bonding agents were tried with varying degrees of success. The primary difficulty with these bonding agents was that they became tacky too quickly and would not permit proper seating of the rings in the seal seat.

Two special silicone rubber seals were molded and tried. Seal flexibility was again a problem. These rings tended to bend over before crushing. To prevent the seal from bending, one of the seals was bonded in place on the seal seat. While the bond held, the seal itself sheared away from the bond area when compressed.

As part of another experiment, Permatex gasket cement was used with good results. It appeared that a satisfactory seal could be obtained with a crushable metal ring in combination with Permatex. The problem was to find a soft metal which was not attached by the mercury. It was found that copper had fair to good resistance to mercury corrosion for the temperature range specified.

The final configuration, therefore, employs a soft copper ring in combination with Permatex at the main seal location between case halves. The rubber O-rings used successfully under the transducer and between the transducer housing and outer case replace the metal O-rings in the final configuration.

4.3 FILLING

The filling procedure was designed for vacuum filling of the accelerometer and to permit sealing of the accelerometer under vacuum conditions with controlled internal pressure of 1 to 2 inches of mercury. The filling was done through a hole in one half of the accelerometer case. The arrangement of valve and ball seals are described in Section 3.

A specially designed fill fitting screwed into the fill hole makes it possible to seal the accelerometer under vacuum. The fitting consists of a hexagonal body with a 1/4 inch diameter tube joined to the side to form a 'T'. A plug is inserted into a hole through the body of the fitting. This plug has a screwdriver slot at the outer end of a screwdriver blade at the end where the fitting screws into the fill hole. A small O-ring seals the assembly. The plug is free to turn in the body of the fitting and is used to screw the sealing valve down on the ball and against the seal seat.

A schematic diagram of the arrangement of components of the vacuum filling operation is given in Figure 5. The tubing used to connect the various parts of the system was 1/4 inch ID Taigon tubing. The mercury reservoir was 1/2 inch ID Taigon tubing with a rubber stopper at one end. Since system pressure normally was between 5×10^{-6} and 2×10^{-5} inches of mercury, 1/8 inch ID restriction was placed between the mercury reservoir and the vacuum diffusion pump, to reduce the boil-off of mercury vapor. In addition the mercury was cooled with ice water.

A cold trap was placed in the line to the vacuum diffusion pan. This was used to supplement a second cold trap which was part of the vacuum diffusion pump. These traps were filled with liquid nitrogen, and were used to trap the mercury vapor boiled off and to improve system pressure.

The fill procedure as finally established consists of several steps. Since the small stainless steel ball used to seal the accelerometer would act as a check valve when filling the accelerometer with mercury, the initial fill is done without the ball and valve in place. The mercury reservoir is placed below the opening to the accelerometer and the accelerometer is outgassed for several hours before pouring the mercury into the sphere. A head of mercury is maintained for from 5 to 10 minutes to allow time for the mercury to flow into all corners and channels. This process is helped by the gold plating on all the interior surfaces. The head of the mercury is then removed except for that remaining in the fill hole of the accelerometer. The system pressure is brought

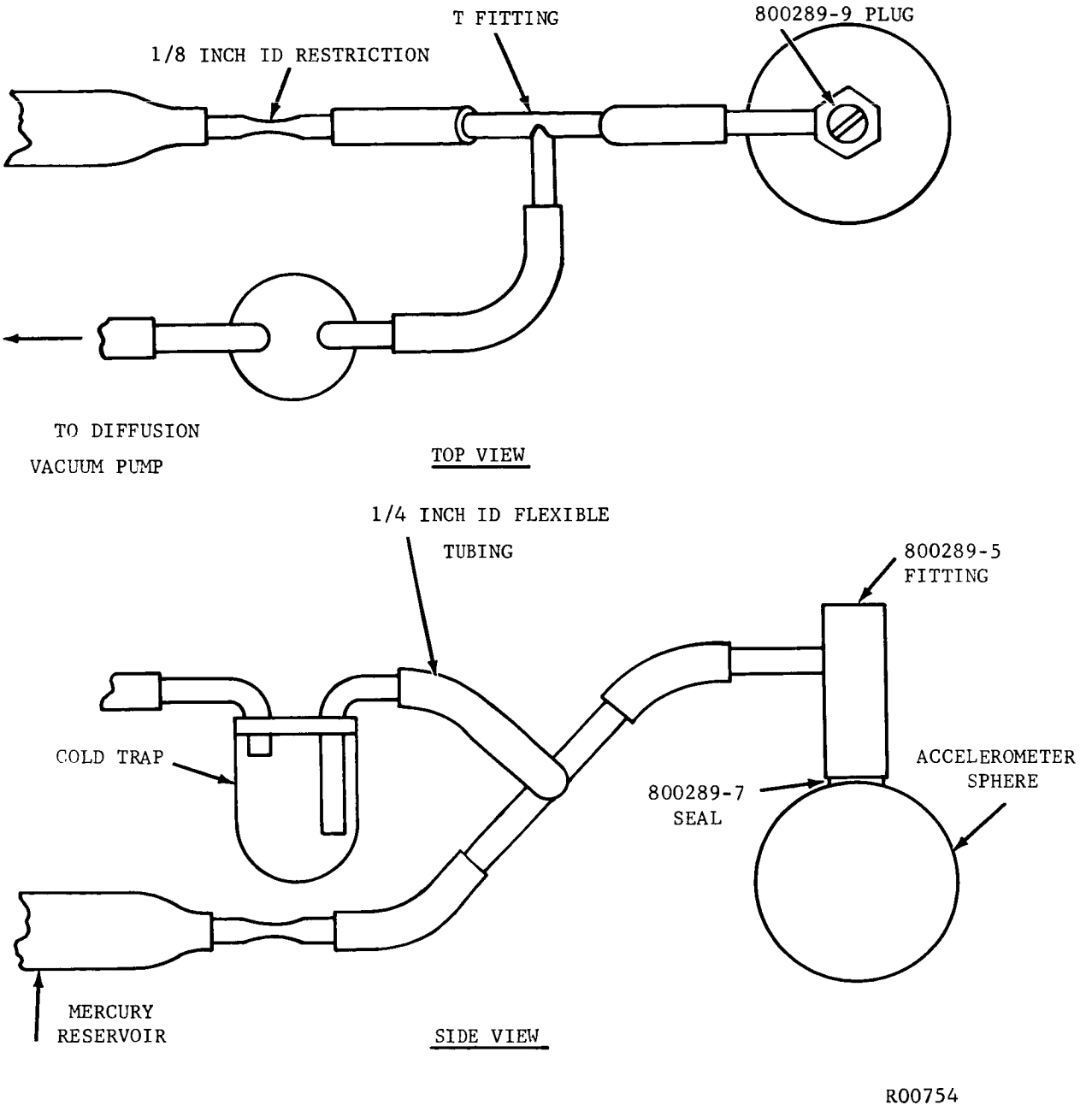

FIGURE 5. ARRANGEMENT OF COMPONENTS FOR VACUUM FILL OPERATION

to atmospheric and the fill fitting is removed. A stainless ball and valve are screwed into the fill hole of the accelerometer displaying the mercury standing in the hole but are not tightened against the seat. Since the mercury is denser than the steel ball, the ball floats on the mercury and is held against the valve away from the seat. The fill fitting is replaced and the system pressure is again reduced to vacuum conditions. A head of mercury is again placed on the sphere and is held to 1 to 2 inches. This produces an internal pressure of 0.5 to 1.0 psi and a corresponding acceleration threshold of 2 to 4 g's. A screwdriver, with the aid of the screwdriver blade on the end of the plug in the fill fitting, is then used to screw the valve and ball against a seat sealing the accelerometer. The fill procedure is completed when the pressure is brought to atmospheric and the fill fitting is removed.

4.4 TEMPERATURE COMPENSATION

In order to protect the transducer diaphragm and to hold pressure-temperature effects to within that permitted by the design specifications, some form of compensation for the differential rate of expansion between mercury and stainless steel must be provided. This is accomplished by rigidly suspending an Invar sphere in the mercury chamber of the accelerometer. For proper compensation the expansion in volume of the mercury plus the Invar sphere should exactly equal the volume expansion of the interior cavity of the case.

Elasticity relations required for the design of a thermally compensated accelerometer are presented in Appendix B. Using these relationships, the thermal expansion equations were obtained from which the required Invar sphere radius for perfect compensation was determined. This calculation is given in Appendix C.

All tolerances were designed to result in an over compensated unit. Coarse adjustment for machining tolerances was obtained by changes in the length of the retainer which holds the transducer in place in the compensator. Fine volume adjustment was provided by a threaded hole in the retainer which could be filled with slugs of stainless steel of the desired length.

Temperature compensation data were obtained by observing the output of the pressure transducer for a sealed accelerometer as a function of temperature. An oven which permitted a temperature variation from 20°F to 125°F was used to control the temperature of the accelerometer. The initial results obtained were unexpected in that considerable

drift and nonlinear effects were noted. As a result of a series of subsequent tests on the transducer by itself, the drift appeared to be due to hysteresis and temperature effects on the transducer.

The nonlinear effects were disturbing since these appeared to indicate a void in the mercury filling the accelerometer. This was confirmed with a series of void volume measurements described in Section 4.5. The nonlinear effects noted tended to disappear as the void size was reduced.

It was found that the small changes in volume produced by varying the length of the slugs in the retainer were masked by the variation in output of the transducer with temperature. Moreover, to accurately determine the compensation the output voltage versus temperature for both the unfilled and filled conditions would be necessary. However, since the total variation in pressure for a 100°F temperature change was normally considerably less than 10 percent on even the initial fill, more extensive effort to further reduce the sensitivity was deemed not fruitful at this time. A curve of output voltage versus temperature is supplied for each unit. This calibration adjustment curve would be required only if a temperature change were to occur during operation after a zero acceleration level had been established.

4.5 MERCURY VOIDS

The most serious problem encountered was the presence of voids in the mercury. A mercury void seriously affects the response characteristics of the accelerometer. The possibility of a void was first noticed in the nonlinear data obtained during temperature compensation runs. Initial results from vibration and shock tests were also characteristic of a large bubble in the mercury. A series of tests using a 2 mm ID manometer tube was run in order to determine void size. The tube was mounted on a fitting which screwed into the accelerometer fill hole. The mercury level under vacuum and at atmospheric pressure was measured and the void volume was determined from the displacement. Data obtained from three accelerometers indicated an average void of 8×10^{-4} cubic inches.

Variations in fill procedure were tried first to eliminate or reduce the void size. These variations included heating the accelerometer to drive off air molecules and replace them with mercury vapor, ultrasonic excitation during filling, and pressurizing the accelerometer after being filled in order to force mercury into small corners. No apparent improvement in fill was noted for these variations in procedure and the original procedure was continued in use.

In order to determine if the bubble was due to trapped gas or to mercury surface tension effects, one accelerometer was vacuum filled with silicone oil. A complete fill was obtained with the oil, therefore, it was felt that the high surface tension of the mercury was the primary cause of the voids.

A series of void volume measurements on various accelerometer cases and interior component configurations were made in order to locate the source of trouble. The volumes were computed for a standard internal pressure of 2 inches of mercury. In part of these tests an improved manometer tube fitting was used which permitted sealing at the bottom of the fill hole instead of at the top of the hole. This eliminated the error caused by mercury flowing up into the threads of the filling below the seal. The average void size determined for the various configurations are:

(1)	Standard Configuration	7.3×10^{-4} cu in
(2)	Standard Configuration, interior gold plated	1.63×10^{-4} cu in
(3)	Accelerometer case and transducer housing; no transducer, spacer or retainer	1.04×10^{-4} cu in
(4)	Accelerometer case only, no interior components	$.523 \times 10^{-4}$ cu in
(5)	Accelerometer case only; no interior components and O-ring seals replaced by Permatex gasket material	$.246 \times 10^{-4}$ cu in
(6)	Theoretical volume change of case due to 15 psi pressure change	$.056 \times 10^{-4}$ cu in

These results are more completely covered in Appendix G.

It can be seen that the high surface tension effects prevent the mercury from wetting the surface completely in the small channels and sharp corners of the interior components. Measures, such as providing mercury channels into crevices and threshold areas, as well as adding RTV fillets in sharp corners did not produce significant improvements. Gold

plating on all interior surfaces promotes wetting and was found to reduce the void size by nearly a factor of five, from 7.3 to 1.6×10^{-4} cu in. An improved main seal was expected to reduce this remaining bubble somewhat further. While a considerable improvement in bubble size was obtained, the void remaining was still considerably larger than the theoretical value of volume change computed for an internal pressure change of 15 psi.

It was felt that this configuration had been carried as far as possible and any additional changes in configuration would destroy the temperature compensation of the unit. The final configuration therefore, employs gold plating and improved seals in order to reduce mercury voids to the lowest possible size.

4.6 PERFORMANCE CHARACTERISTICS OF TEST MODELS

It was noted in Section 4.2 that because of a threshold pressure effect the accelerometer must be sealed with an internal pressure of about 1 to 2 inches of mercury in order to measure accelerations as low as 5 g. This threshold may best be described if the accelerometer is considered to have a given internal pressure and is in a zero g field. The pressure will then be the same at the top, middle and bottom of the accelerometer cavity. When subjected to a small externally applied acceleration the pressure at the top of the accelerometer cavity will be lowered while that at the bottom of the cavity will be increased at the same rate. The hydrostatic pressure at the center, however, will be the average of the top and bottom and will remain constant until zero pressure is reached at the top of the accelerometer cavity.

This effect was confirmed with a test on the centrifuge of an accelerometer vacuum filled with mercury but sealed at atmospheric pressure. The lowest acceleration that could be measured was 30 g. This corresponds to a pressure of 15 psi for the 1 inch interior diameter of the cavity. A curve of the data obtained is presented in Figure 6. The smooth transition in slope around 30 g's is due to non-linear effects and to small pressure changes created by deflections of the case, seals and transducer diaphragm.

Several units, sealed at 2 inches of Hg, were subjected to steady state accelerations up to 150 g in a centrifuge. Hysteresis and directional sensitivity were found to be less than 0.5 percent. The output of the accelerometer in millivolts/g was also found to be quite linear and was well within specifications.

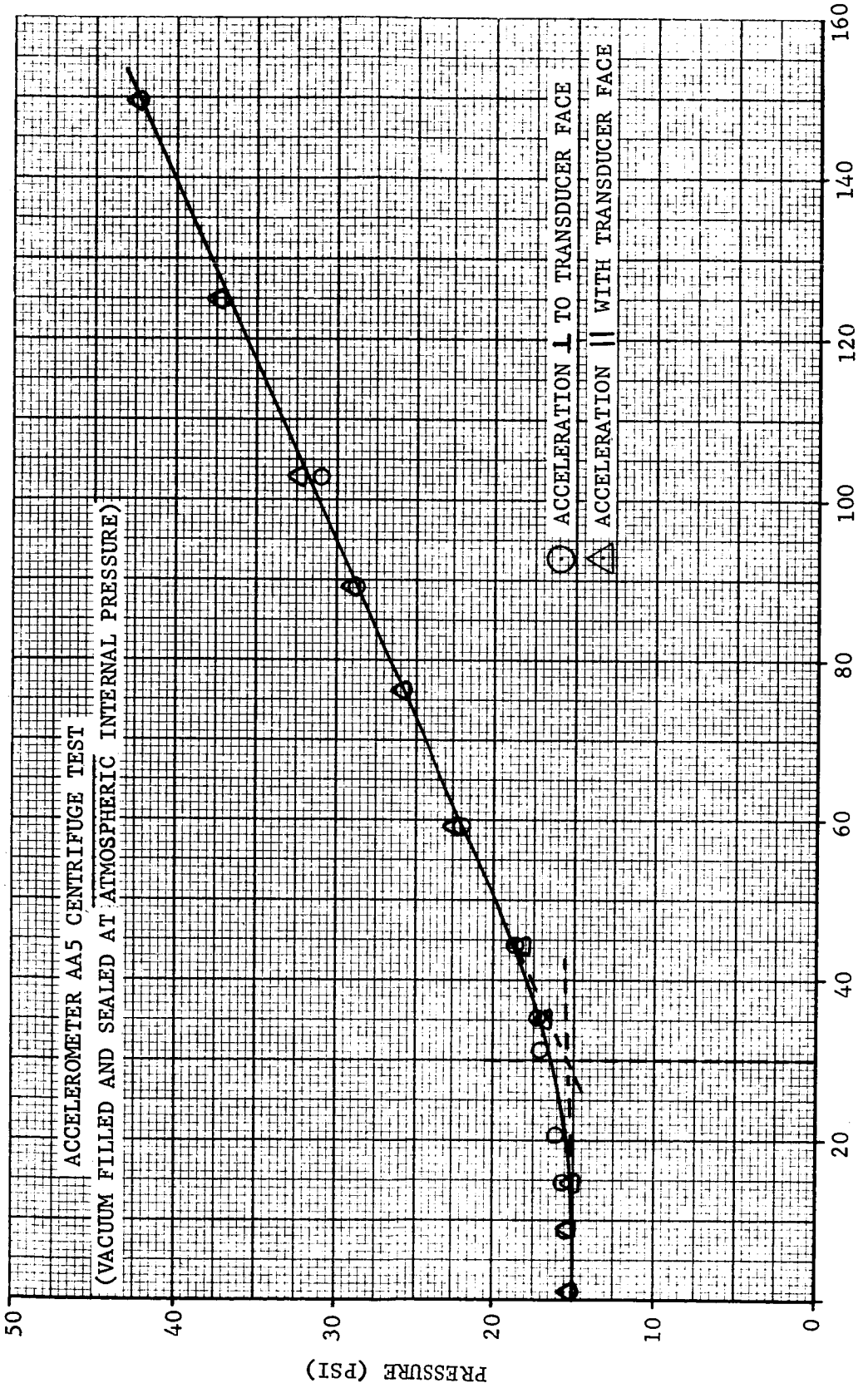

R00695

FIGURE 6. PRESSURE THRESHOLD EFFECT

Initial results from vibration and shock tests were disappointing. The data obtained were characteristic of large voids in the mercury filling the accelerometer. The output obtained at low frequencies was rectified sine wave with a superimposed transient. As the frequency of excitation increased the transient also increased in amplitude badly distorting the basic rectified sine wave. Shock response curves obtained with a simple drop test also showed a superimposed transient on the basic shock pulse. These effects were similar to those observed for a large void in the mercury obtained during development tests of a dual-transducer configuration.

Since essentially the only additional equipment required for the drop tests was recording equipment, subsequent performance testing performed during the engineering development period was concentrated on tests using controlled drop heights and impact limiters. Response data from a shock calibrated Endevco accelerometer was used for comparison purposes. Very smooth, nearly 1/2 sine, pulses were obtained from impacts against a shaped nylon limiter.

Some typical early shock time histories are shown in Figures 7 through 10 together with the comparison curve obtained from the crystal accelerometer. The data shown in Figure 7 are characteristic of data obtained with the original configuration. Although the velocity change indicated by the area under the acceleration-time curve for the omni-accelerometer appears to agree fairly well with that measured by the crystal accelerometer, the transient, characteristic of a large bubble badly distorts the basic acceleration pulse shape. When an accelerometer of the original configuration was vacuum filled and sealed with atmospheric pressure the acceleration histogram obtained from a similar shock test shows some improvement in characteristics. The curve obtained is given in Figure 8. The amplitude and number of cycles of the superimposed transient are somewhat smaller and the shape of the curve obtained with the omni-accelerometer. This is primarily due to the reduced bubble size obtained by sealing the accelerometer after allowing the pressure to rise to atmospheric with a head of mercury remaining in the fill fitting. Because of the threshold pressure effect, however, measurement of accelerations below 30 g's would not be possible when sealed at atmospheric pressure.

To reduce mercury bubble size by promoting wetting of the surfaces, one accelerometer with all interior surfaces gold plated was tested. The acceleration histogram obtained with this configuration, for the same drop and limiter conditions as used previously, is shown in Figure 9. A definite improvement can be noted although a rather sharp initial peak due to the transient is still present. In connection with this initial peak there also always appears to be a lag in the initial response of the omni-accelerometer.

ACCELEROMETER AA7
78" DROP ⊥ TO TRANSDUCER FACE

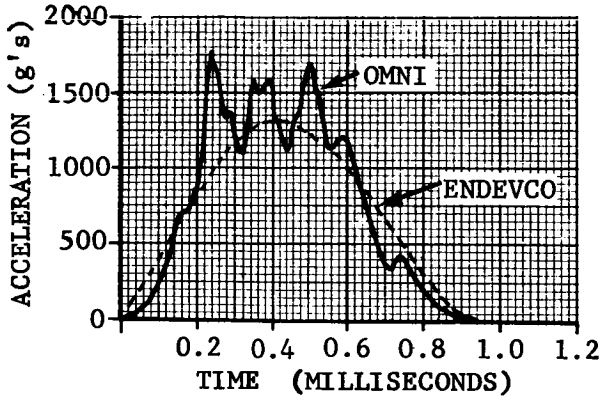

FIGURE 7. IMPACT TRACE WITH LARGE BUBBLE

ACCELEROMETER AA5
78" DROP ⊥ TO TRANSDUCER FACE
INTERNAL PRESSURE, 15 PSI

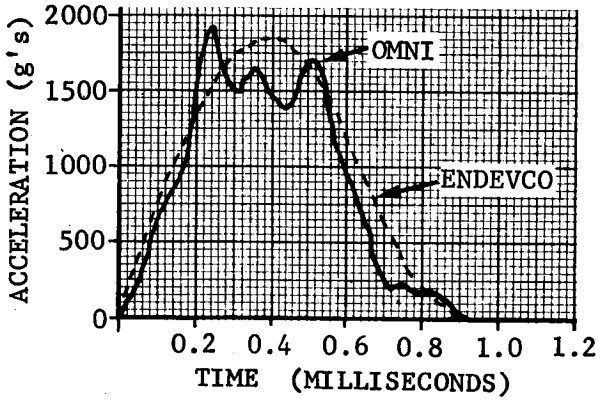

R00714

FIGURE 8. IMPACT TRACE WITH ATMOSPHERIC FILLING

ACCELEROMETER AA-2
78" DROP ⊥ TO TRANSDUCER FACE, GOLD-PLATED INTERNAL SURFACES

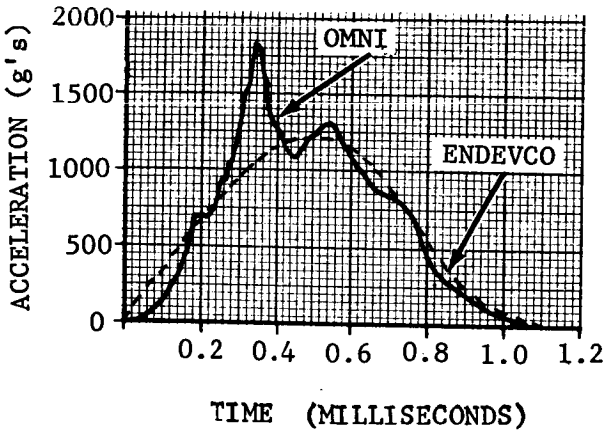

FIGURE 9. IMPACT TRACE WITH GOLD PLATING

ACCELEROMETER AA-2
78" DROP || TO TRANSDUCER FACE, GOLD-PLATED INTERNAL SURFACES

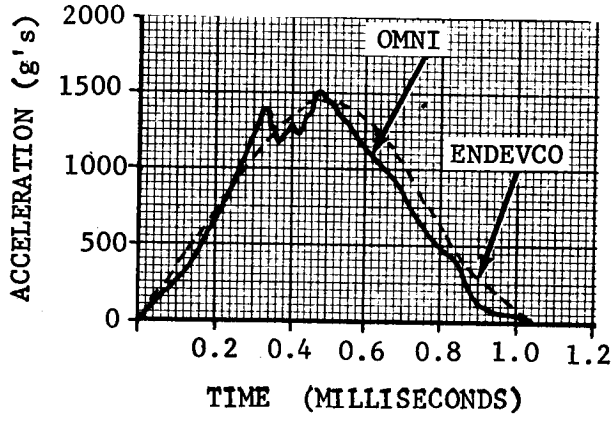

R00696

FIGURE 10. IMPACT TRACE WITH TRANSVERSE DROP

In all the tests described above, the omni-accelerometer was dropped in a direction perpendicular to the face of the transducer. The gold plated accelerometer was also tested in a direction parallel to the transducer face. The acceleration histogram for this orientation is shown in Figure 10. In this orientation the transient appears to be reduced and the resulting curve seems to match the trace obtained with the crystal accelerometer more closely. This characteristic may be due to the internal arrangement of channels from the annular space around the compensator to the plenum chamber at the face of the transducer inside the compensator. These channels are arranged in a plane parallel to the face of the transducer. When impacted in a direction perpendicular to the transducer face the pressure pulse must travel a longer distance to the diaphragm and same form of standing wave may be formed due to the pressure of the mercury bubble resulting in the observed transients.

The gold plated accelerometer used flexible rubber O-rings to seal the various joints. These may have compromised the results obtained slightly, due to increased flexibility and a tending to leak. Engineering development was stopped at this point and the design was fixed. In the final configuration, the rubber O-ring at the main joint was replaced with a copper ring to improve elasticity effects and to reduce surface tension effects at the seal.

SECTION 5

ASSEMBLY AND CALIBRATION

5.1 ASSEMBLY

Ten accelerometers numbered AA 3 through AA 12 were assembled as described in Section 4. AA 12 was somewhat of an exception in that the accelerometer was subjected to a temperature of 260°F for twenty-four hours after filling with mercury, but before sealing, to verify that the assembly can satisfactorily withstand sterilization procedures. After the twenty-four hour bake, the accelerometer was sealed under vacuum. The accelerometers were assembled with minor structural variations from unit to unit as indicated in the simplified diagram of Figure 11.

5.2 CALIBRATION

Each accelerometer was subjected to centrifuge and shock tests in order to establish curves of acceleration versus transducer output voltage. Accelerometer AA 10 was also tested to determine its frequency response characteristics and susceptibility to fifty percent overload (3000 g shock). Curves of accelerometer output voltage versus temperature were also established over the range of +20°F to + 125°F. The electrical characteristics were measured in every case, having the model RC-01 transducer driver in the circuit between the power supply and accelerometer.

The following procedures were followed in the calibration testing:

Ford Motor Company
AERONUTRONIC DIVISION

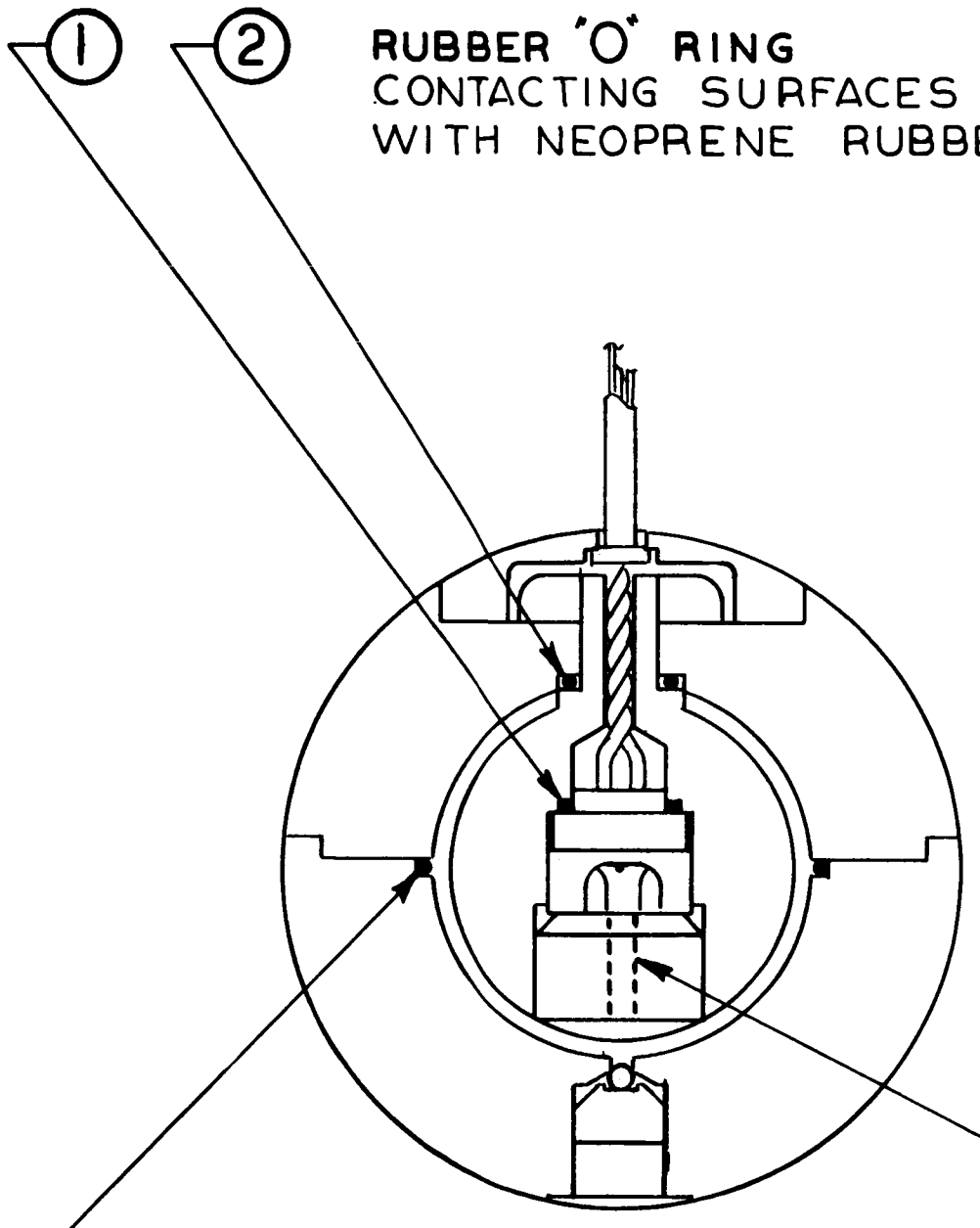

UNIT NUMBER	METHOD USED							
	1	2	3	4	5	6	7	8
AA 2	XDUCER DESTROYED							
AA 3	X	X	X		X		X	
AA 4	X	X	X		X		X	
AA 5	X	X		X		X	X	
AA 6	X	X		X		X	X	
AA 7	X	X		X		X	X	
AA 8	X	X		X		X	X	
AA 9	X	X	X		X		X	
AA 10	X	X		X		X		X
AA 11	X	X		X		X		X
AA 12	X	X		X		X		X
AB 39	SPARE XDUCER							

R00761

FIGURE 11. FINAL ASSEMBLY CONFIGURATIONS

a. Temperature Effects

Output voltage for each accelerometer as a function of temperature was determined with a Leeds and Northrup millivolt potentiometer and a temperature chamber. The accelerometer was allowed to stabilize at five temperatures over the range of +20°F to +125°F and the respective output voltages were recorded. The internal accelerometer temperature was considered stable at that time when the output voltage did not drift faster than 0.1 millivolt per half hour.

b. Sensitivity to Sustained Acceleration

Each accelerometer was mounted on a centrifuge and subjected to sustained accelerations to 100 g's. Data was taken for the two cases of increasing acceleration and decreasing acceleration along the major axis. Accelerometer AA 10 was also subjected to the same test with the acceleration applied along two transverse axes. No attempt was made to distinguish transverse axes since the accelerometer has symmetry about its major axis.

c. Sensitivity to Shock Accelerations

Output voltage as a function of shock deceleration at 1000 g's and 2000 g's was determined using the drop test set-up shown in Figure 12. The omni-directional accelerometer was potted into the test fixture with low-melting cerrobend and the reference Endevco accelerometer was mounted to the fixture. The fixture was dropped from pre-set heights along vertical guide wires onto a specially calibrated nylon impact surface. In general, two drops heights were used to give approximately 1000 and 2000 g's. A photograph of the reference accelerometer and omni-directional accelerometer output voltages as displayed on the oscilloscope were taken for each shock. Each drop was repeated three times to verify reproducibility.

Omni-directional accelerometer AA 10 was subjected to a more complete routine. It received shocks along the major axis and one transverse axis, three times each at 5000 g's, 1000 g's and 2000 g's. To test its susceptibility to shocks exceeding the 2000 g rating, two 3000 g shocks were applied along the major axis followed by four 1000 g shocks to be compared with the earlier shocks.

Calibration of the reference accelerometer was accomplished using the signal insertion method recommended by its manufacturer.

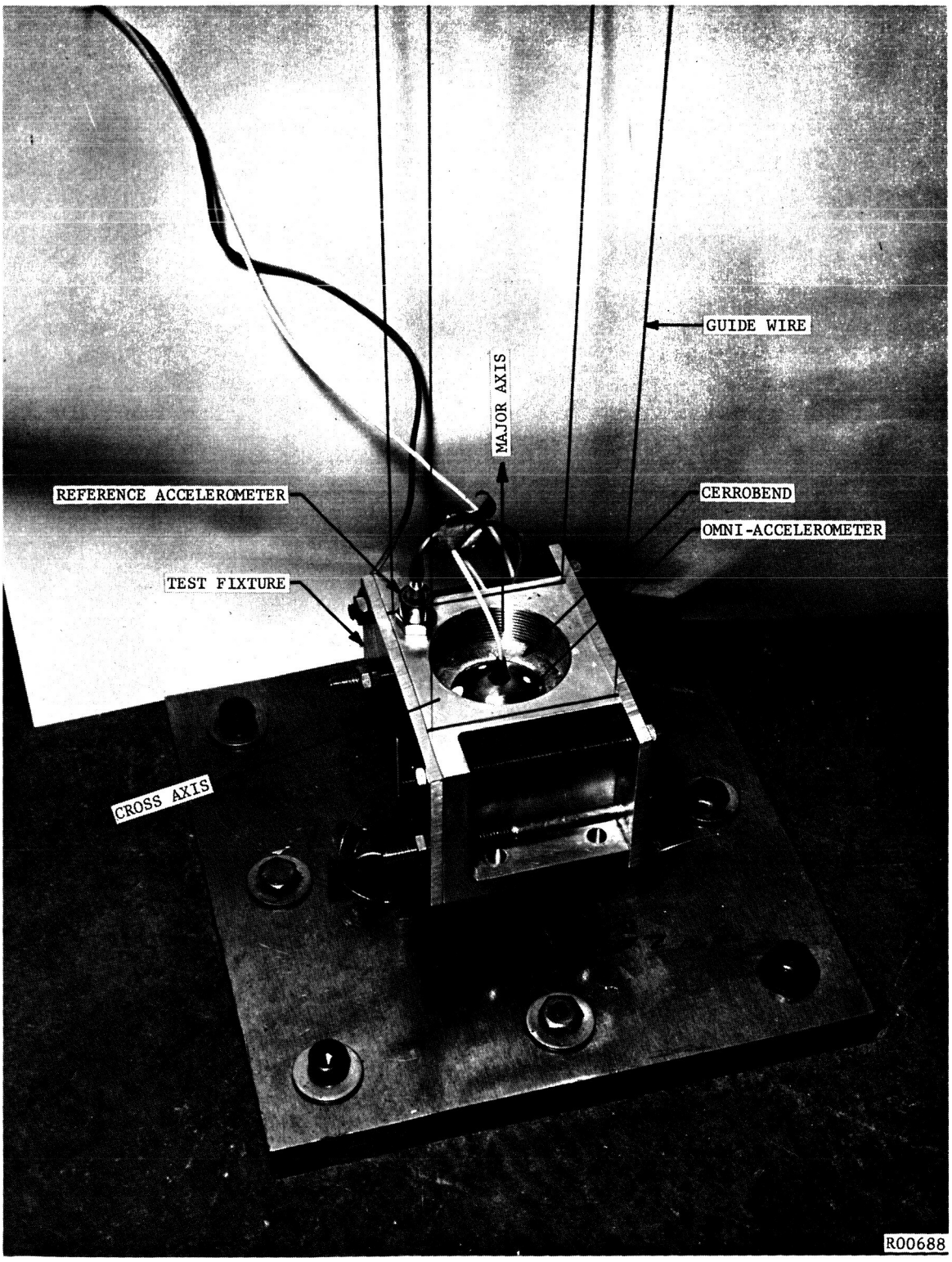

FIGURE 12. OMNIDIRECTIONAL ACCELEROMETER IN SHOCK TEST SETUP

d. Sensitivity to Sinusoidal Acceleration

The response of accelerometer AA 10 to sinusoidal vibration along its major axis and one transverse axis for frequencies to 2000 cps at 10 g's and 40 g's was obtained. The specimen accelerometer in its test fixture was mounted on a vibration table. The output of the reference accelerometers was monitored on a separate oscilloscope and distortion analyzer. The signal from the omni-directional accelerometer was then observed on an oscilliscope using a differential preamplifier. Waveforms were photographed at several frequencies.

e. Sterilization

Accelerometer AA 12 was subjected to a twenty-four hour bake at sterilization temperature (+260°F) after filling with mercury, but before sealing. Sealing was not accomplished prior to sterilization because the accelerometer was not fully temperature compensated for the extreme range. With a properly compensated unit, the elevated temperature would create no pressure problems.

5.3 INSTRUMENTATION ERRORS

A list of the test instruments used in each of the tests along with their probable errors, including readability, is tabulated below. The probable error in the data is thus indicated.

a. Temperature Effects

Measurement	Instrument	Error
Output Voltage	Millivolt pot, L&N 8686, Ser. 1582889	± 0.05 mv
Temperature	Temp. Pot, L&N 8692, Ser. 1559120	± 2°F

b. Centrifuge

Measurement	Instrument	Error
Radius	6 foot rule	± 0.6 %
RPM	Counter, HP 522B, Serial 3609	± 0.1 %
Output Voltage	Millivolt Pot, L&N 8686	± 0.06%

Maximum error in data = ± 0.8% of reading.

c. Shock

Measurement	Instrument	Error
Acceleration	Accelerometer, Endevco 2225, Ser. GA23	± 5%
Calib. Voltage	AC VTVM, HP400D, Ser. 26588	± 2%
Acceleration	Amplifier, Endevco 2702B, Ser. CA50	± 1%
Acceleration	Oscilloscope, Tektronix 531, Ser. 5034	--
Acceleration	Preamp., Tektronix CA, Ser. 15879	± 5%
Output Voltage	Oscilloscope, Tektronix 531, Ser. 5034	--
Output Voltage	Preamp, Tektronix CA, Ser. 15879	± 5%

Probable error in data = 8.9 percent

d. Vibration

Measurement	Instrument	Error
Vibr. Level	Accelerometer, Endevco 2225, Ser. GA23	± 5%
Vibr Level Calib	AC VTVM, HP 400D, Ser. 26588	± 2%
Vibr Level	Oscilloscope, Tektronix 531, Ser 5034	--
Vibr Level	Preamp, Tektronix, CA, 15879	± 5%
Vibr Distortion	Distortion Analyzer, HP330D, Ser 5300	(N. A.)
Vibr Level	Amplifier, Endevco 2702B, Ser. CA50	± 1%
Output Voltage	Oscilloscope Preamp, Tektronix 53/54D, Ser. 2711	± 5%

Probable Error in data = ± 8.9 % of reading

e. Sterilization

Measurement	Instrument	Error
Temperature	Temp Pot, L&N 8692, Ser. 1559120	± 2°F

5.4 CALIBRATION RESULTS

The following results were obtained from the calibration testing:

a. Output Voltage as a Function of Temperature

Every accelerometer showed a positive temperature coefficient of output voltage having very little slope in the region of room temperature but increasing at high temperatures. This would indicate the presence of

a small void in the mercury due to incomplete wetting of the accelerometer interior as discussed in Section 4. The knee in the voltage versus temperature curves is not well defined due to the limited number of data points. These curves are presented in Figures 13 through 15.

b. Sustained Acceleration as a Function of Output Voltage

The units discussed in this report did not perform as well on the centrifuge as did the earlier dual-transducer unit and the first test assembly of the single-transducer design. The hysteresis and nonlinearities are poorer than expected. Accelerometer AA 10 is particularly interesting since the indicated acceleration is a double-valued function of output voltage for accelerations less than about 35 g's. Curves of acceleration as a function of output voltage are presented in Figures 16 through 27.

c. Shock Sensitivity and Waveform Conformity

In general, the onmi-directional accelerometer produced a quite representative trace of the impacts. In those accelerometers showing some spurious responses to shock decelerations, the peak output voltage during each shock was used to compute the acceleration sensitivity. Tests with accelerometers AA 9 and AA 10 in which the shock was applied along a transverse axis, showed improved correspondence of output voltage to the applied shock. AA 10 showed a reproducible decrease in sensitivity of about 25 percent after being subjected to a 3000 g shock.

Figures 28 through 39 were reconstructed from oscillographs taken during the shock tests. The peak amplitude of the omni accelerometer output voltage has been adjusted to match the peak of the acceleration curve generated by the reference accelerometer. Units AA 3 and AA 10 are examples of the best conformity, while units AA 6 and AA 12 gave the poorest conformity.

d. Output Voltage as a Function of Acceleration to 2000 g's

Figures 40 through 49 show the pressure sensitivity of the transducers used in the accelerometers. The pressure sensitivities have been converted to acceleration sensitivities by the conversion factor, 0.244 psi = 1 g, a function of the accelerometer's internal geometry. Data points taken from the shock tests are shown on the graphs for comparison. The dynamic shock output is seen to be generally higher than the static output predicted from the pressure calibration.

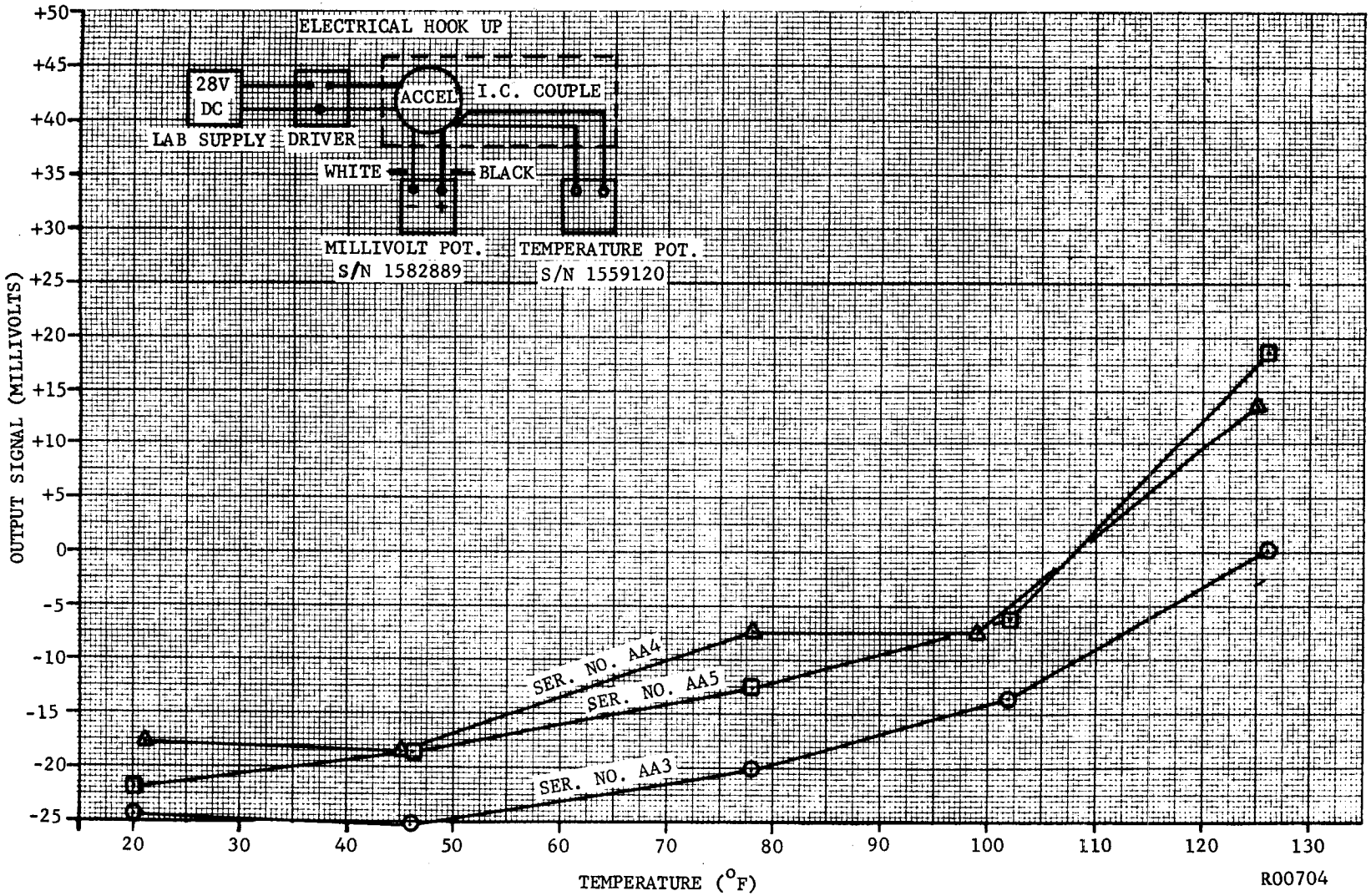

FIGURE 13. TEMPERATURE CHARACTERISTICS FOR ACCELEROMETERS AA3, 4 , 5

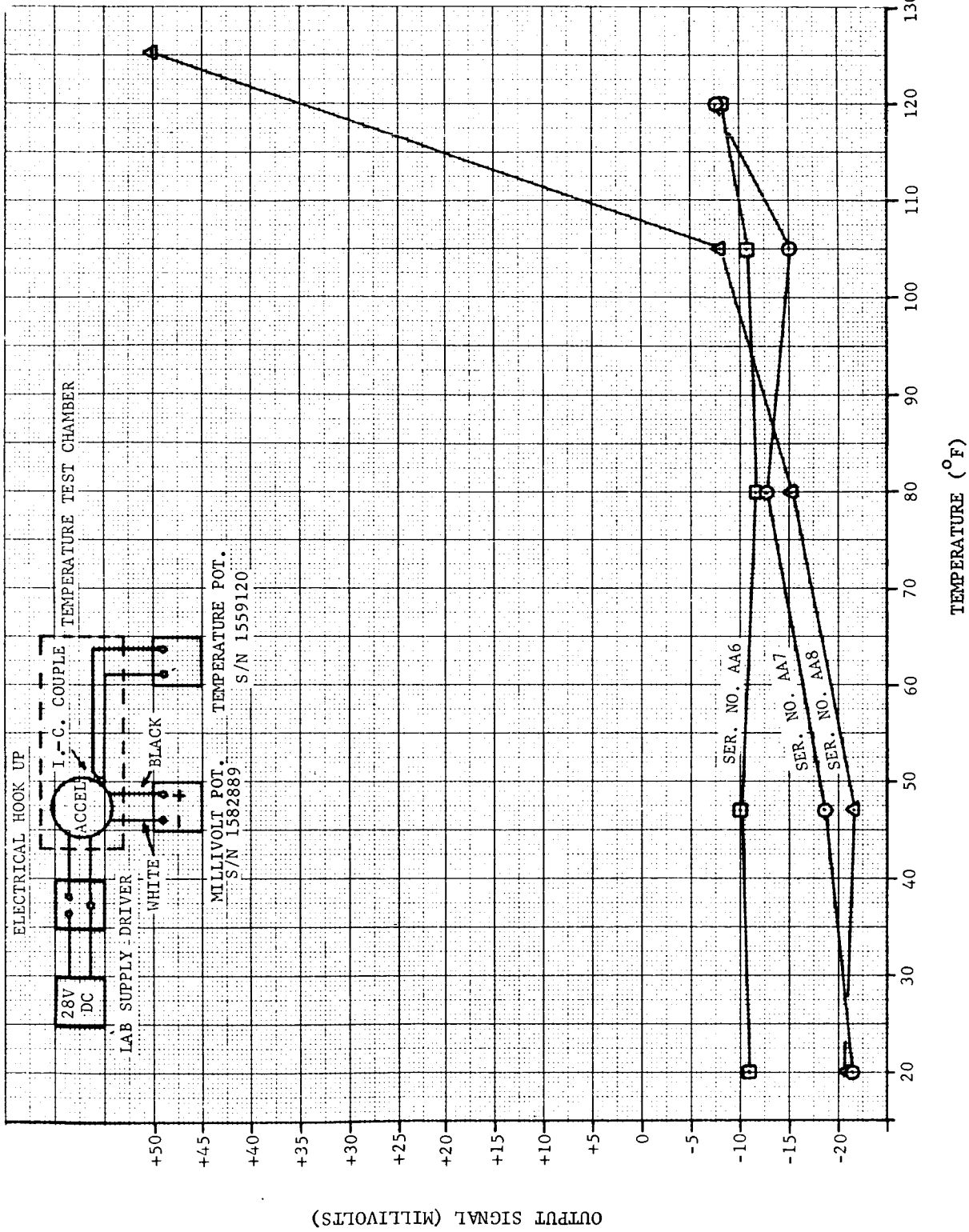

R00715

FIGURE 14. TEMPERATURE CHARACTERISTICS FOR ACCELEROMETERS AA6, 7, 8

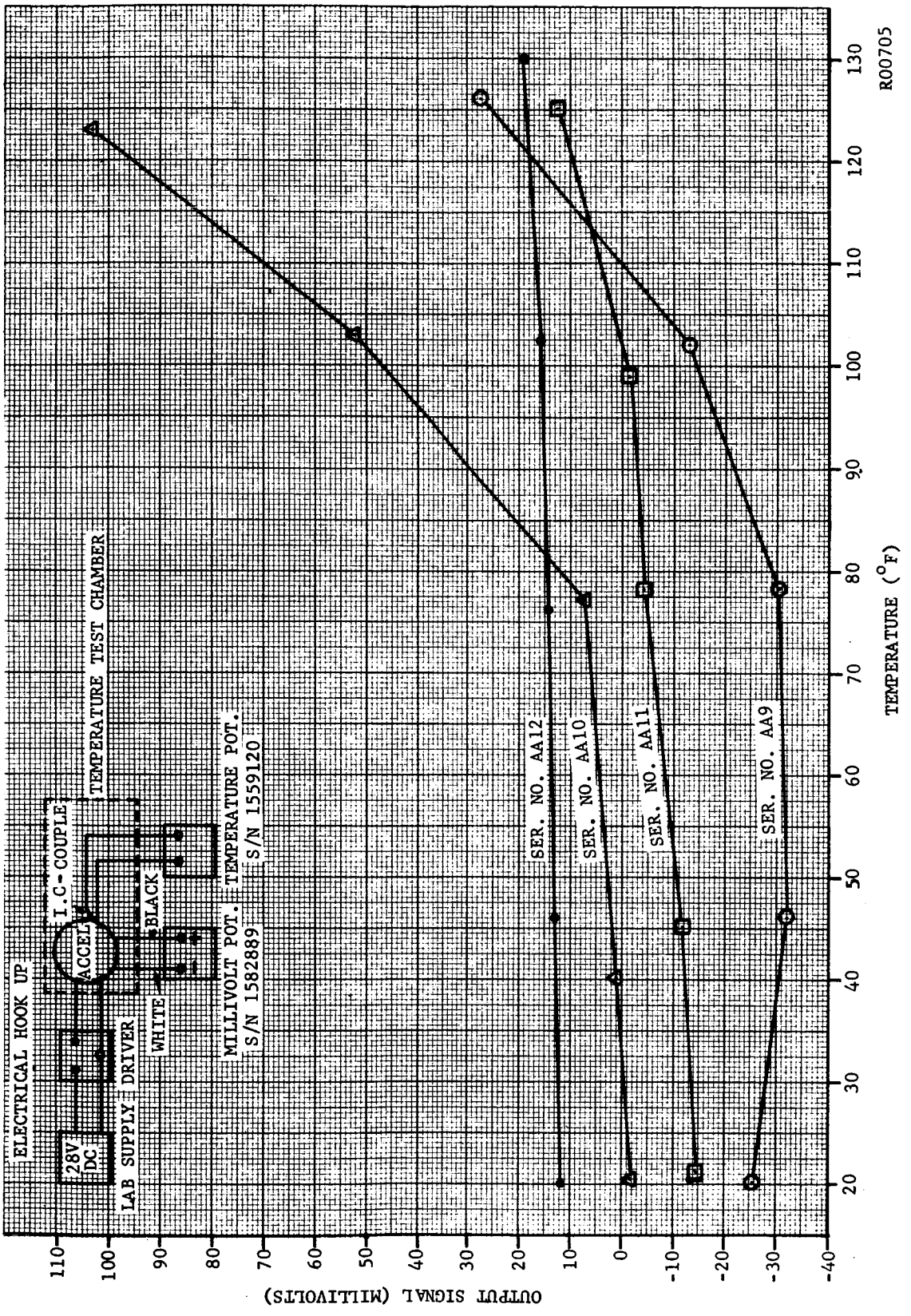

FIGURE 15. TEMPERATURE CHARACTERISTICS FOR ACCELEROMETERS AA9, 10, 11, 12

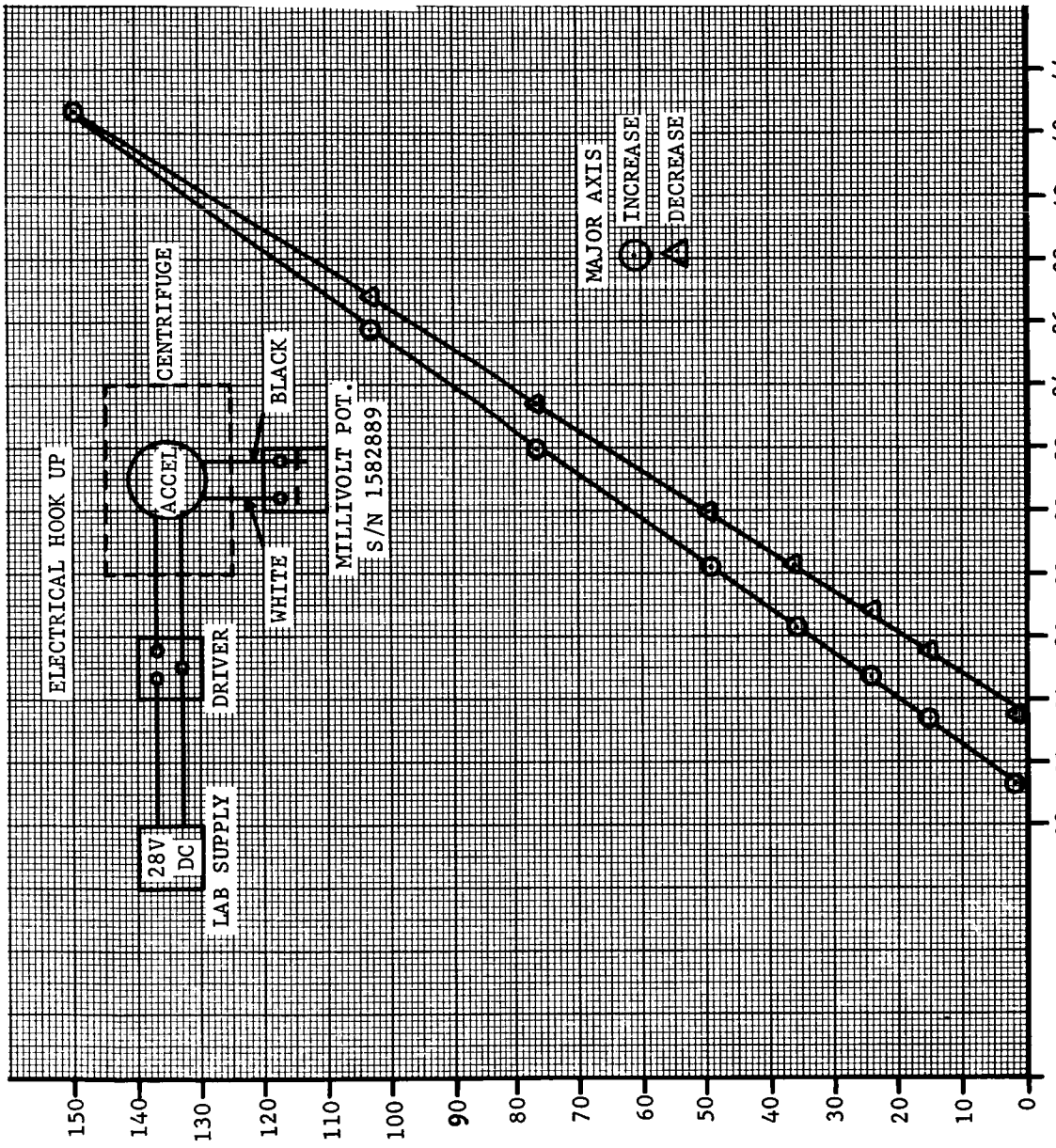

R00720

FIGURE 16. OUTPUT VOLTAGE VERSUS SUSTAINED ACCELERATION FOR ACCELEROMETER AA3

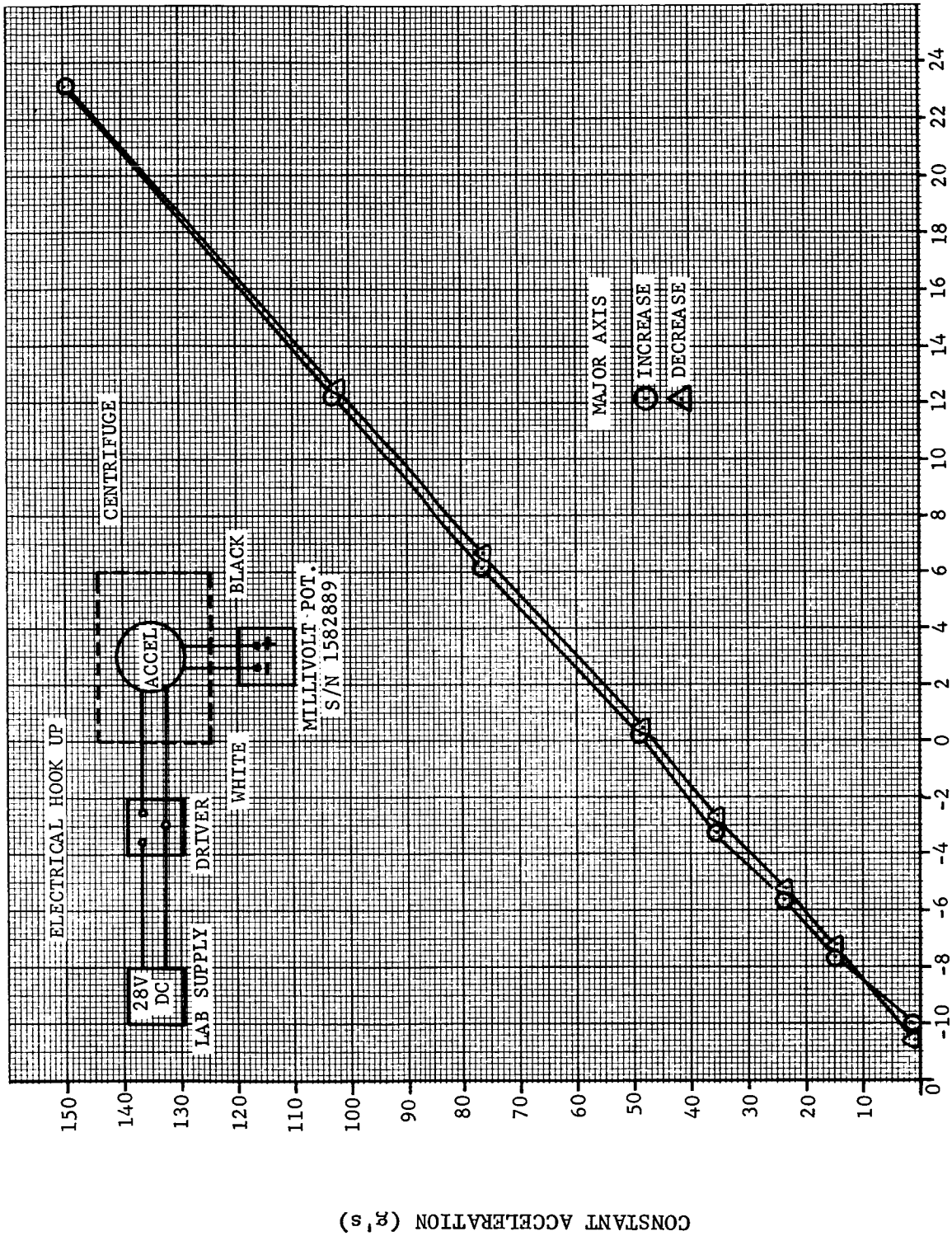

R00699

TRANSDUCER OUTPUT (MILLIVOLTS)

FIGURE 17. OUTPUT VOLTAGE VERSUS SUSTAINED ACCELERATION FOR ACCELEROMETER AA4

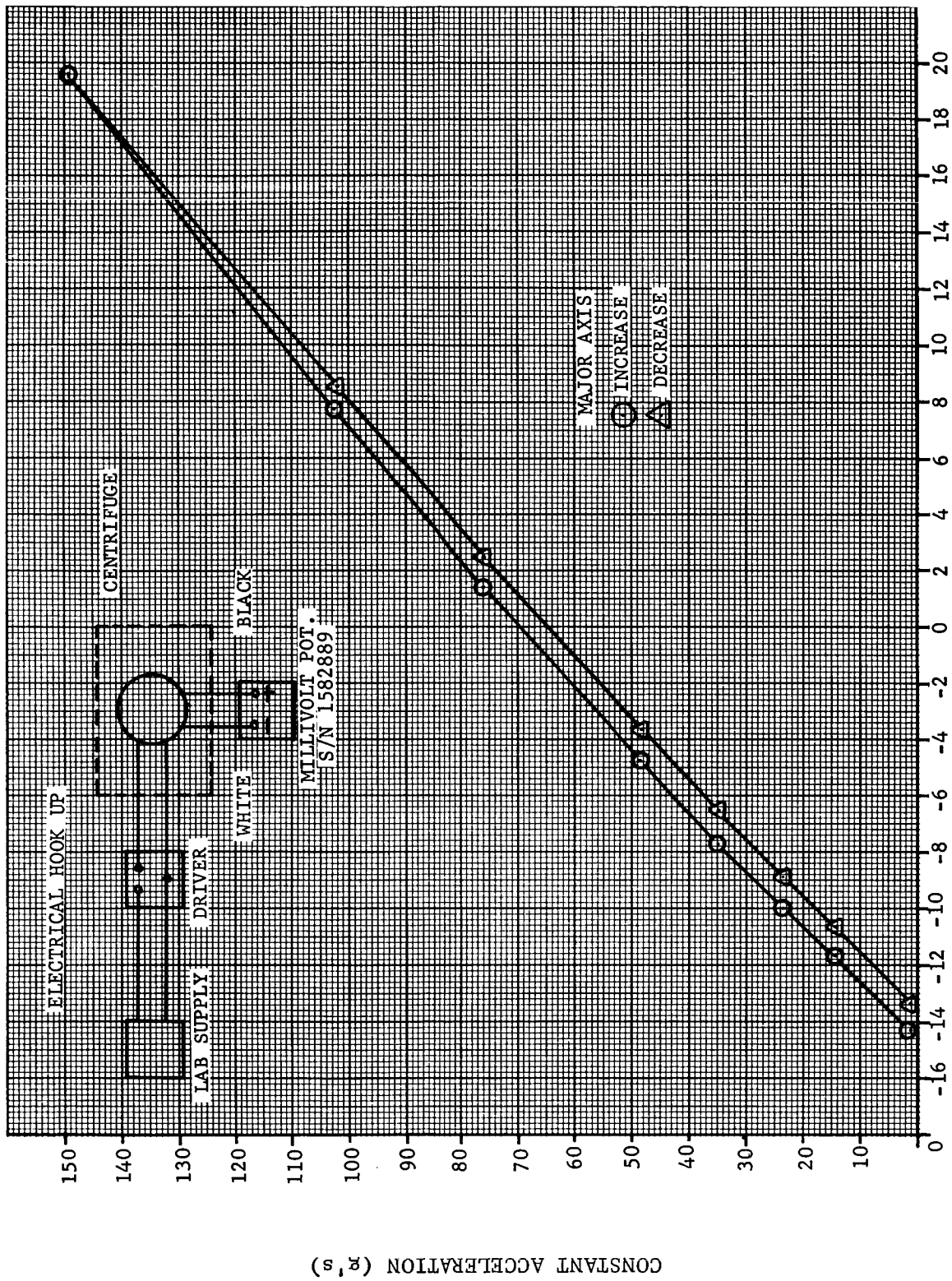

R00701

FIGURE 18. OUTPUT VOLTAGE VERSUS SUSTAINED ACCELERATION FOR ACCELEROMETER AA5

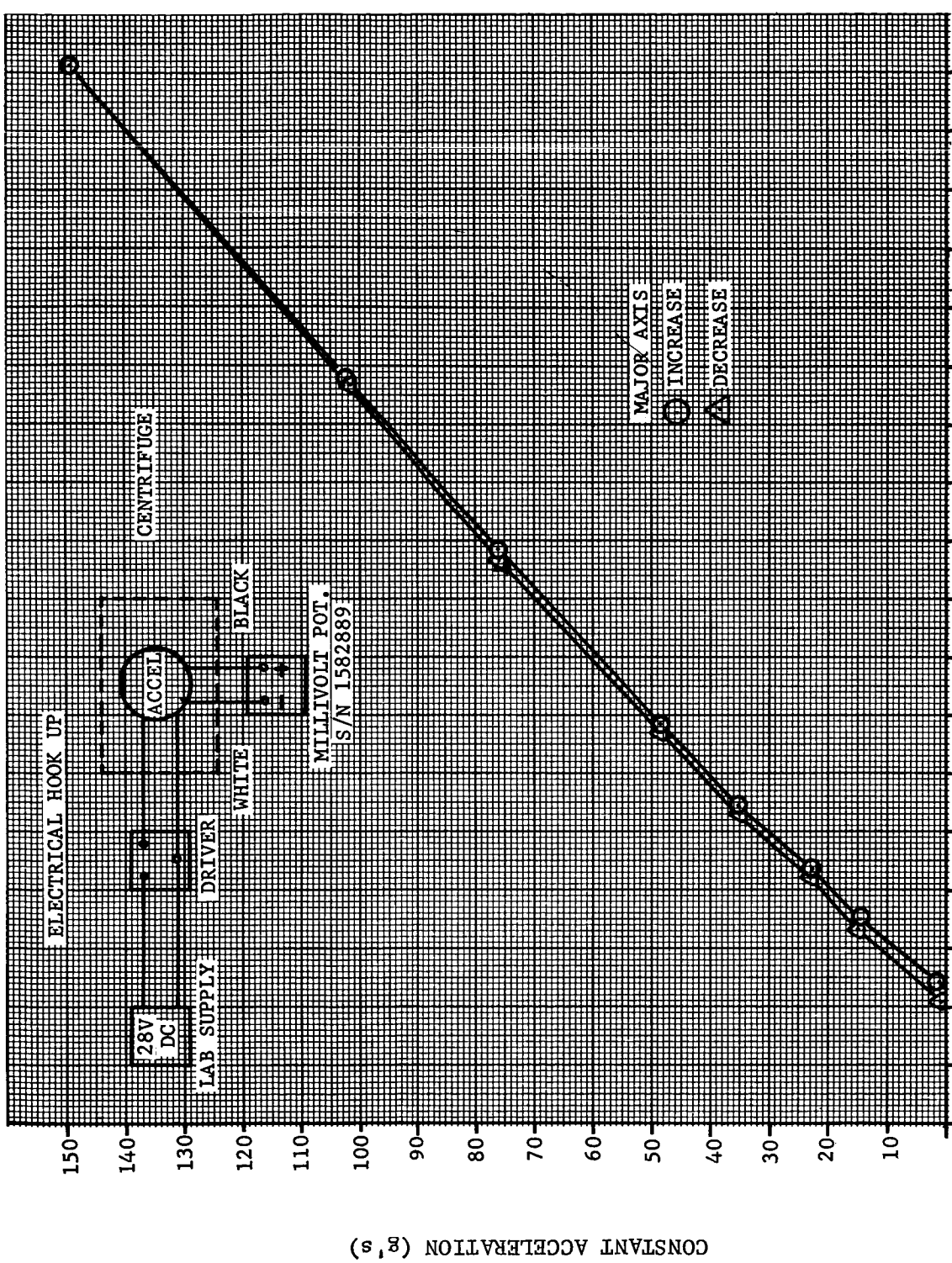

R00700

FIGURE 19. OUTPUT VOLTAGE VERSUS SUSTAINED ACCELERATION FOR ACCELEROMETER AA6

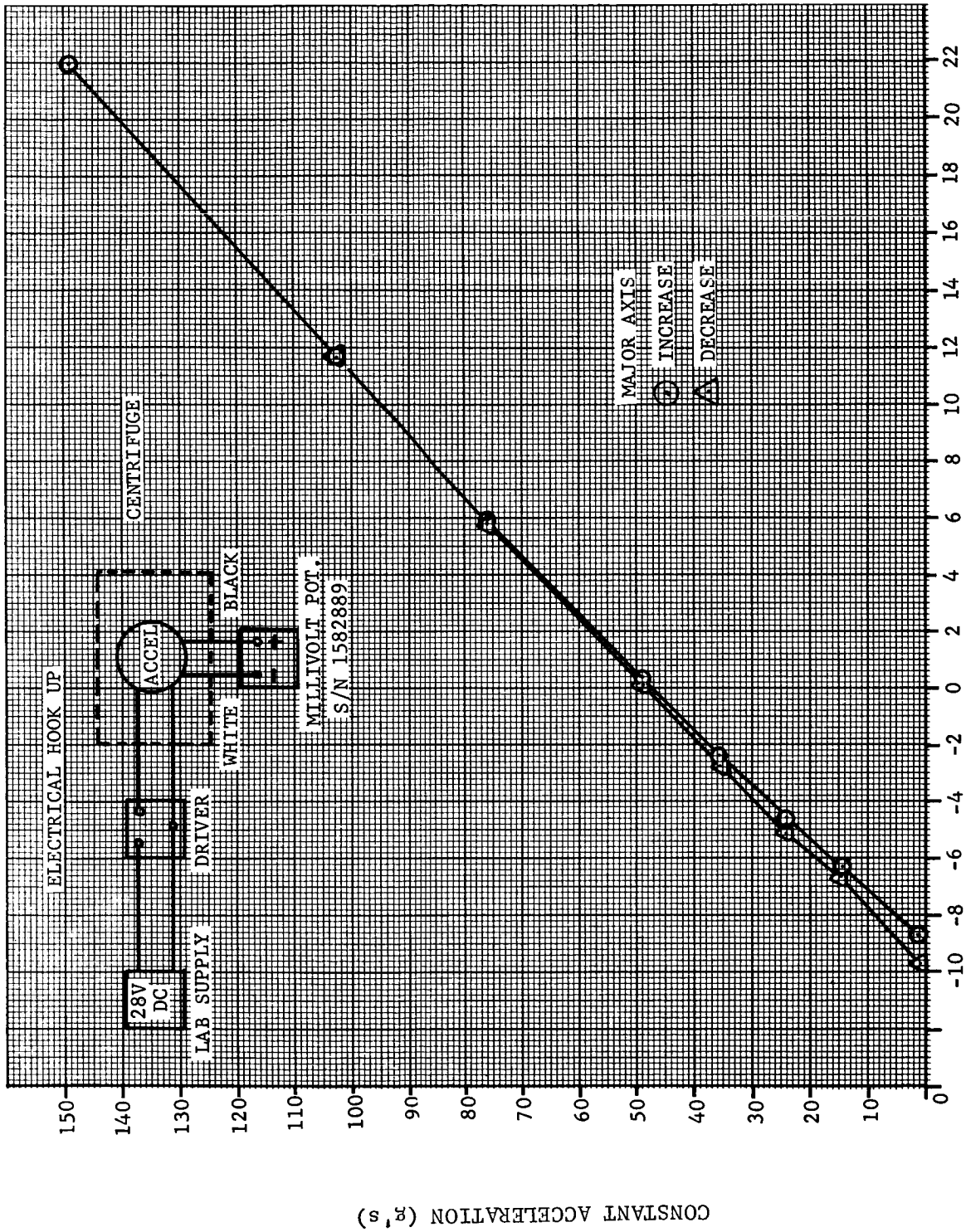

FIGURE 20. OUTPUT VOLTAGE VERSUS SUSTAINED ACCELERATION FOR ACCELEROMETER AA7

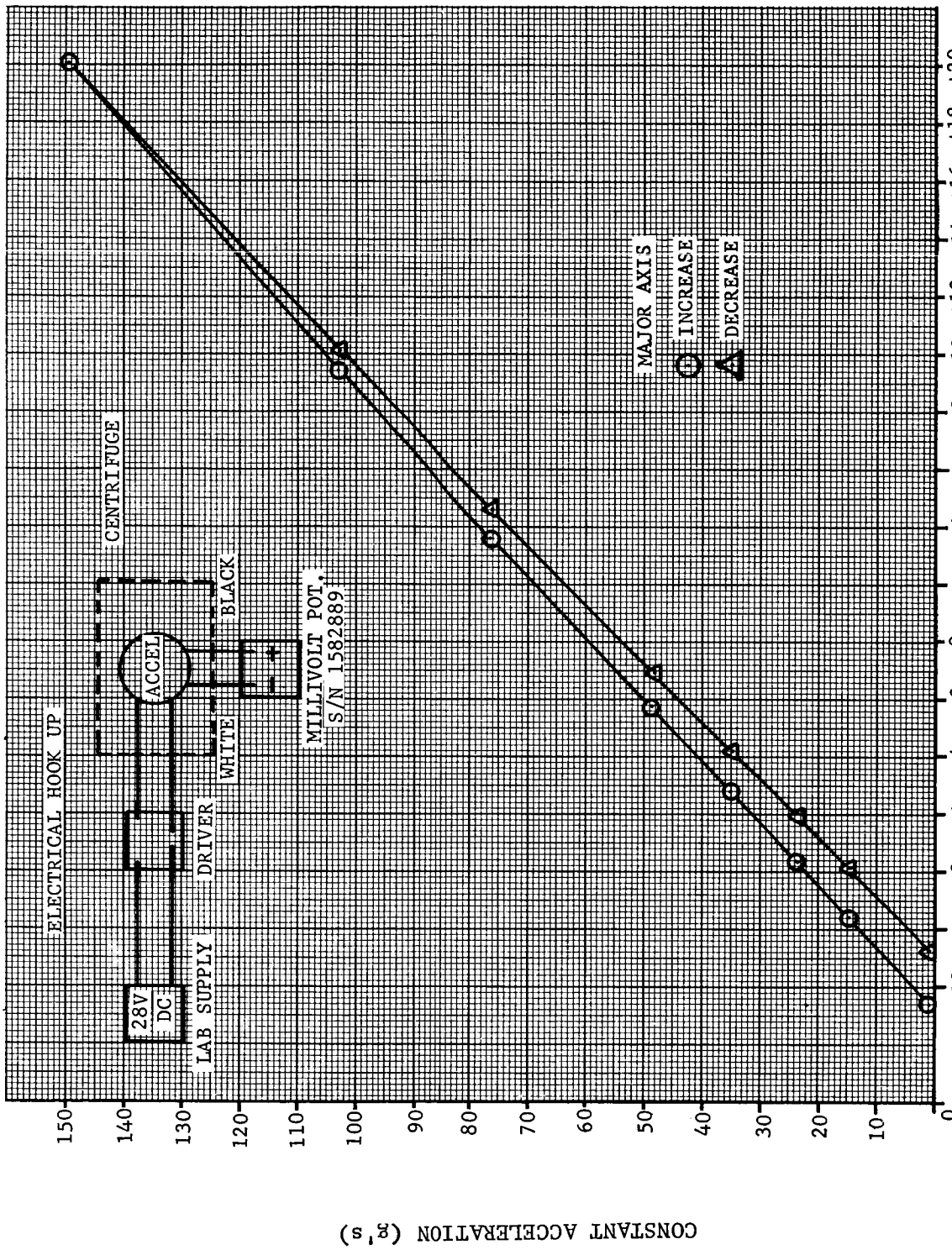

R00693

FIGURE 21. OUTPUT VOLTAGE VERSUS SUSTAINED ACCELERATION FOR ACCELEROMETER AA8

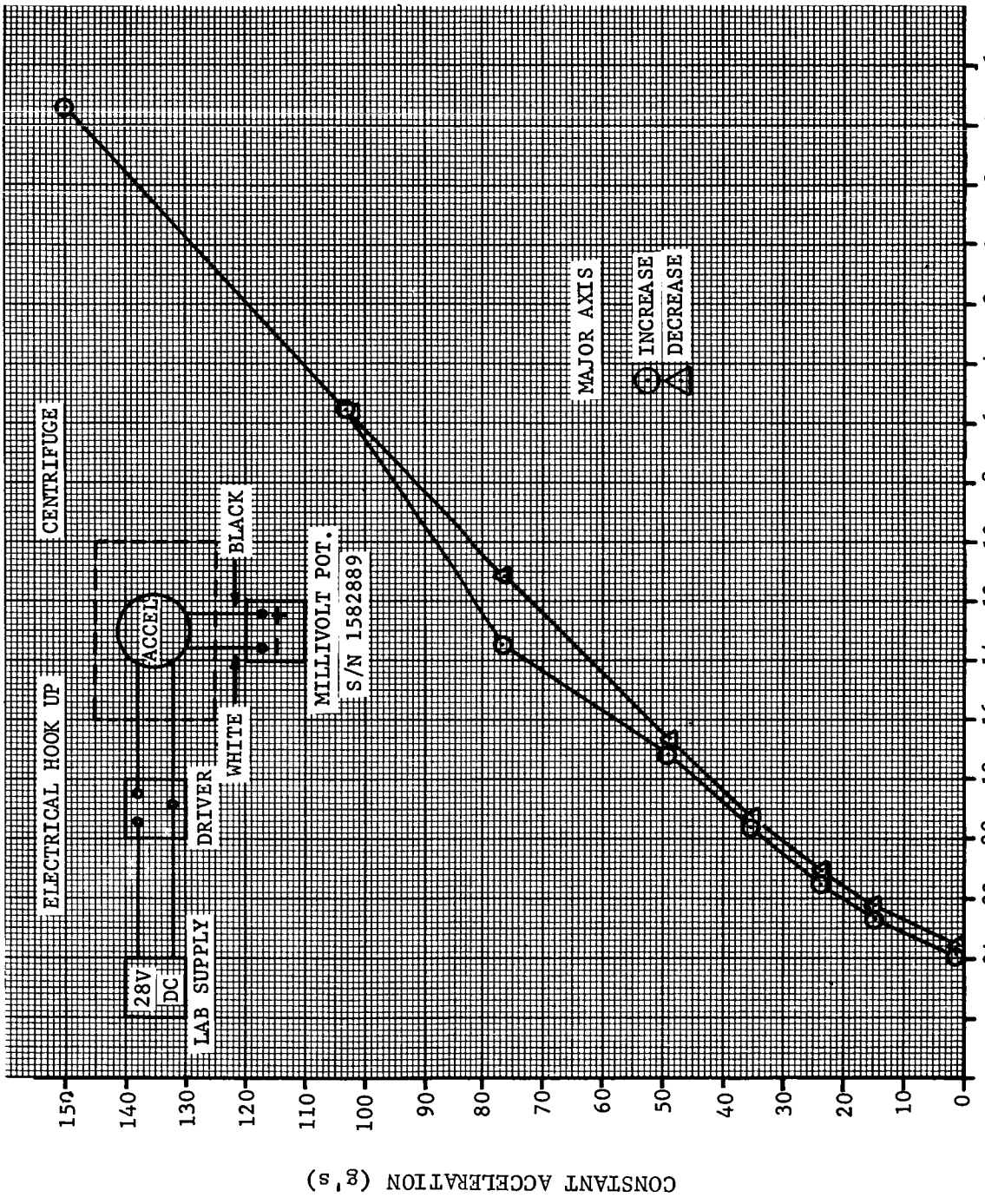

R00698

FIGURE 22. OUTPUT VOLTAGE VERSUS SUSTAINED ACCELERATION FOR ACCELEROMETER AA9

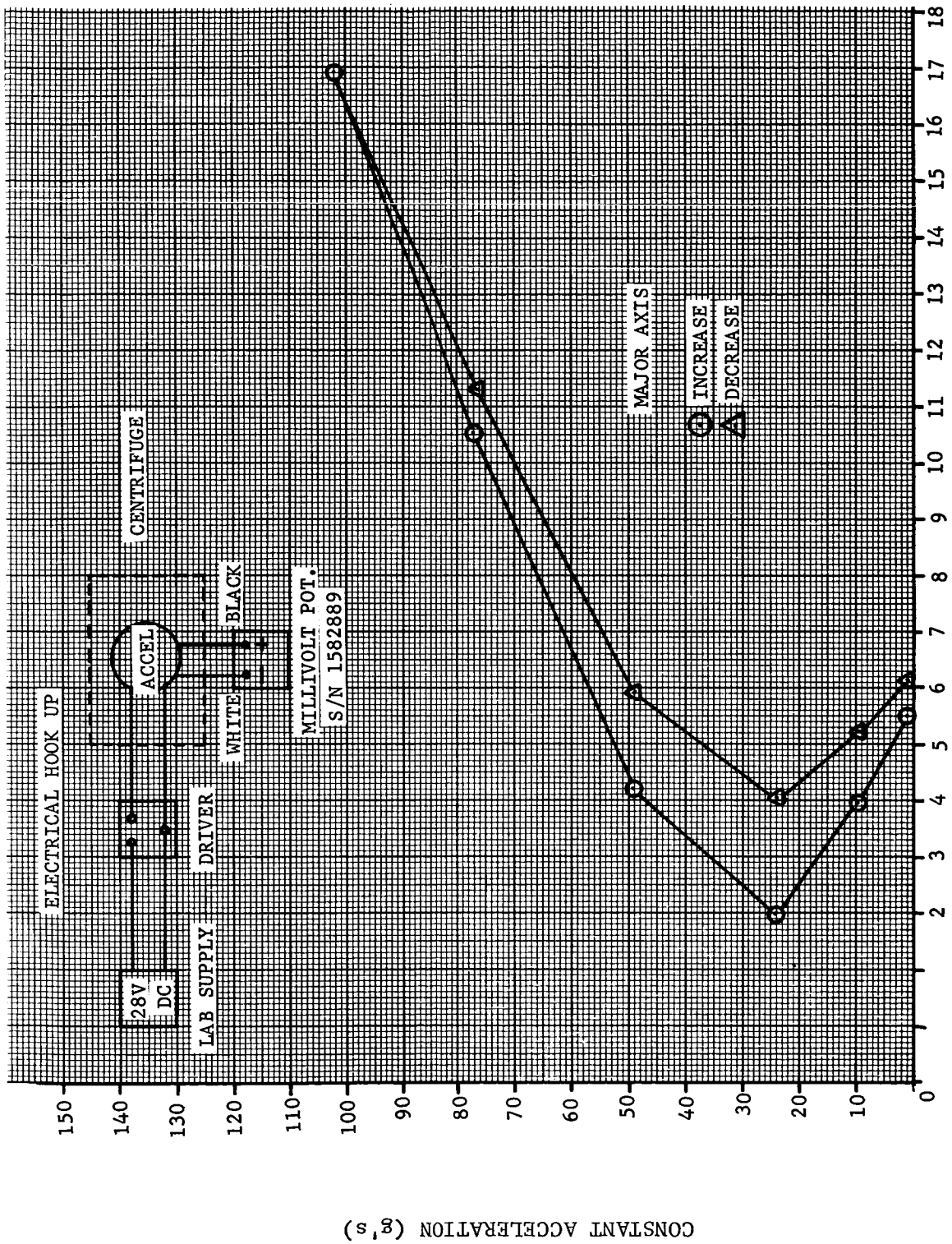

R00703

FIGURE 23. OUTPUT VOLTAGE VERSUS SUSTAINED ACCELERATION FOR ACCELEROMETER AA10

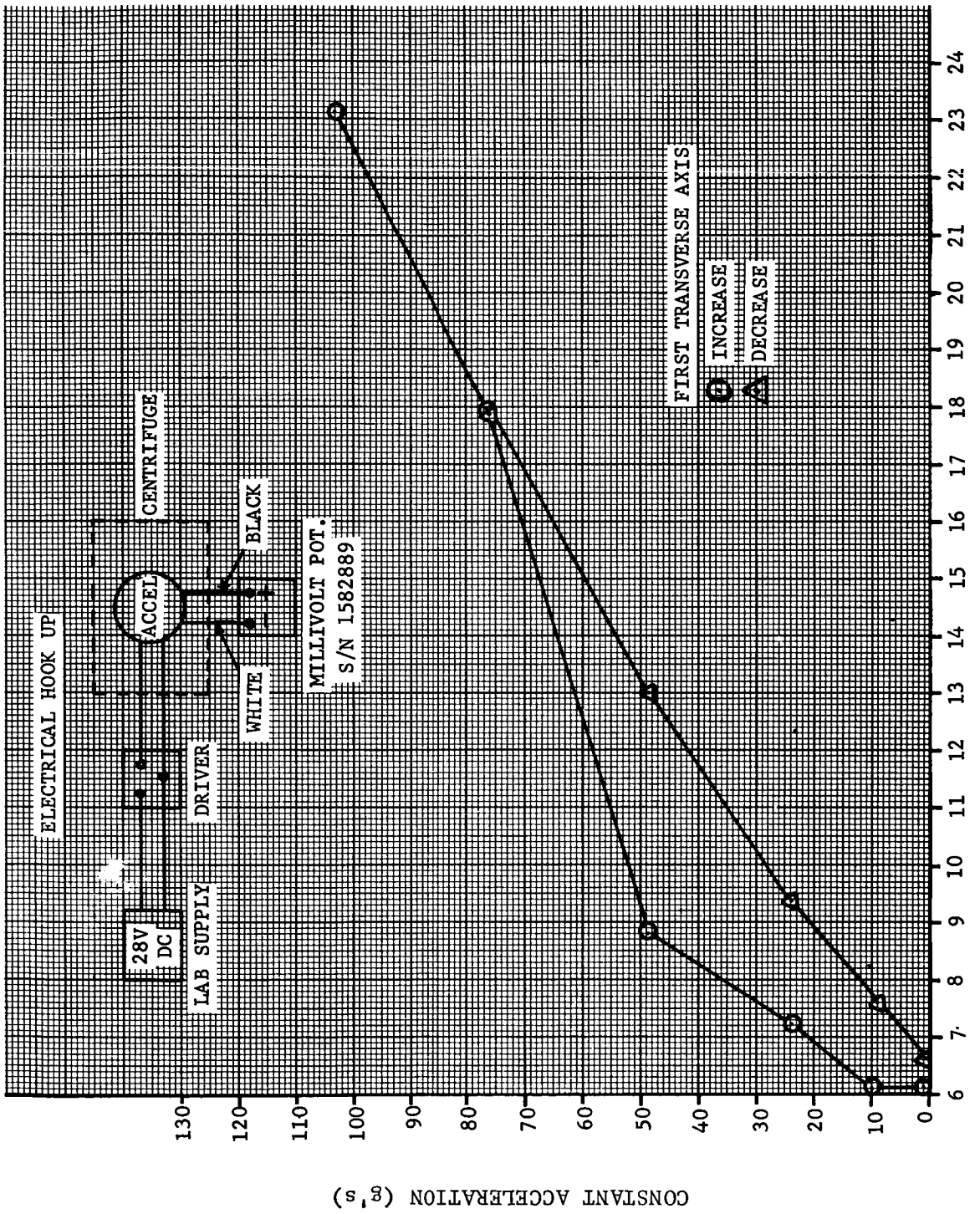

R00716

FIGURE 24. OUTPUT VOLTAGE VERSUS SUSTAINED TRANSVERSE (AXIS NO. 1) ACCELERATION FOR ACCELEROMETER AA10

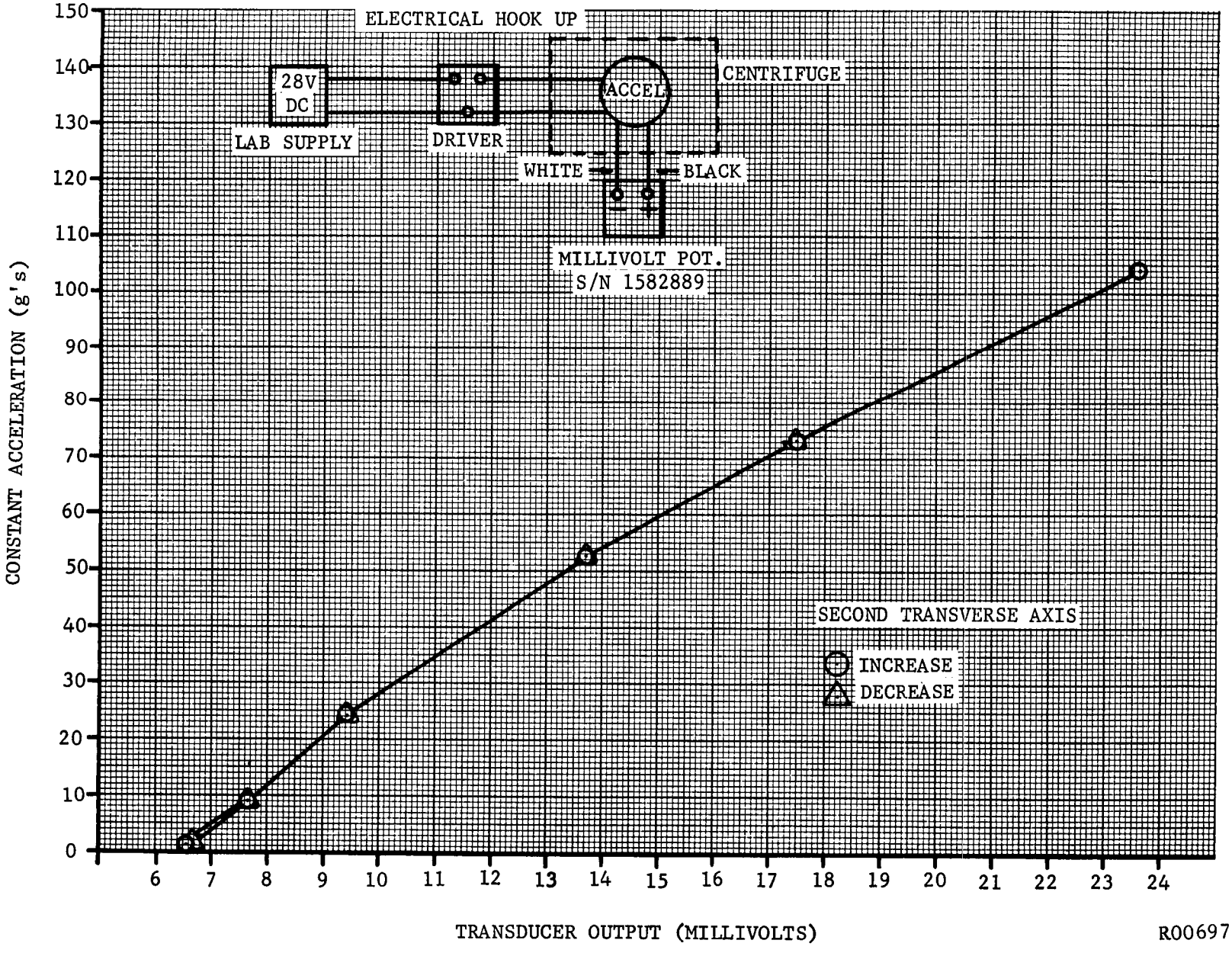

R00697

FIGURE 25. OUTPUT VOLTAGE VERSUS SUSTAINED TRANSVERSE (AXIS NO. 2) ACCELERATION FOR ACCELEROMETER AA10

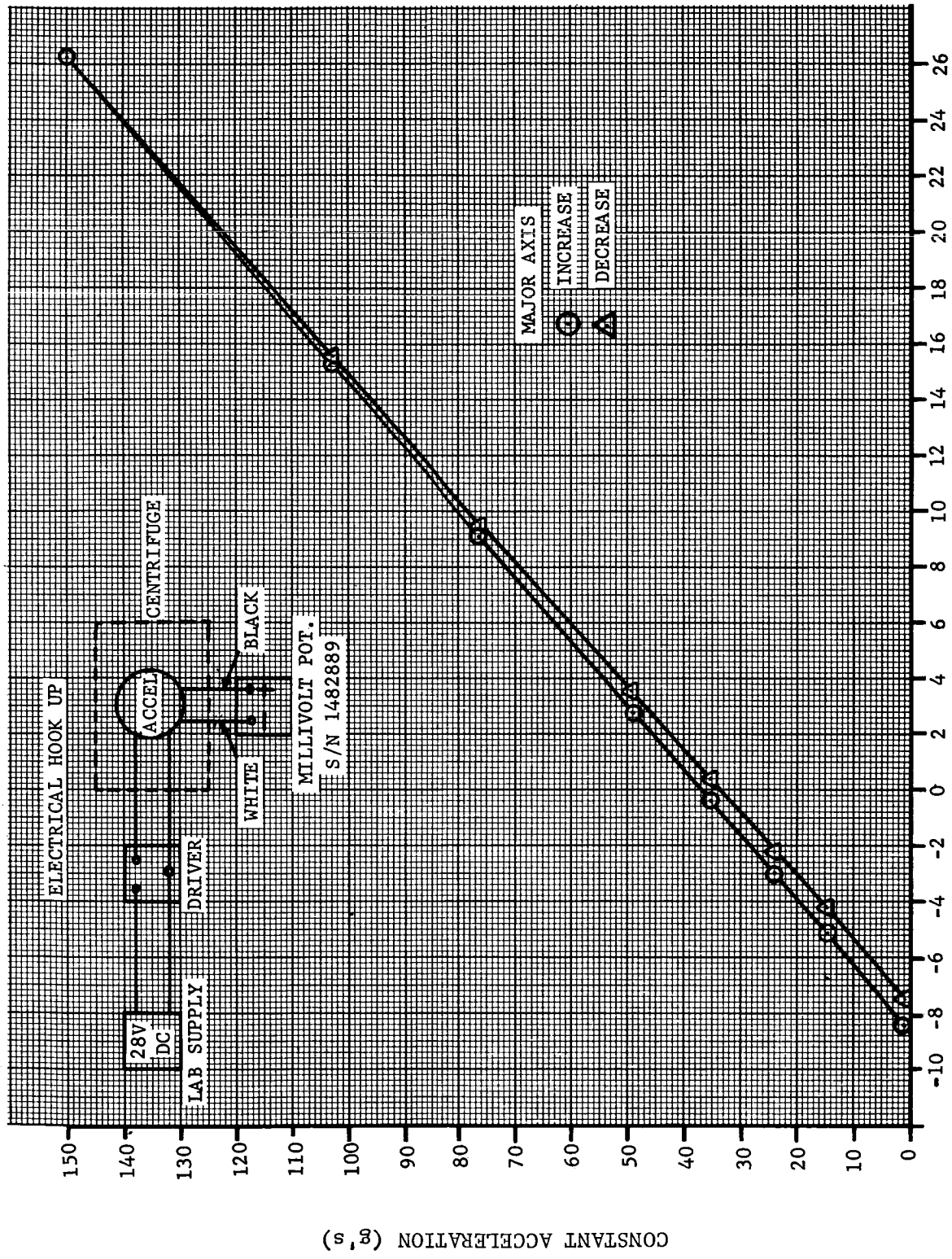

R00719

FIGURE 26. OUTPUT VOLTAGE VERSUS SUSTAINED ACCELERATION FOR ACCELEROMETER AA11

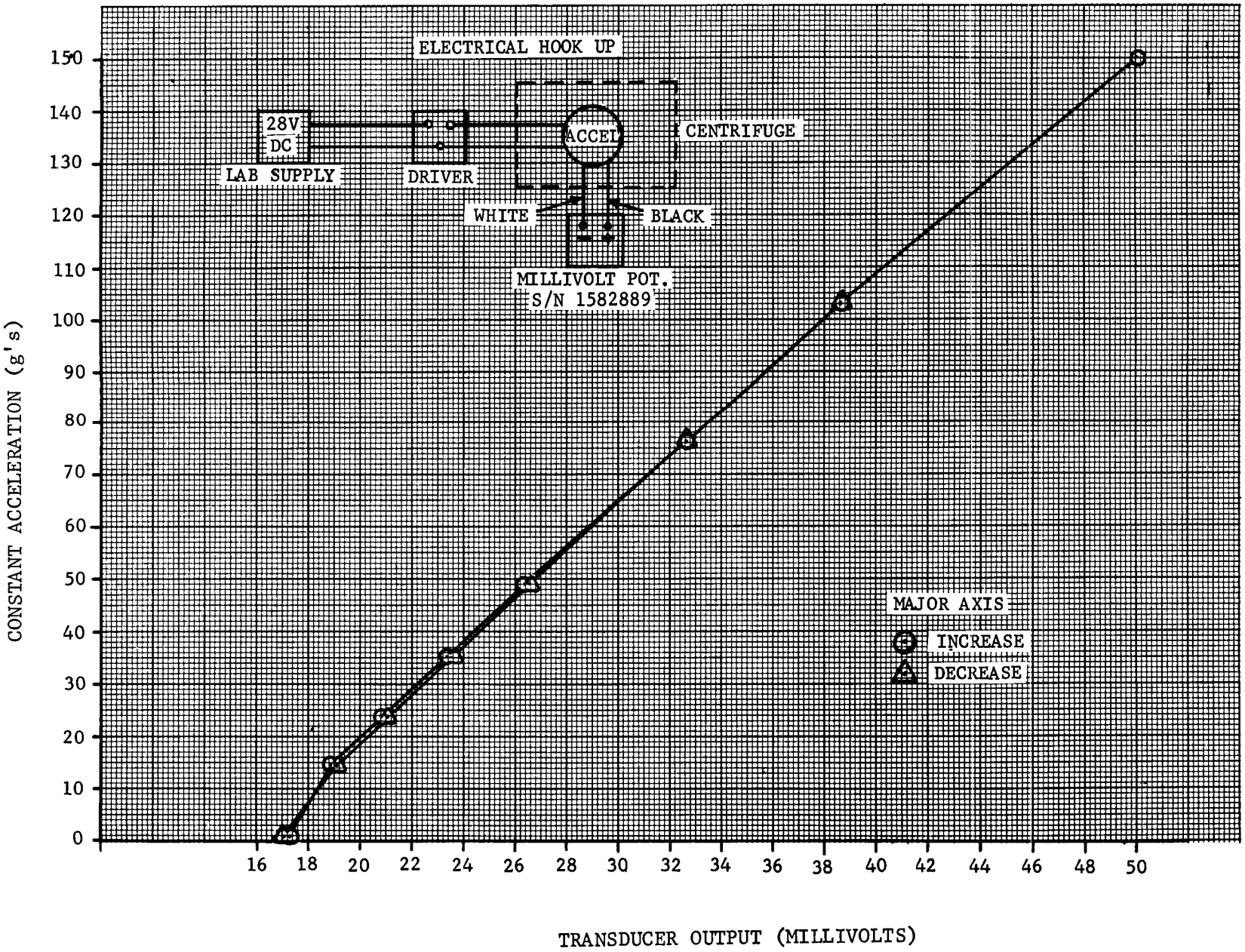

R00717

FIGURE 27. OUTPUT VOLTAGE VERSUS SUSTAINED ACCELERATION FOR ACCELEROMETER AA12

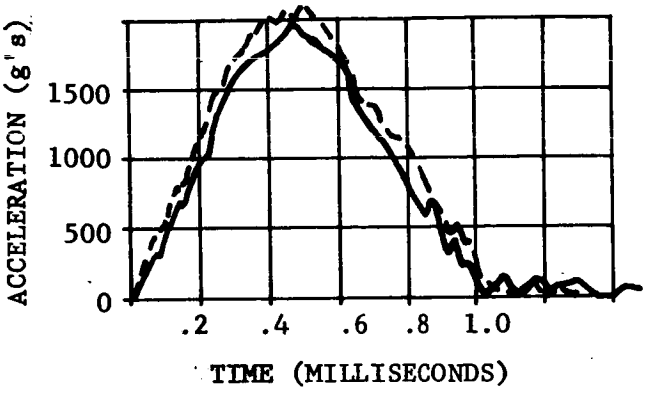

——— OMNIDIRECTIONAL ACCELEROMETER

– – – REFERENCE ACCELEROMETER

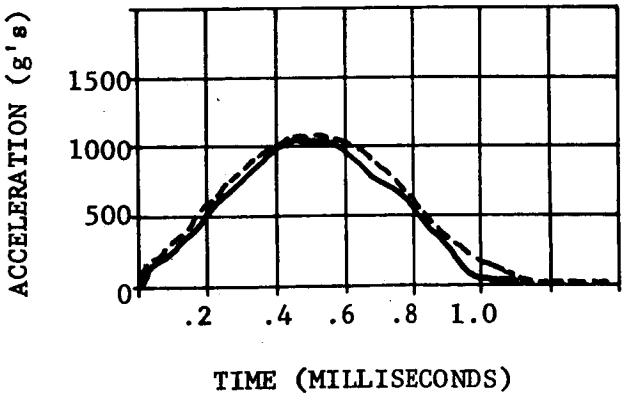

R00743

FIGURE 26. IMPACT CHARACTERISTICS OF ACCELEROMETER AA3

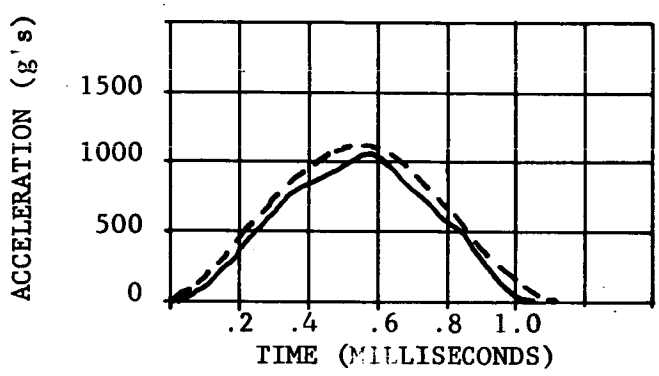

OMNIDIRECTIONAL ACCELEROMETER

REFERENCE ACCELEROMETER

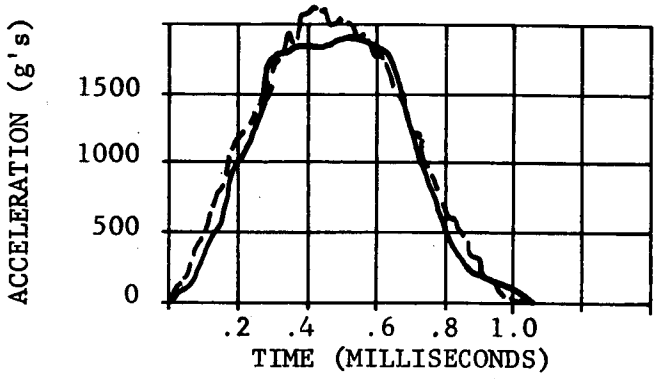

R00749

FIGURE 29. IMPACT CHARACTERISTICS OF ACCELEROMETER AA4

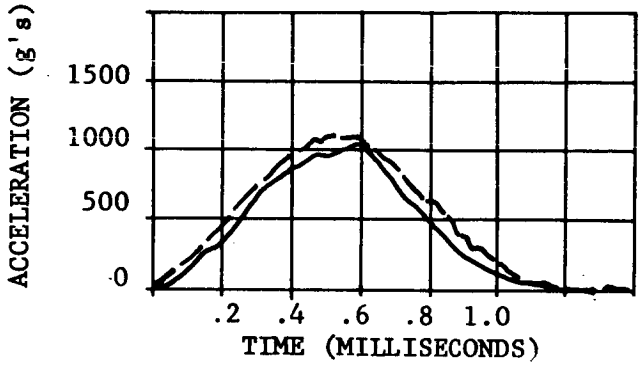

OMNIDIRECTIONAL ACCELEROMETER

REFERENCE ACCELEROMETER

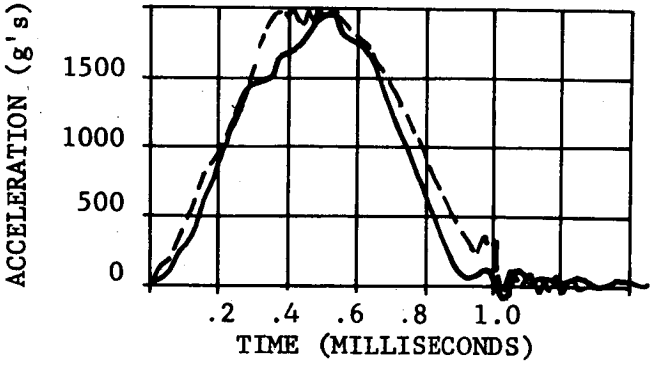

R00747

FIGURE 30. IMPACT CHARACTERISTICS OF ACCELEROMETER AA5

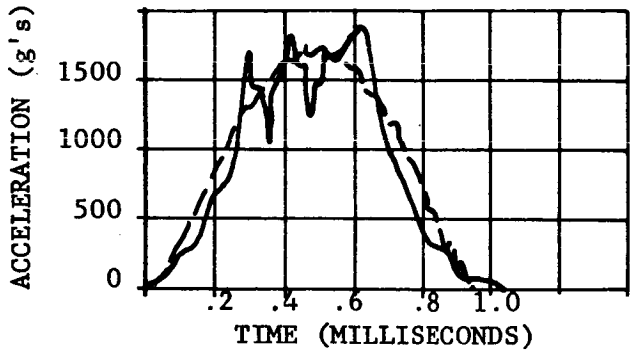

OMNIDIRECTIONAL ACCELEROMETER

REFERENCE ACCELEROMETER

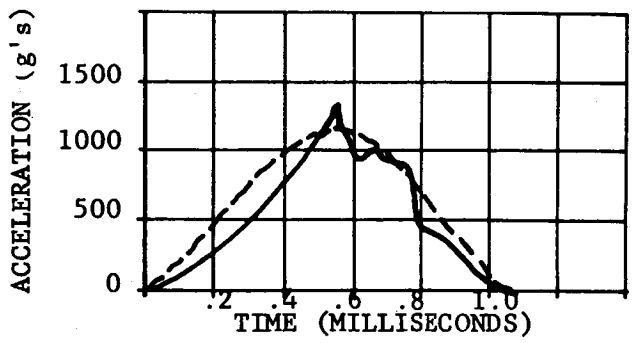

R00748

FIGURE 31. IMPACT CHARACTERISTICS OF ACCELEROMETER AA6

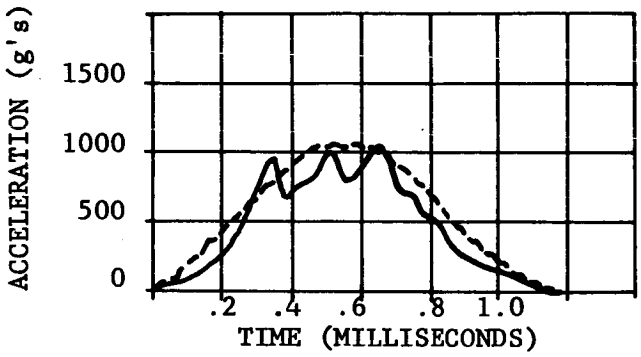

OMNIDIRECTIONAL ACCELEROMETER

REFERENCE ACCELEROMETER

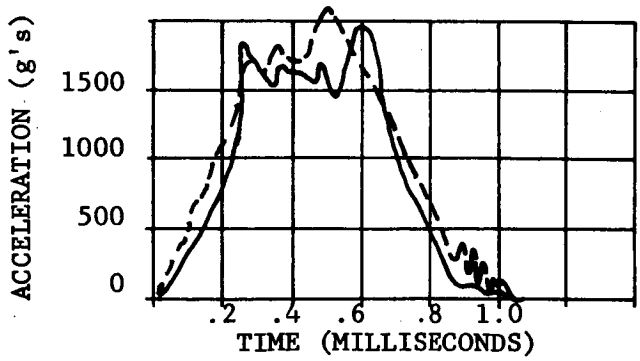

R00746

FIGURE 32. IMPACT CHARACTERISTICS OF ACCELEROMETER AA7

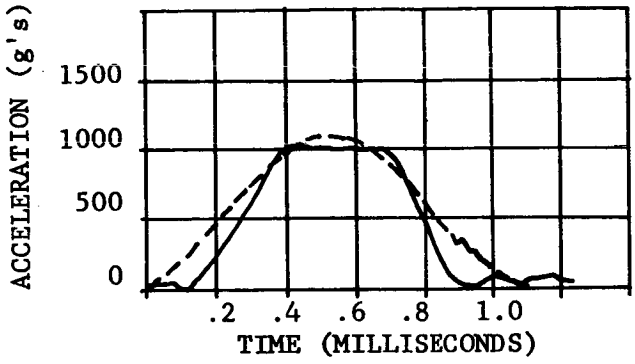

——— OMNIDIRECTIONAL ACCELEROMETER

– – – REFERENCE ACCELEROMETER

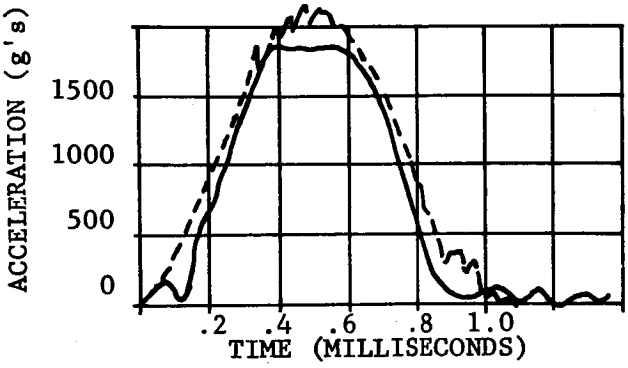

R00745

FIGURE 33. IMPACT CHARACTERISTICS OF ACCELEROMETER AA8

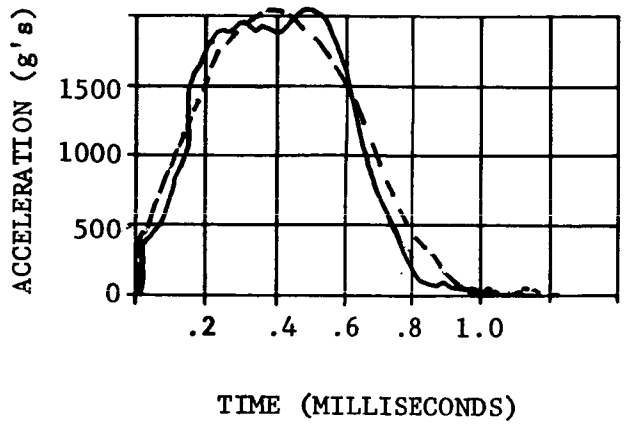

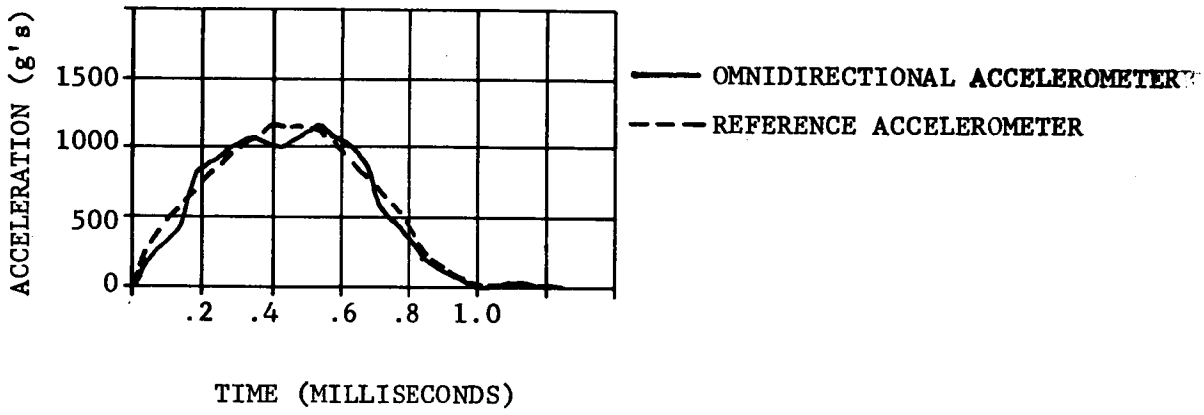

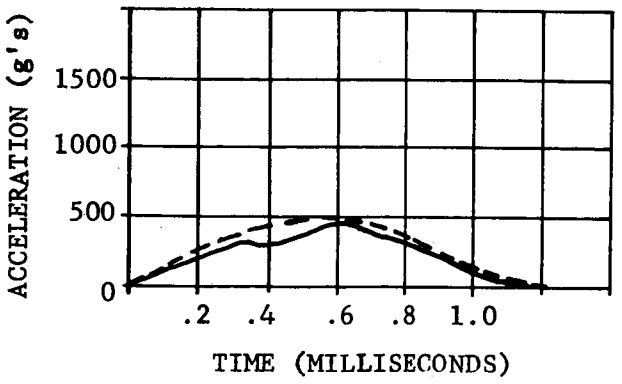

FIGURE 34. IMPACT CHARACTERISTICS OF ACCELEROMETER AA9

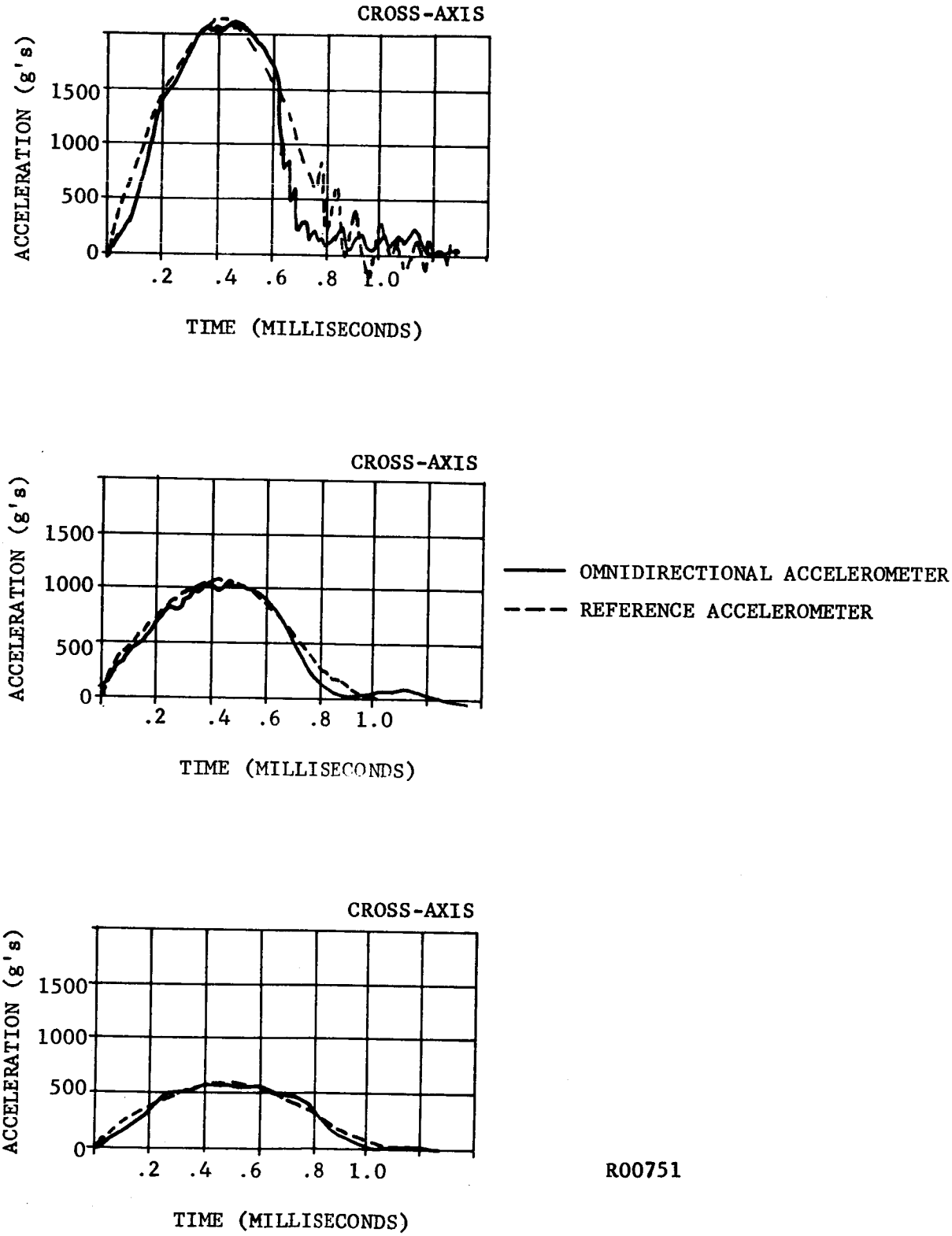

FIGURE 35. IMPACT CHARACTERISTICS OF ACCELEROMETER AA9

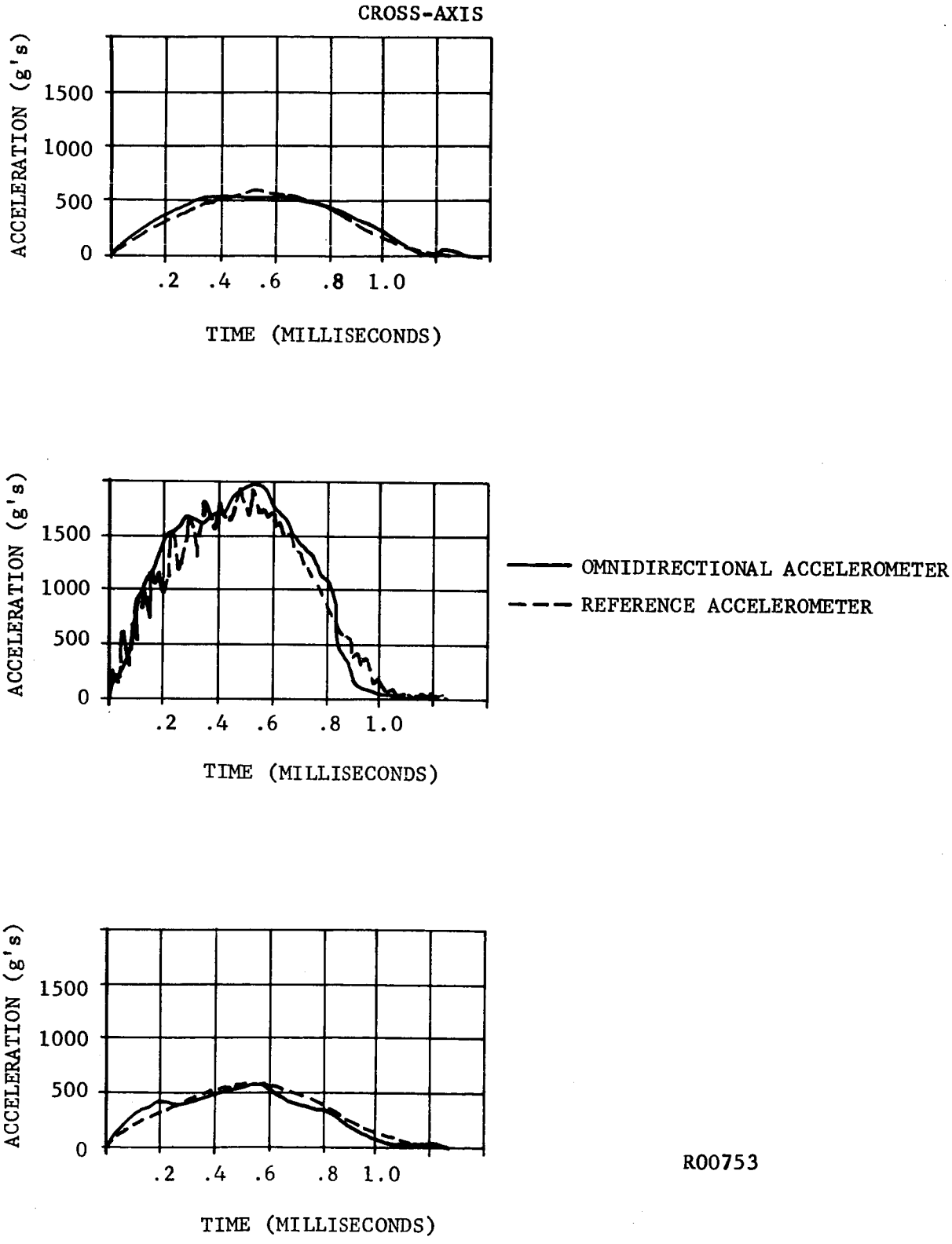

FIGURE 36. IMPACT CHARACTERISTICS OF ACCELEROMETER AA10

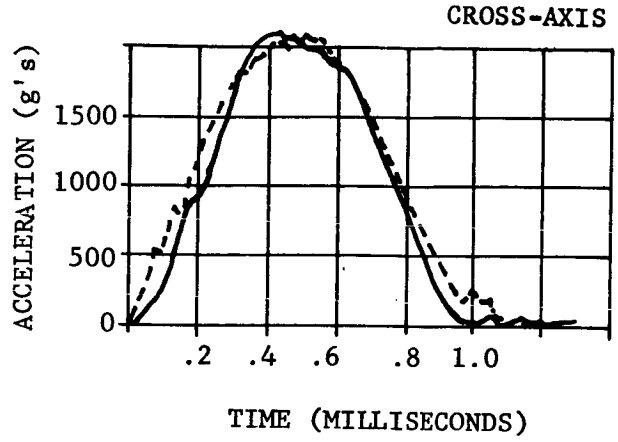

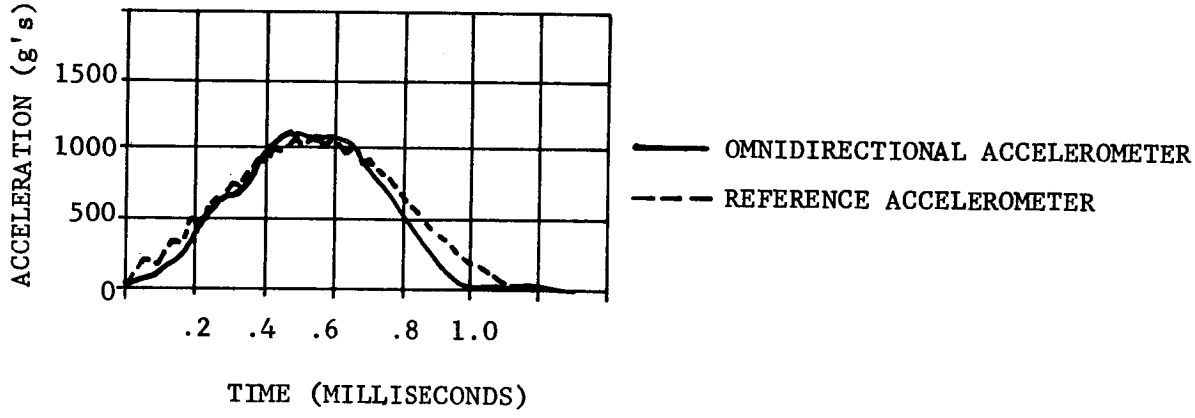

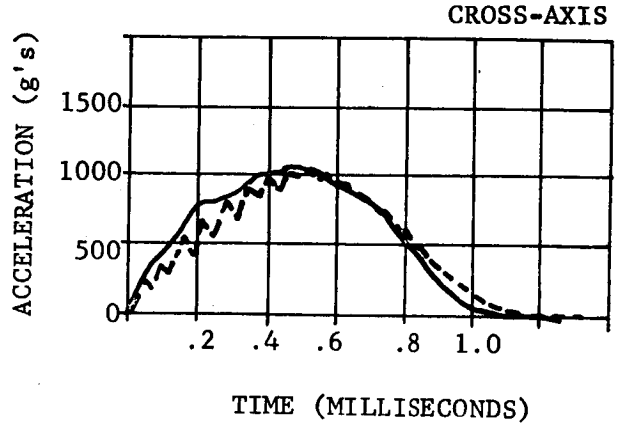

R00752

FIGURE 37. IMPACT CHARACTERISTICS OF ACCELEROMETER AA10

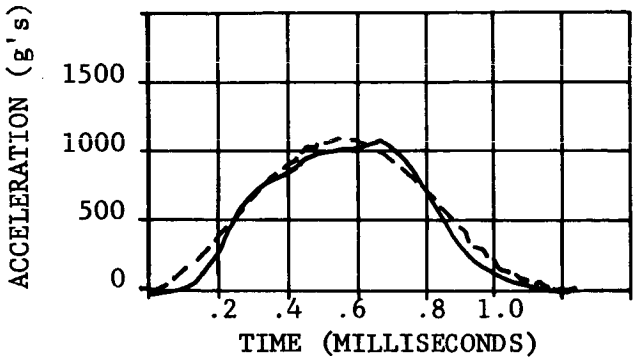

——— OMNIDIRECTIONAL ACCELEROMETER

– – – REFERENCE ACCELEROMETER

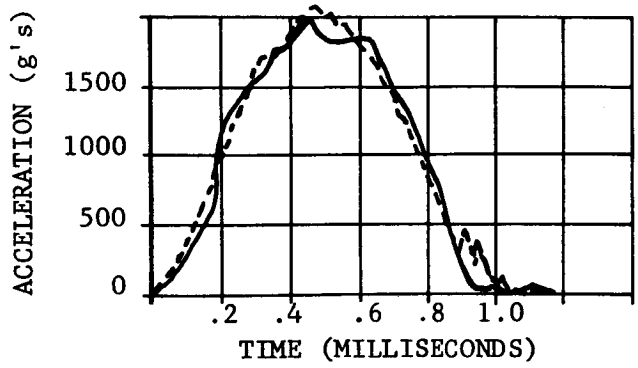

R00744

FIGURE 38. IMPACT CHARACTERISTICS OF ACCELEROMETER AA11

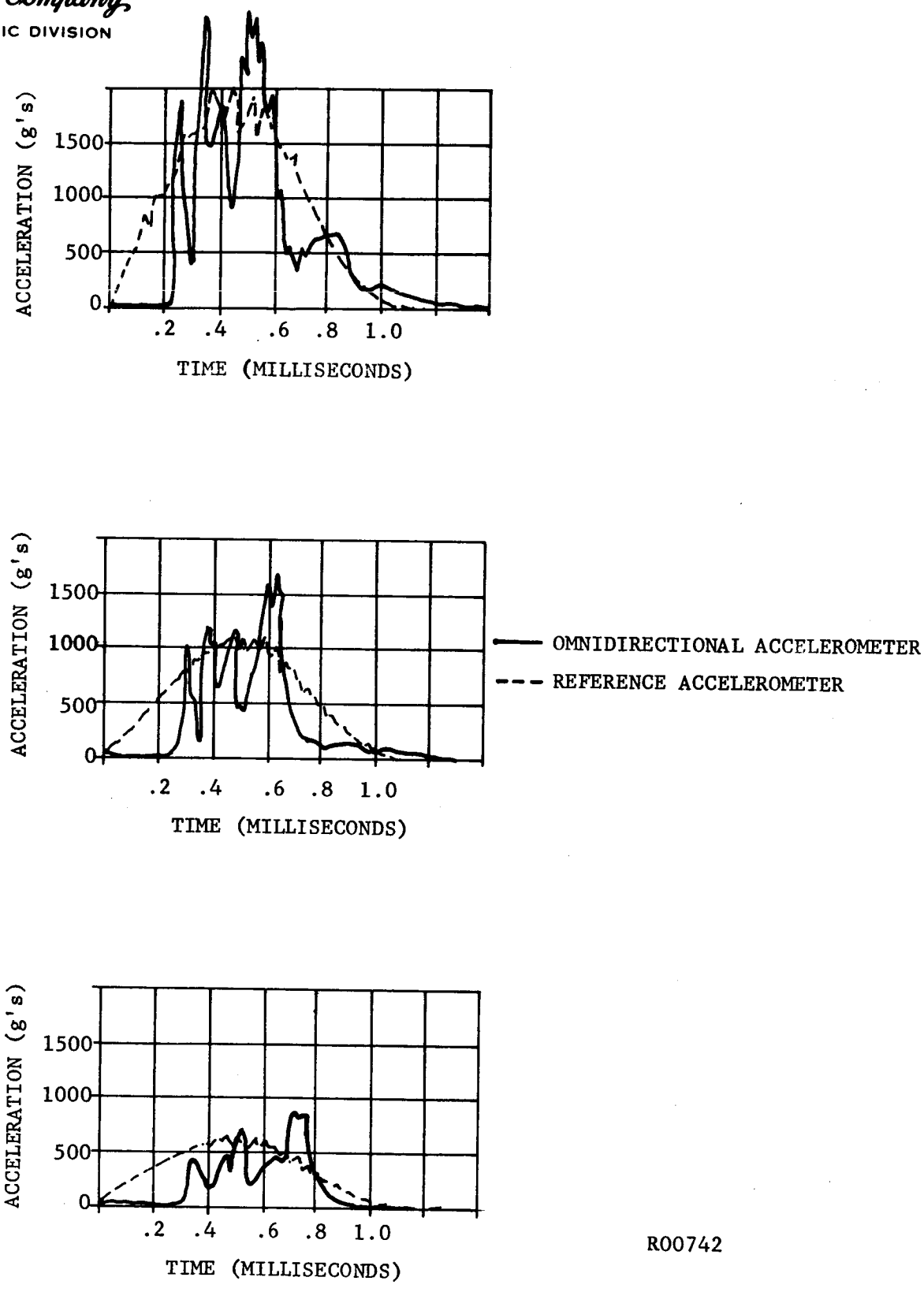

FIGURE 39. IMPACT CHARACTERISTICS OF ACCELEROMETER AA12

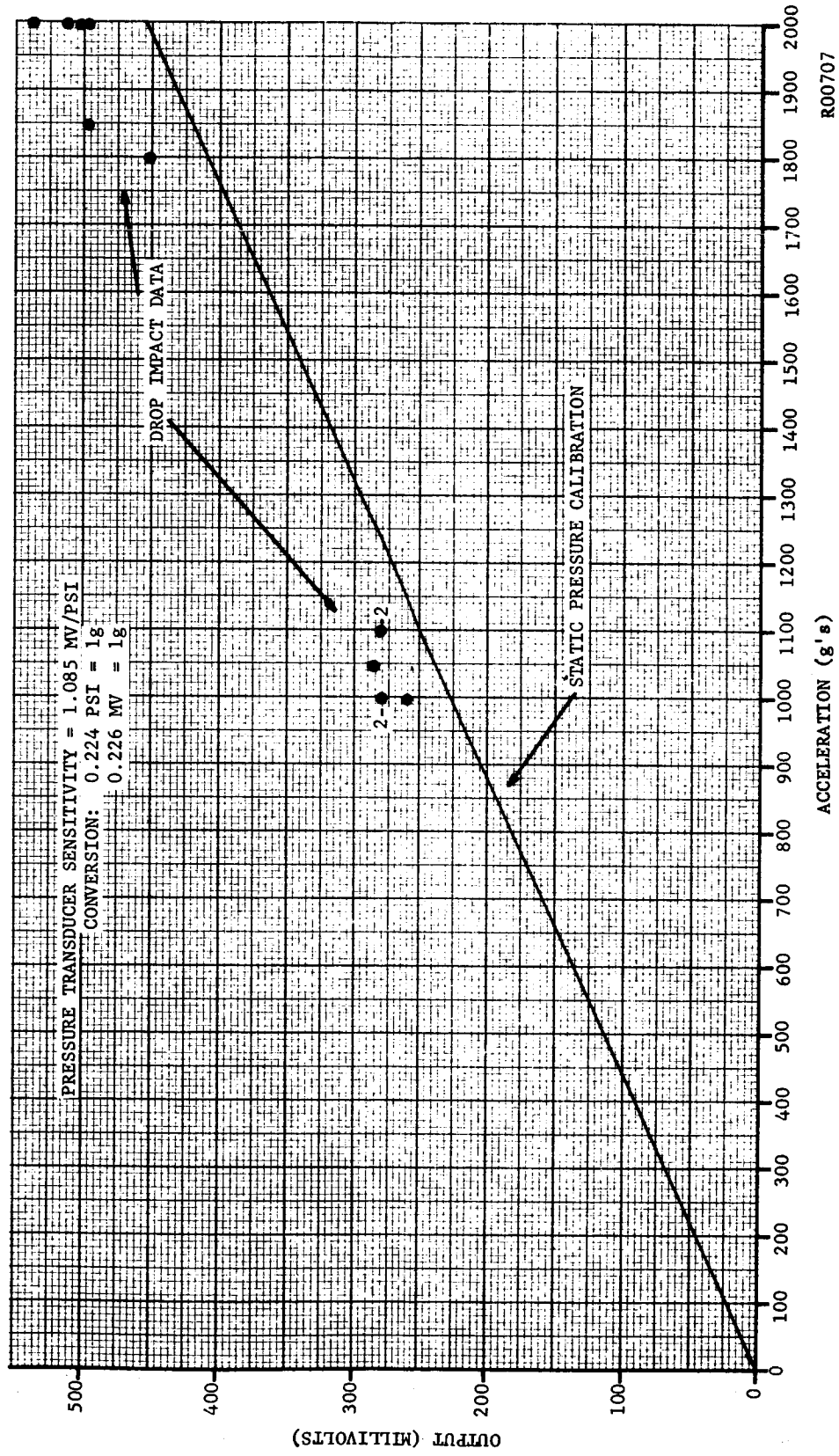

FIGURE 40. CALIBRATION DATA ON ACCELEROMETER AA3

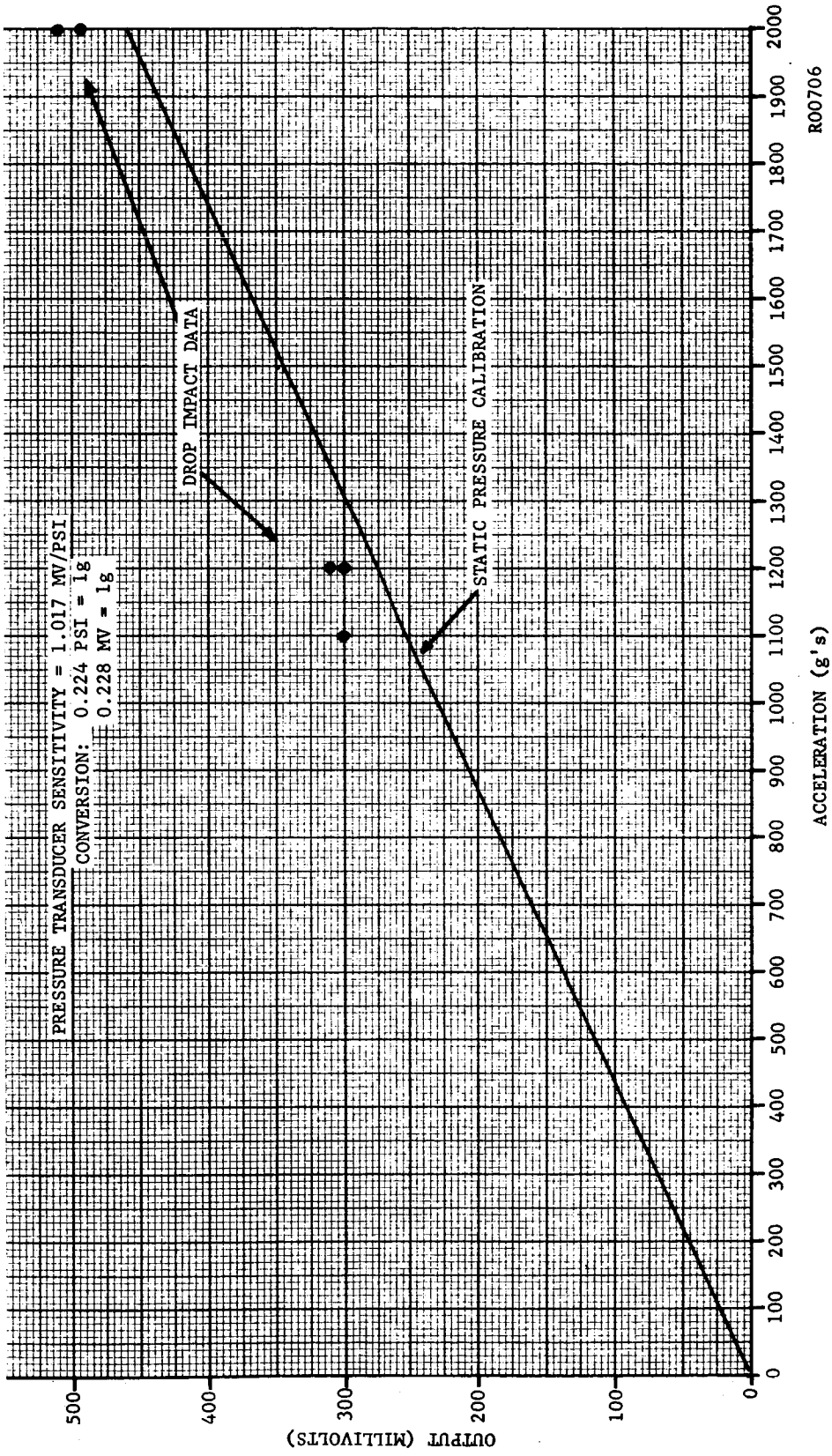

FIGURE 41. CALIBRATION DATA ON ACCELEROMETER AA4

Ford Motor Company
AERONUTRONIC DIVISION

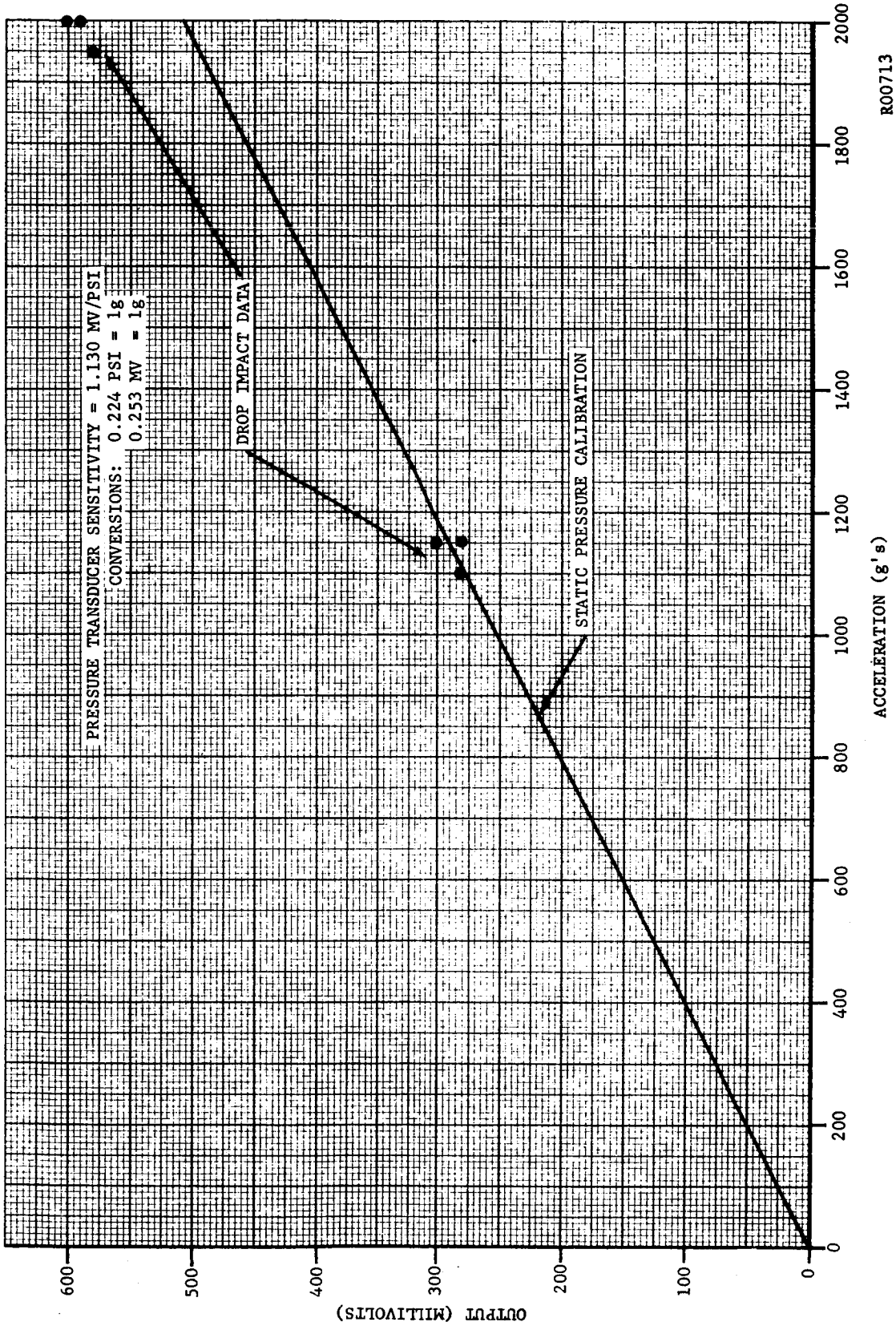

FIGURE 42. CALIBRATION DATA ON ACCELEROMETER AA5

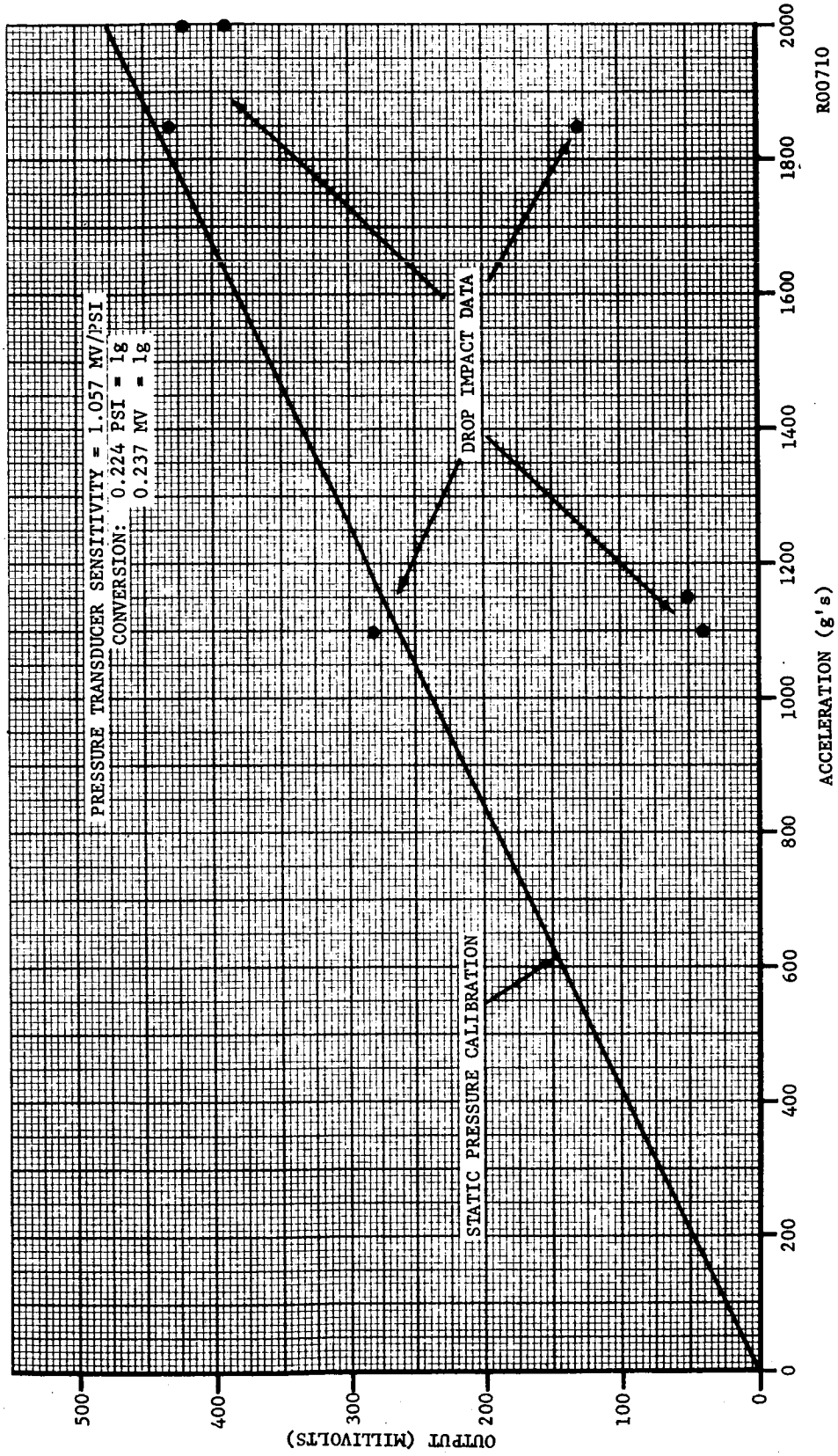

FIGURE 43. CALIBRATION DATA ON ACCELEROMETER AA6

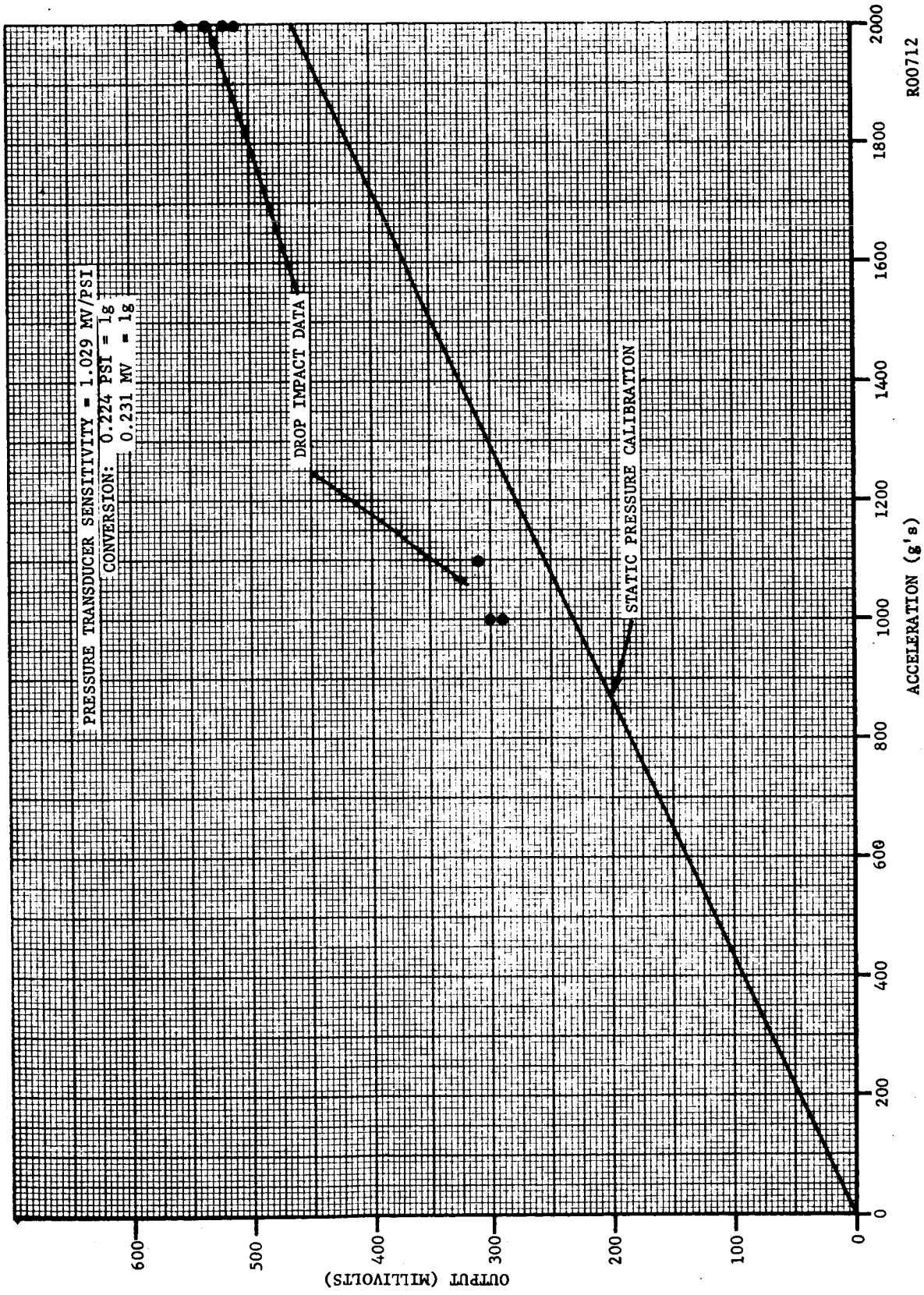

FIGURE 44. CALIBRATION DATA ON ACCELEROMETER AA7

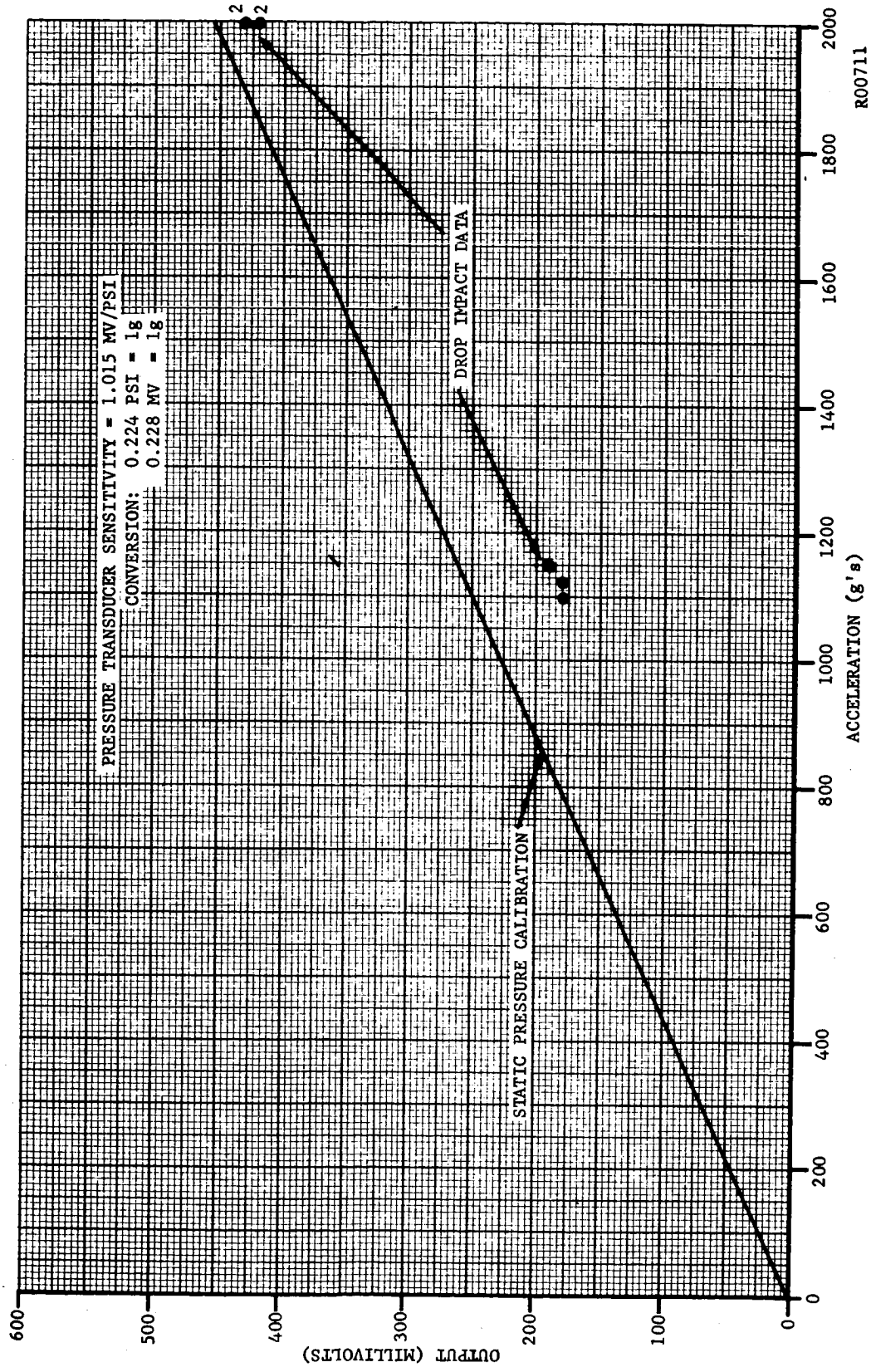

FIGURE 45. CALIBRATION DATA ON ACCELEROMETER AA8

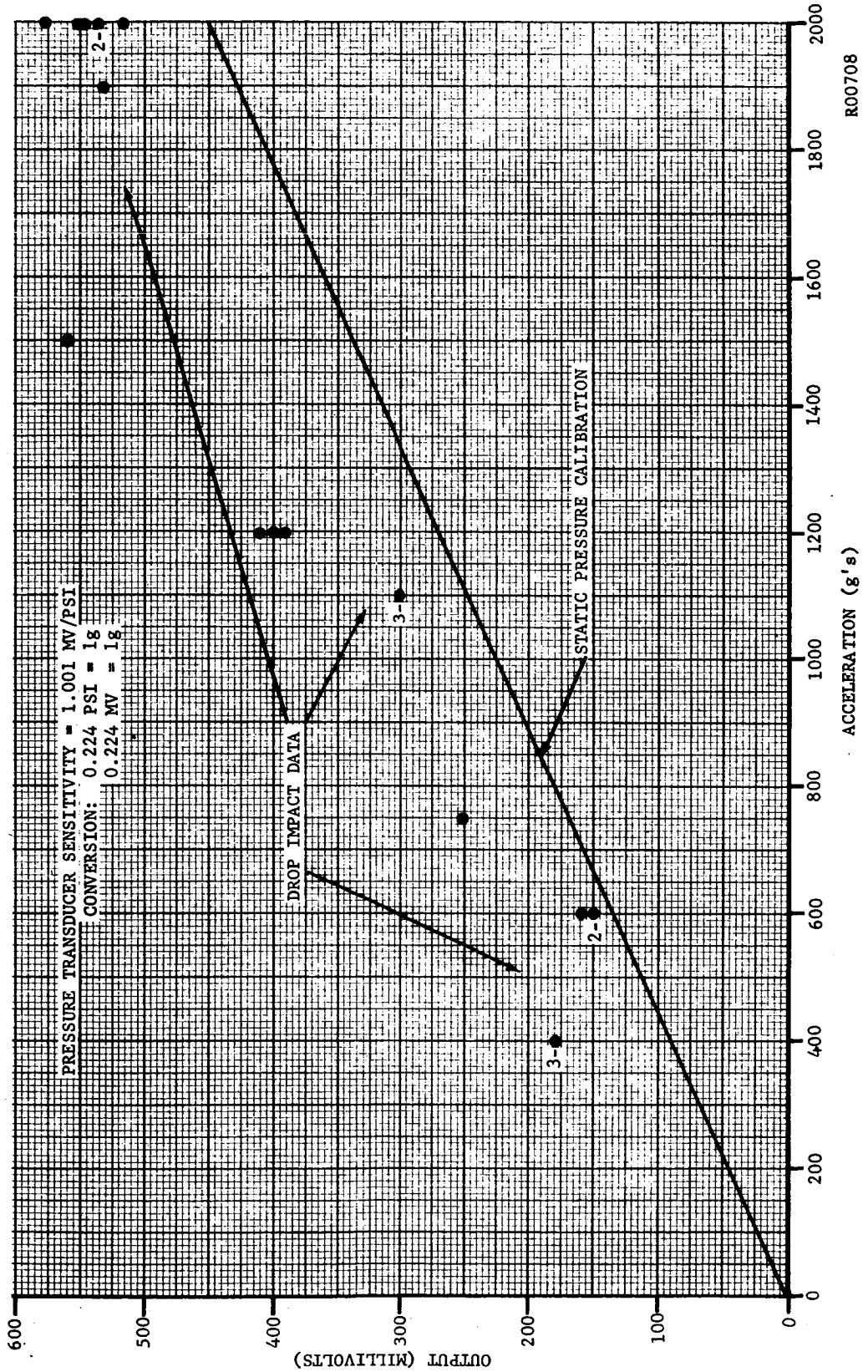

FIGURE 46. CALIBRATION DATA ON ACCELEROMETER AA9

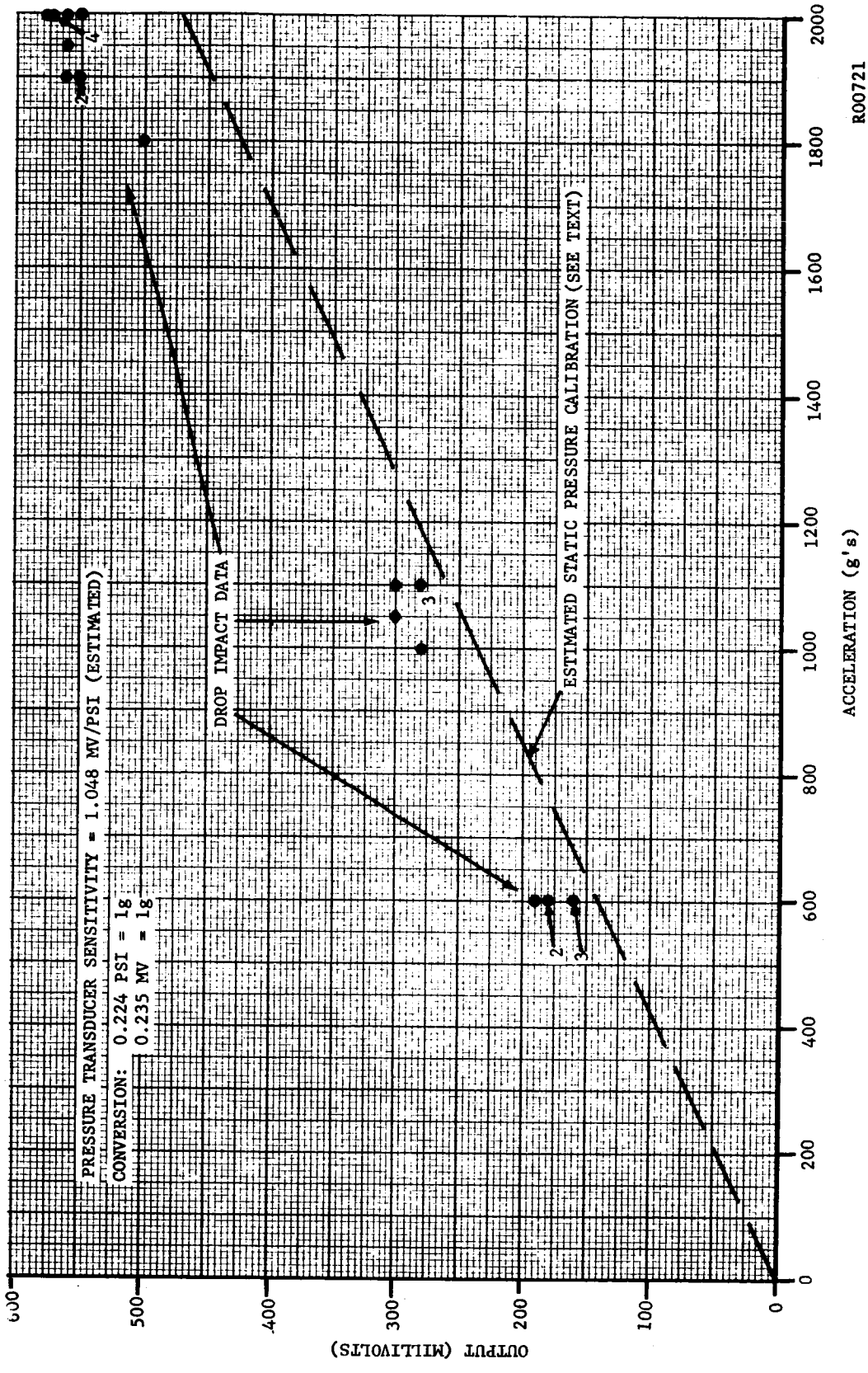

FIGURE 47. CALIBRATION DATA ON ACCELEROMETER AA10

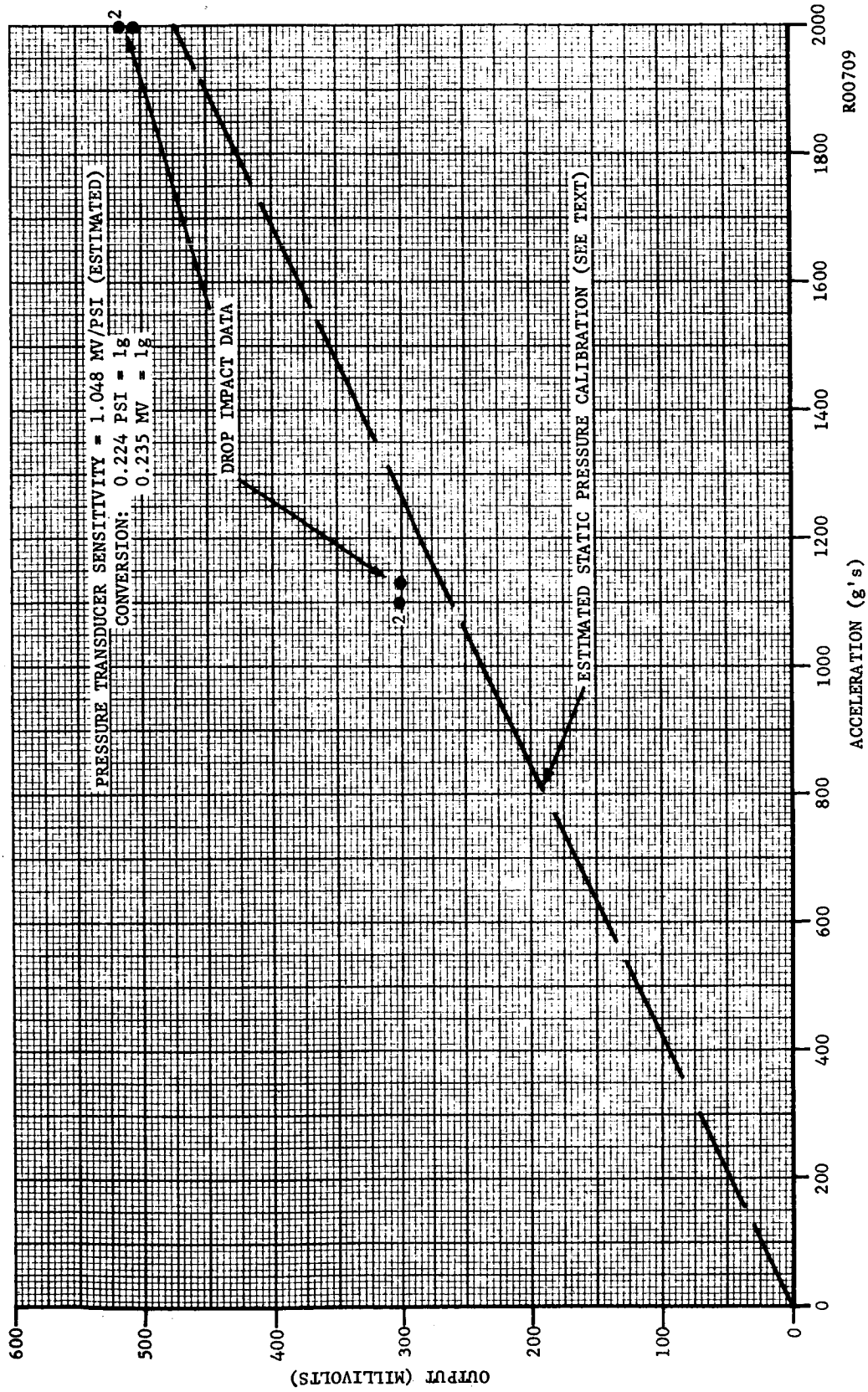

FIGURE 48. CALIBRATION DATA ON ACCELEROMETER AA11

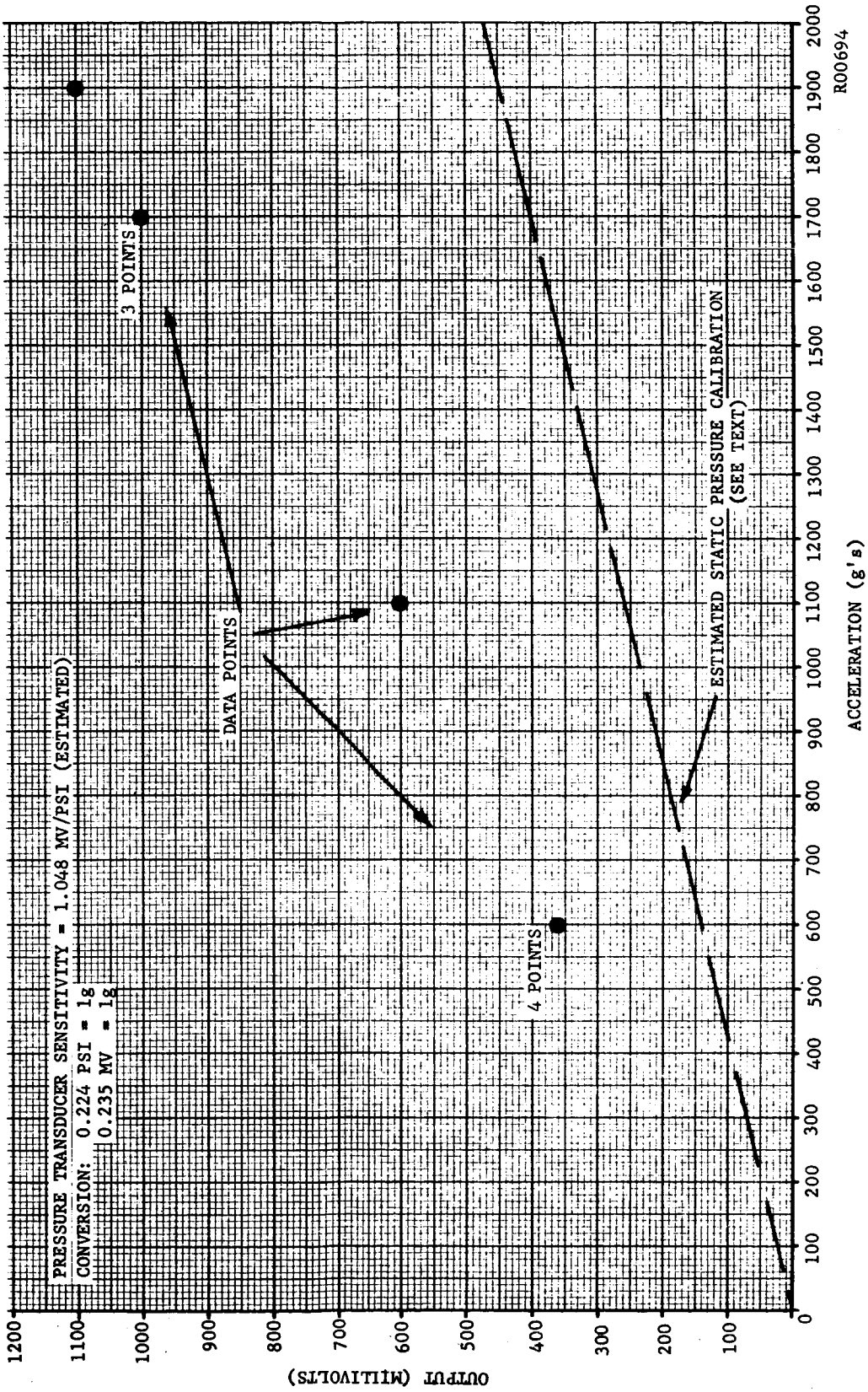

FIGURE 49. CALIBRATION DATA ON ACCELEROMETER AA12

Pressure sensitivity data for transducers AA 10 through AA 12 were not available. The sensitivities for these three transducers were estimated as the average of the other seven, or 1.048 mv/psi.

e. Frequency Response of AA 10

The vibration tests revealed a very reduced sensitivity to sinusoidal vibration at 10 g's and 40 g's. Figures 50 and 51 show the frequency response of AA 10 normalized to the accelerometer sensitivity obtained on the centrifuge at 100 g's. The theoretical rectifying property of the accelerometer upon the output voltage was clearly discernible only at select frequencies (e.g., 1850 cps). Spurious responses and waveform breakup observed during earlier tests using accelerometers with large mercury voids were greatly reduced during these tests. As 100 g's is only 5 percent of the design range of the accelerometers, better response would have been expected had test equipment permitted higher acceleration levels.

f. Sterilization of AA 12

AA 12 was baked at +260°F for twenty-four hours prior to any testing. Tests of the accelerometer on the centrifuge indicate that its sensitivity was the same as the sensitivities of the other accelerometers, about 0.23 millivolts per g.

Measurement of temperature effects and shock sensitivity indicated the presence of a rather large void in the mercury. Further, the voltage sensitivity to shock was about 2-1/2 times that which was expected, indicating "water hammer" effects associated with larger voids. It is probable that the baking speeded the amalgamation of the mercury with the gold plating and destroyed its wetting characteristics prior to the final post-bake fill operation, producing an over-size void.

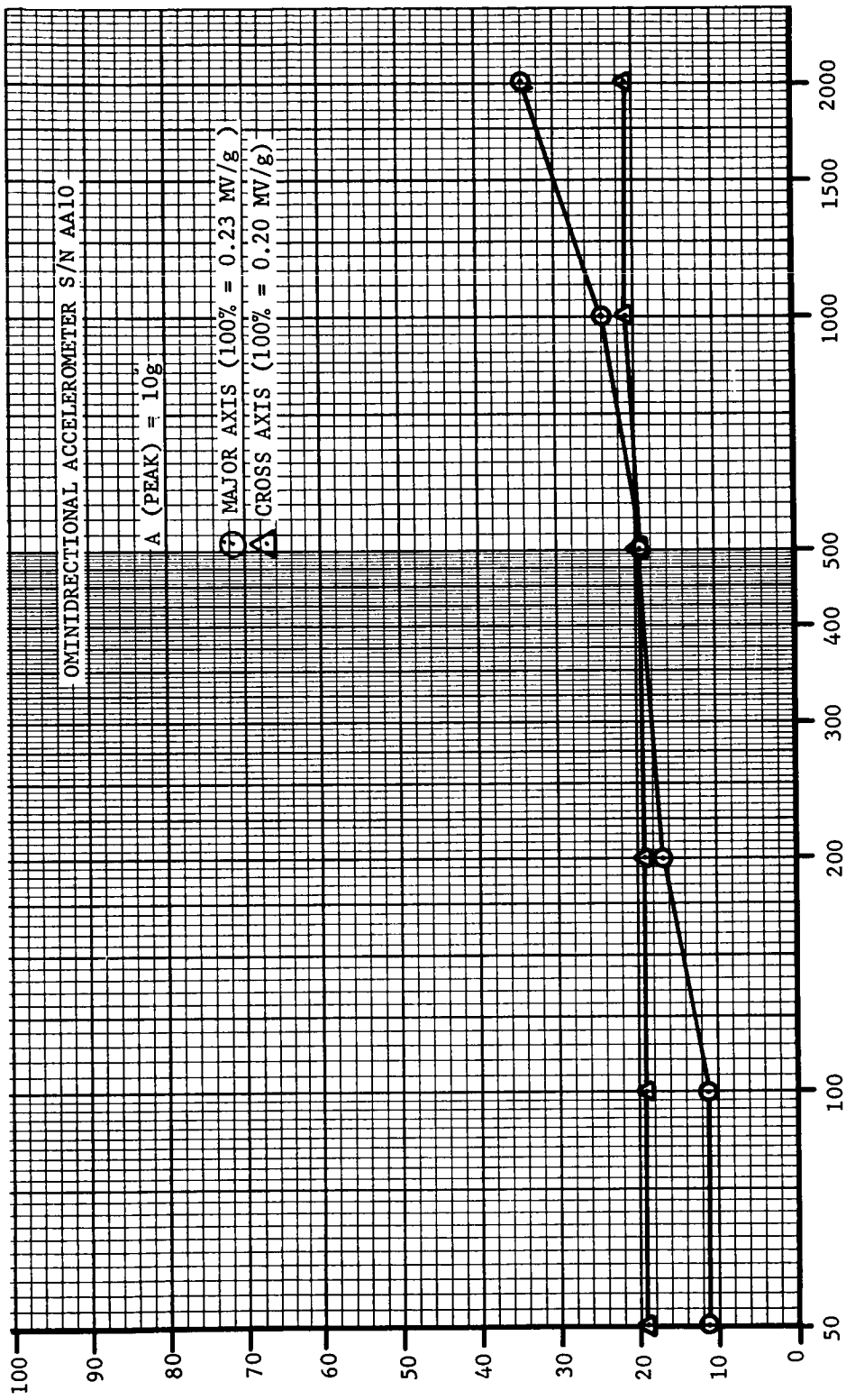

R00718

FIGURE 50. RESPONSE TO 10g SINUSOIDAL VIBRATION AS A FUNCTION OF VIBRATION FREQUENCY

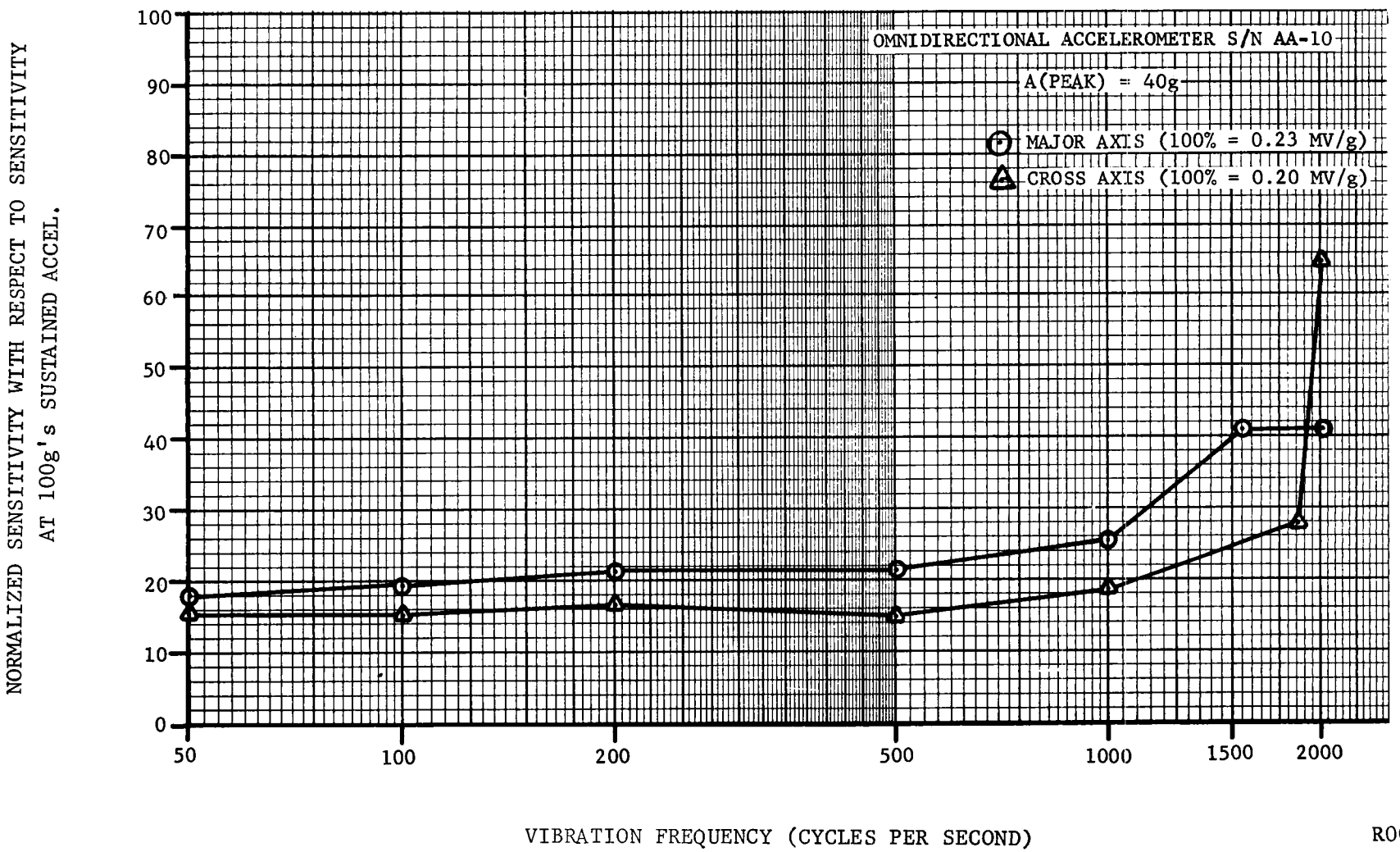

FIGURE 51. RESPONSE TO 40g SINUSOIDAL VIBRATION AS A FUNCTION OF VIBRATION FREQUENCY

SECTION 6

PERFORMANCE OF FINAL ASSEMBLIES

The performance of the delivered units, serial numbers AA-3, -4, -5, -7, -8, -9, and -11 was in general superior to the test units, particularly in output response to uni-directional acceleration impulse. However, the same sensitivity to the presence of voids exist in these as did in the test units.

The output response to the small displacement, low-g, oscillating motion imparted by the vibration machine was particularly poor except when displacement was at a very maximum and so efforts to obtain frequency response of the accelerometer on the vibration machine were discontinued. However, during uni-directional impacts at 2000 g's the response was fairly good to a .001 second half sine pulse. Normally this performance would require a system capable of at least 1000 cycle response, indicating that the accelerometer response is at least capable of 1000 cycles response to uni-directional impact acceleration inputs. The impact pulse was not steep enough to determine whether or not the accelerometer is capable of 2000 cycle response.

Accuracy of the accelerometer output was tested in two ways, one in a centrifuge and the other by peak output during impact. The calibration of the units was originally done by reading output as a function of pressure on the transducer faces and converting the pressure to g's as a function of the equivalent hydrostatic head of mercury. In comparing the data from the two types of accuracy tests, it can be seen that the centrifuge data compares favorably, with few exceptions, with the pressure calibration. The impact data on the other hand, was almost entirely off of the curve in the direction of high output for any given g level. Part of this discrepancy can be attributed to the accuracy limitation on the system used as a standard, since it is

limited to ± 8 percent of full scale reading. However, assuming it to be absolutely accurate, then the omni-accelerometer can only be said to be accurate with respect to its calibration to the nearest 10 percent of full scale, not to the nearest 10 percent of reading as specified. If on the other hand the error is in the standard, then based on the excellent repeatability exhibited by the omni-accelerometer its accuracy is well within the specified 10 percent of reading. From all this, it is advised that the accelerometer be checked against an acceptable unidirectional standard in the environment for which this unit will be used, in order to get comparable results.

Due primarily to the overshadowing effects of voids and thermal drift of the sensor, no precision trimming of the temperature compensation in the accelerometers was attempted in this program. Therefore, while considerable compensation is present, it is not complete and major shifts in sensitivity can be expected above 100°F. This compensation range can be readily extended but only after complete disassembly of each unit.

A test to determine the sterilization sensitivity of the unit encountered difficulty when, due to the lack of adequate compensation, it was necessary to heat the assembly in the unsealed condition. Gold is used to improve the wetting of internal surfaces with mercury and at the elevated sterilization temperatures the gold became amalgamated, the mercury retracted from all the crevices in the accelerometer chamber and voids formed. The performance after subsequent sealing indicated the presence of large voids. However, since no other ill effects were shown, indications are that the unit could be sterilized by either separately sterilizing the mercury and the assembly or by sterilizing it as a unit with adequate thermal compensation present.

After subjecting one of the units to a 3000 g shock a general reduction of sensitivity in the order of 25 percent was noted. Thus, while it is not destroyed by such a shock, recalibration of the accelerometer is required in its present form.

In an effort to improve response by opening up additional fluid access to the transducer from the perimeter of the mercury cavity, three of the accelerometers had holes drilled through the cap in the compensator plug. This change had no significant effect on impact response but may have further offset thermal compensation by a small amount.

Of all the units, the undelivered numbers AA 6 and AA 12 are particularly low in performance. The problem in AA 12 stems from the

presence of a large void, while AA 6 evidences unduly high fill pressure. These units could likely be much improved upon complete reassembly, including gold plating, and refilling.

In the breadboard development program, it was noted that the insertion of the Invar compensator made the accelerometer more void sensitive. Apparently this was due to the restriction by the compensator of partial access to the transducer of the mercury volume. In the single-transducer model this access is even more restricted and it seems that the unit is much more void sensitive. It is believed that a redesign of the Invar compensator to provide more direct access of the mercury to the transducer, with a corresponding decrease in spherical gap around the compensator in order to maintain the proper volume relationship, could greatly reduce void sensitivity of the accelerometer.

SECTION 7

REFERENCES

1. Aeronutronic Publication No. U-1775, "Final Report, Advanced Development of an Omni-Directional Accelerometer", dated 20 July 1962.

Intra-Company Communication

LC(b)-418
11/9/62

To: W. W. Hawley

From: D. Arnold

Title: Calculated Dynamic (Impact) Load Factors for Elastic and Plastic Covered Omni-Directional Accelerometer Sphere

Object: The primary objective of this report was to analytically study a method for limiting the impact "g" levels of the omni-directional accelerometer sphere now in the development phase at Aeronutronic. An impact velocity of 30 ft./sec. and sphere of 2 in. diameter and 1.1 pounds were used in this report.

Statement of Problem: If the bare accelerometer sphere were required to impact at 30 ft./sec. on a hard surface the "g" forces would be quite high.* If these forces exceed a certain value (approximately 6000 g's) then the internally contained pressure sensor might be damaged. One possible way of preventing this overload is to encase the sphere in a cover of elastic or plastic material chosen so that it deforms at a "g" level less than that required to damage the pressure sensor.

Results Obtained: 1. Elastic Covering

Pages 4 thru 9 give the analysis for the elastically covered sphere impacting on a flat, elastic plane. Figure 1, Page 8 illustrates the more significant results obtained. From this it is seen that if the covering is chosen so that the maximum "g" load is limited to 2800 (for this design E_1 = 36,000 psi) then this sphere would indicate only 1730 "g's" for an impact in which a rigid sphere (E_1 = ∞) would record 2000 g's. Therefore, in this instance the error is 13.3%.

*For instance, Figure 1 shows that a rigid sphere, impacting on a flat plane whose elastic modulus is 5 x 10^7 psi, would develop approximately 50,000 "g's".

177V

A further inspection of Figure 2 shows that the error (at 2000 g's impact) would be reduced considerably and the sphere covering material selection less tedious if the transducer and covering were selected for a slightly higher maximum load factor. For instance, following is a list of the per cent error at 2000 g's, maximum pressure at the transducer, and covering modulus as a function of the maximum design load factor:

Design Load Factor, Maximum	Transducer Pressure, Maximum	Per Cent Error at 2000 g's	Elastic Modulus of Cover
2000	500 psi	24.2	16,420 psi
2800	700	13.3	35,900
4000	1000	6.2	87,500
5000	1250	3.6	153,800
6000	1500	2.3	242,500

2. Plastic Covering

Pages 10 and 11 give the analysis for a plastically covered sphere impacting on a flat, rigid plane. The results obtained indicate that for various maximum design load factors the following crushing strength materials are needed:

Design Load Factor, Maximum	Crushing Strength of Cover
2000	2100 psi
2800	4000
4000	8200
5000	13,000
6000	19,000

D. Arnold

D. Arnold

cc: C. F. Husen
W. D. Longyear
W. F. Mac Innes
R. S. Kraemer
N. Quackenbush

NOMENCLATURE

SYMBOL	DESCRIPTION	USUAL UNITS
E	MODULUS OF ELASTICITY	PSI.
F	FORCE	LB.
g	GRAVITATIONAL ACCELERATION = 386.4	IN./SEC.^{2}
h_f	HEIGHT OF FREE FALL = $V_o^2/2g$	IN.
n	LOAD FACTOR = F/W	#/#
R	RADIUS OF CURVATURE OF BODY	IN.
t	TIME AFTER INITIAL CONTACT	SEC.
U	POTENTIAL OR STRAIN ENERGY	IN. LB.
V	KINETIC ENERGY OF SPHERE = $\frac{1}{2}\frac{W}{g}V_o^2$	IN. LB.
V_o	INITIAL CONTACT VELOCITY OF SPHERE AND FLAT PLANE	FT./SEC.
W	WEIGHT OF SPHERE	LB.
x	PENETRATION DEPTH OR DISTANCE TRAVELED BY SPHERE C.G. AFTER INITIAL CONTACT	IN.
μ	POISSON'S RATIO	
σ_o	CRUSHING OR FLOW STRESS OF PLASTIC SPHERE	PSI.
τ	TIME, BEGINNING AT INITIAL CONTACT, REQUIRED TO STOP THE DOWNWARD MOTION OF SPHERE	SEC.
∞	INFINITY	

IMPACT OF AN ELASTIC SPHERE ON AN ELASTIC, FLAT PLANE

THE SOLUTION TO THIS PARTICULAR PROBLEM IS GIVEN IN REF. a. RESULTS OBTAINED ARE;

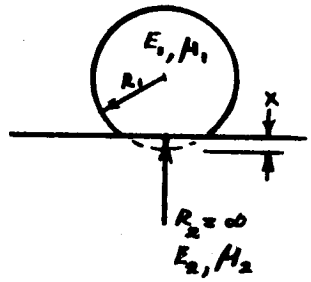

$$F = \frac{4 E_1 R_1^{1/2} x^{3/2}}{3\left[(1-\mu_1^2) + (1-\mu_2^2)\frac{E_1}{E_2}\right]}$$

$$x_{MAX.} = \left\{\frac{15\left[(1-\mu_1^2) + (1-\mu_2^2)\frac{E_1}{E_2}\right] W h_f}{8 E_1 R_1^{1/2}}\right\}^{2/5}$$

$$x \approx x_{MAX.} \sin\left(\frac{1.512\, t\sqrt{g h_f}}{x_{MAX.}}\right)$$

$$\tau \approx 1.040 \frac{x_{MAX.}}{\sqrt{g h_f}}$$

$$n_{MAX.} = \frac{5}{2}\frac{h_f}{x_{MAX.}}$$

FOR A 2 IN. DIAMETER SPHERE, WHICH WEIGHS 1.1 #, THAT IMPACTS AT 30 FT./SEC. THEN,

$$h_f = (30)^2/64.4 = 14.0 \text{ FT.} = 168 \text{ IN.}$$

$$x_{MAX.} = \left\{\frac{15\left[.91 + .91\, E_1/E_2\right](1.1)(168)}{8E_1}\right\}^{2/5}$$

$$= 10\left(\frac{1 + E_1/E_2}{E_1}\right)^{2/5}$$

$$\tau = .00408\, x_{MAX.}$$

$$n_{MAX.} = \frac{5}{2}\frac{168}{x_{MAX.}} = 420/x_{MAX.}$$

REF. a GOLDSMITH, WERNER; IMPACT, THE THEORY AND PHYSICAL BEHAVIOR OF COLLIDING SOLIDS, PP. 83 - 91

IMPACT OF AN ELASTIC SPHERE ON AN ELASTIC FLAT PLATE - CONT'D

①	②	③	④	⑤	⑥	⑦	⑧
DISPLACEMENT, $X_{MAX.}$ IN.	LOAD FACTOR, n	CONTACT TIME, τ, SEC.	ELASTIC MODULUS OF SPHERE, E_1, PSI.				
			$\frac{E_1}{E_2} = 0$	$\frac{E_1}{E_2} = .50$	$\frac{E_1}{E_2} = 1$	$\frac{E_1}{E_2} = 10$	$\frac{E_1}{E_2} = 100$
.05	3400	.000204	565,000	847,000	1,128,000	6,220,000	88,000,000
.10	4200	.000408	99,600	149,500	199,500	1,096,000	10,050,000
.15	2800	.000612	36,300	54,600	72,600	400,000	3,629,000
.20	2100	.000816	12,650	26,450	35,300	194,000	1,789,000
.25	1680	.001020	10,200	15,150	20,200	111,000	1,020,000
.30	1400	.001224	6410	9,610	12,800	70,500	640,000
.35	1200	.001430	4870	6580	8,740	48,100	442,000
.40	1050	.001632	3120	4700	6,250	34,400	315,000

COLUMN ④ OF THE ABOVE TABLE GIVES THE CASE OF IMPACT OF THE ELASTIC SPHERE ON A RIGID FLAT PLANE. IT IS SEEN THAT IF THE ELASTIC MODULUS OF THE SPHERE IS 36,300 PSI. THEN ONE COULD EXPECT THE CONTACT SURFACE TO DISPLACE BY 0.15 AT IMPACT. THE MAXIMUM "g" LOAD IN THIS INSTANCE IS 2800. ONE MIGHT NEXT ASK, "WHAT IS THE EFFECT, ON DISPLACEMENTS AND "g" LOADS, OF IMPACTING THIS PARTICULAR SPHERE (E_1 = 36,300 PSI.) ON A ELASTIC FLAT PLANE WHOSE ELASTIC MODULUS IS LESS THAN INFINITY"? THE TABLE AT THE TOP OF PAGE 6 LISTS THE RESULTS OBTAINED FOR THAT PROBLEM;

IMPACT OF AN ELASTIC SPHERE ON AN ELASTIC, FLAT PLANE - CONT'D.

RATIO OF MODULII E_1/E_2	MODULUS OF PLANE E_2	MAXIMUM PENETRATION $X_{MAX.}$	MAXIMUM LOAD FACTOR $\eta_{MAX.}$	DURATION OF CONTACT τ
0	∞	.150 IN.	2800	.000612 SEC.
.5	72,600 PSI.	.176	2380	.000718
1.0	36,300	.198	2120	.000808
5	7,260	.305	1380	.001245
10	3630	.391	1074	.001595
100	363	.945	445	.00385

ANOTHER PROBLEM OF TECHNICAL INTEREST IS THE CASE WHERE THE FLAT PLANE IS ELASTIC BUT THE IMPACTING SPHERE IS QUITE RIGID. THEN FROM PAGE 4 ONE OBTAINS,

$$X_{MAX.} = 10/(E_2)^{.45}$$

$$\tau = .00408 X_{MAX.}$$

$$= .0408/(E_2)^{.45}$$

$$\eta_{MAX.} = 420/X_{MAX.}$$

$$= 42\,(E_2)^{.45}$$

IMPACT OF AN ELASTIC SPHERE ON AN ELASTIC, FLAT PLANE - CONT'D.

MODULUS OF PLANE E_2	MAXIMUM PENETRATION $X_{MAX.}$	MAXIMUM LOAD FACTOR $n_{MAX.}$	DURATION OF CONTACT, τ
∞	0	∞	0
10^{10}	.001 in.	420,000	.00000408 sec.
10^8	.00633	66,400	.0000258
10^6	.040	10,500	.0001635
72,600	.1138	3,690	.000464
36,300	.1500	2800	.000612
7,260	.286	1470	.001165
3630	.378	1112	.001542
363	.948	443	.00387

①	$n_{MAX.}$	2000	2800	4000	5000	6000
②	$X_{MAX.} = 420/n_{MAX.}$	.210	.150	.105	.084	.070
③	$E_1 = (10/②)^{4/2}$	16,420	35,900	87,500	153,800	242,500
④	E_2	16,000	16,000	16,000	16,000	16,000
⑤	$X_{MAX.,2000} = 10\left[\frac{1+E_1/E_2}{E_1}\right]^{2/5}$	.2735	.2420	.2230	.2168	.2140
⑥	$n_{MAX.,2000} = 420/⑤$	1516	1734	1876	1928	1954
⑦	% ERROR $= \frac{2000-⑥}{2000} \times 100$	24.2	13.3	6.20	3.60	2.30

ALSO; AT $n_{MAX.} = 10{,}000$ g's., $n_{MAX.,2000} = 1984$, % ERROR = 0.8

FIGURE 1

- IMPACT OF AN ELASTIC SPHERE ON AN ELASTIC, FLAT PLANE -
CALCULATION OF MAXIMUM LOAD FACTOR INDUCED

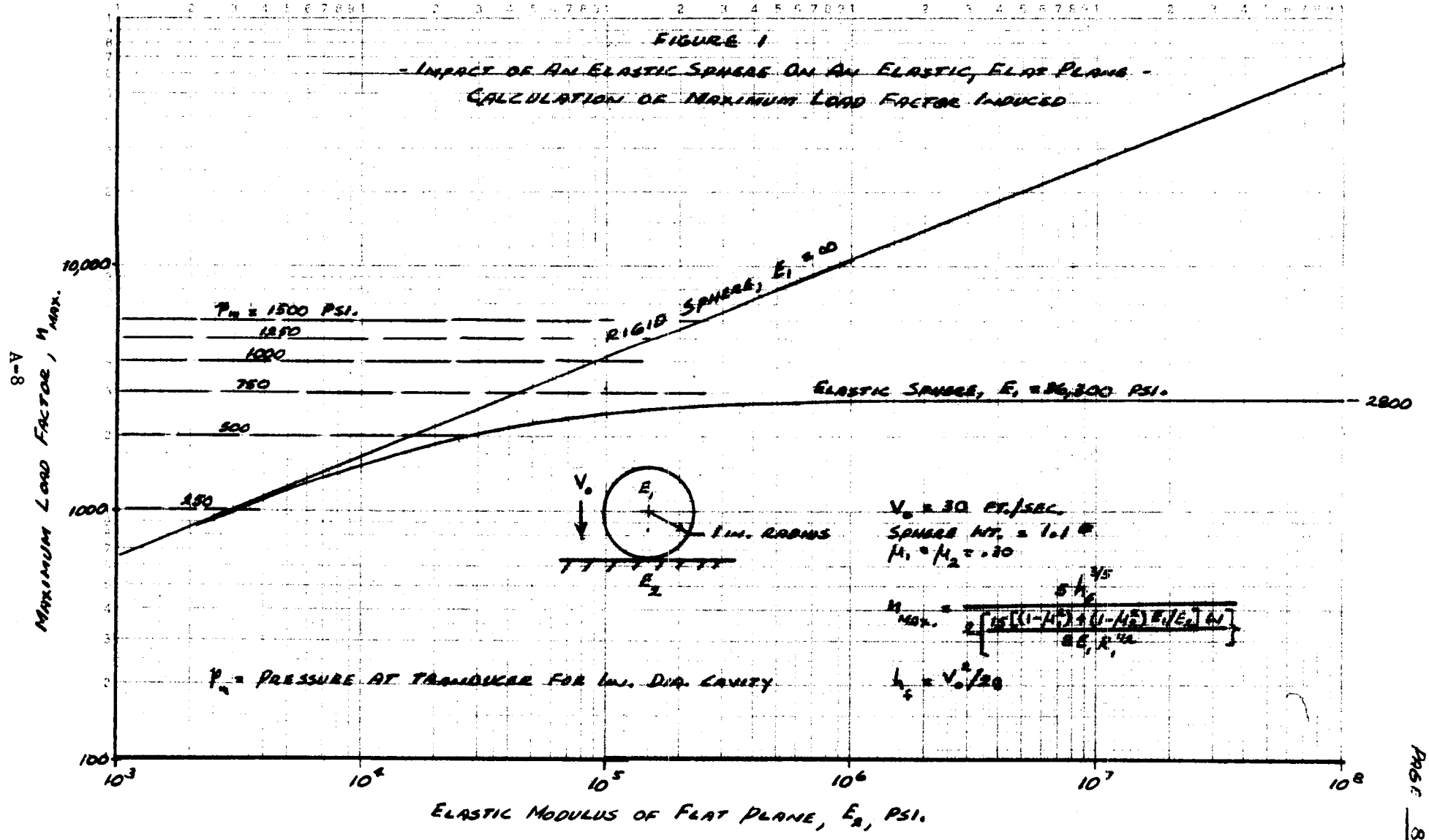

D. ARNOLD

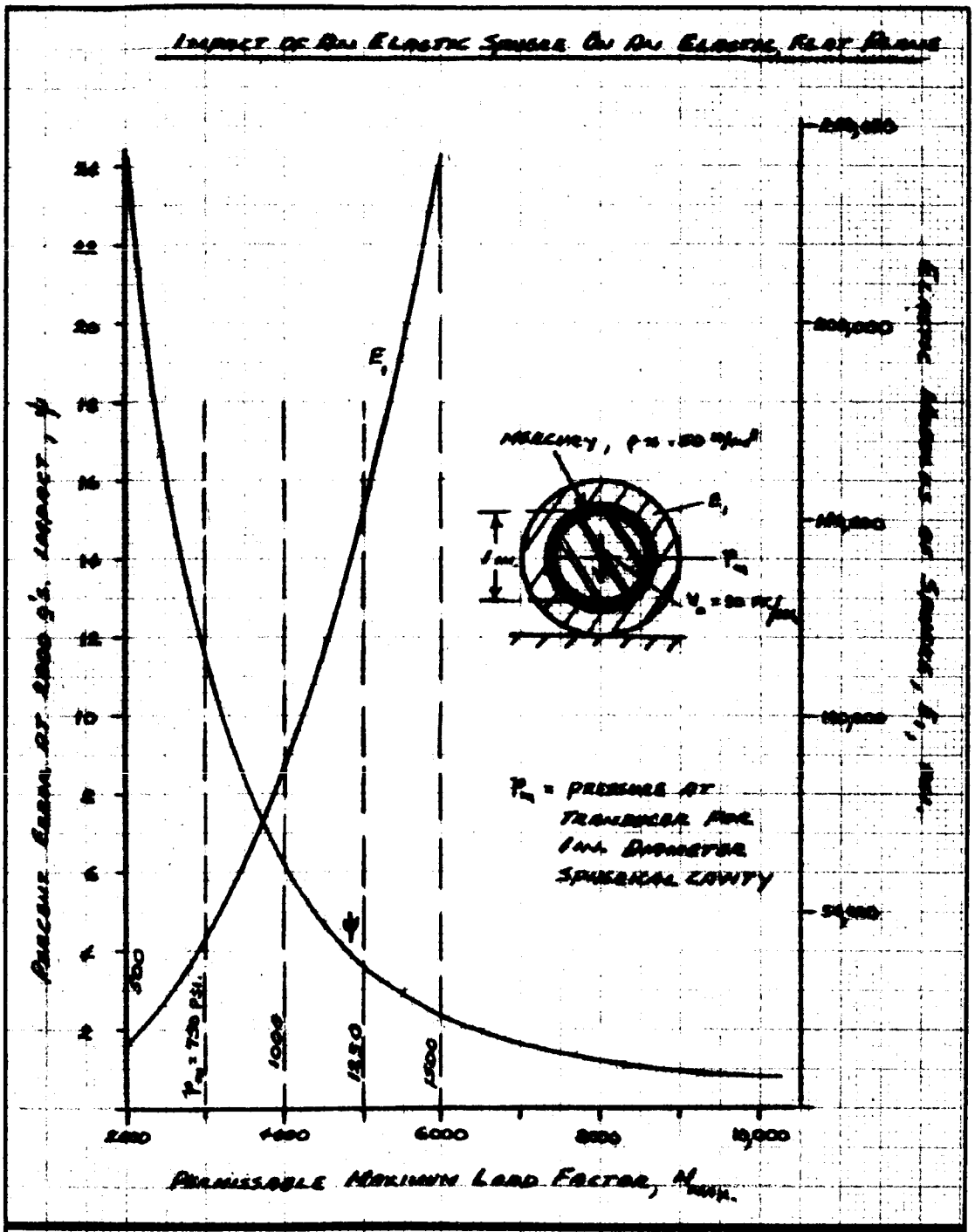

AERONUTRONIC SYSTEMS INC. — DOCUMENT ILLUSTRATION	
TITLE: Effect of Design Load Factor on Signal Error in Omni-Accelerometer	FIG. NO: 2
	REP. NO:
BY: D. Arnold	DATE:

FORM T1-26C
NOV. 56

IMPACT OF A PLASTIC SPHERE ON A RIGID, FLAT PLANE

$$F = \sigma_0 \pi (2R_1 X - X^3)$$

$$U = \int_0^X F\,dx = \sigma_0 \pi (R_1 X^2 - X^3/3)$$

$$= \sigma_0 \pi R_1 X^2 \qquad \text{FOR } X \ll 3R_1$$

$$= \frac{1}{2} F X$$

$$= \frac{1}{2} n W X$$

$$V \approx W h_f = \frac{1}{2} \frac{W}{g} V_0^2$$

SETTING $U = V$ GIVES,

$$n_{MAX.} = 2 \frac{h_f}{X_{MAX.}} = 336 / X_{MAX.}$$

$$X_{MAX.} = \sqrt{\frac{W h_f}{\pi \sigma_0 R_1}} = \frac{2.67}{\sqrt{\sigma_0}}$$

$$\tau \approx 1.10 \frac{X_{MAX.}}{\sqrt{g h_f}} = .00432\, X_{MAX.}$$

THE TABLE WHICH FOLLOWS GIVES THE MAXIMUM DISPLACEMENT, LOAD FACTOR, CRUSHING STRENGTH, AND CONTACT TIME,

MAXIMUM PENETRATION $X_{MAX.}$	MAXIMUM LOAD FACTOR $n_{MAX.}$	CRUSHING STRENGTH σ_0	DURATION OF CONTACT τ
.05 IN.	6720	23,500 PSI.	.000216 SEC.
.10	3360	5,880	.000432
.15	2240	2,620	.000648
.20	1680	1,470	.000864
.25	1344	940	.001080
.30	1120	654	.001295
.35	960	480	.001510
.40	840	368	.001728

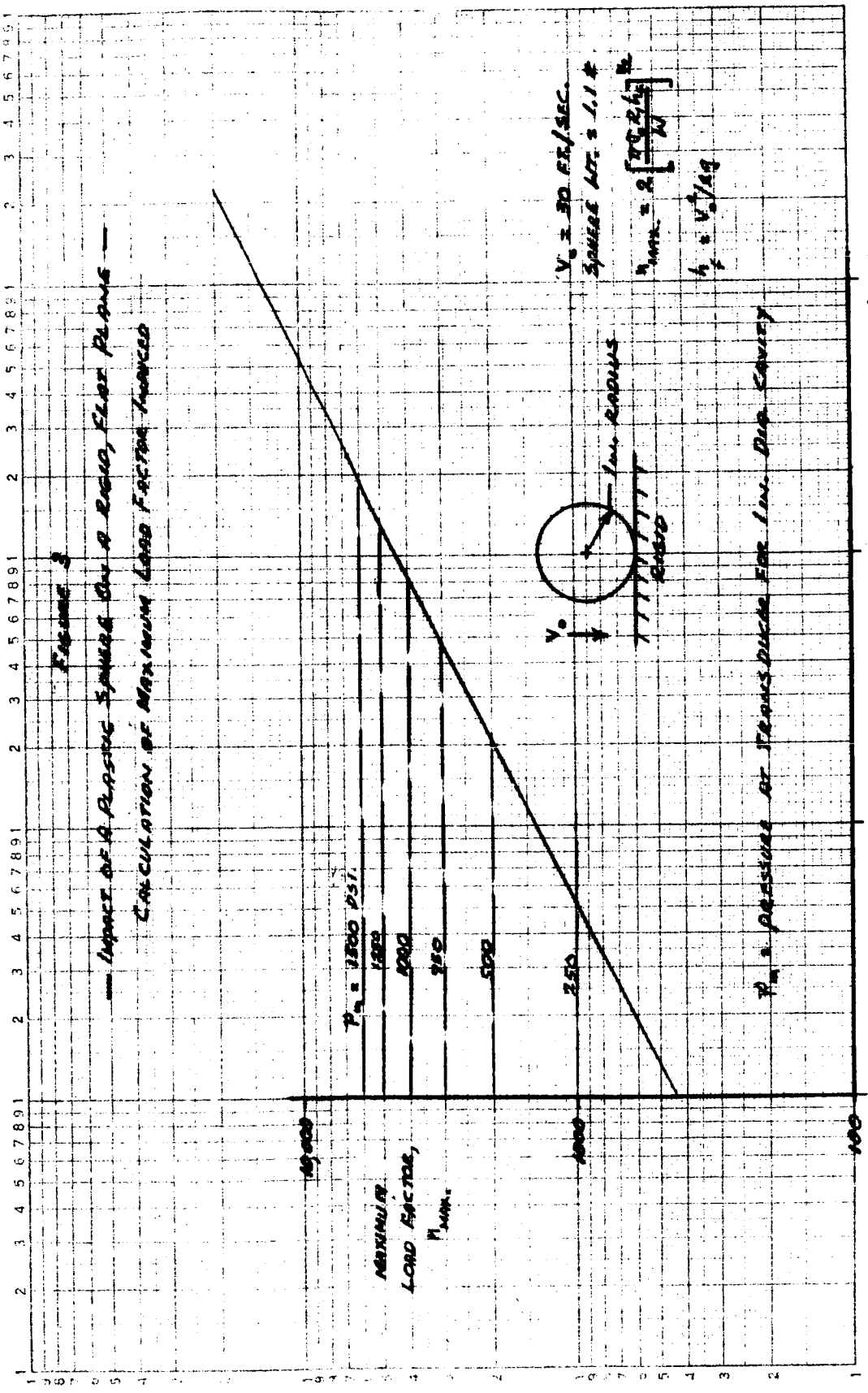
FIGURE 3
— IMPACT OF A PLASTIC SPHERE ON A RIGID, FLAT PLANE —
CALCULATION OF MAXIMUM LOAD FACTOR INDUCED
MAXIMUM LOAD FACTOR, $n_{MAX.}$
$P_{n_{MAX.}}$ = 1800 PSI.
1500
1000
750
500
250
V_o
V_o = 30 FT./SEC.
SPHERE WT. = 1.1 #
1 IN. RADIUS
RIGID
$n_{MAX.} = 2\left[\frac{\frac{1}{2}\rho V_o^2 A_p}{W}\right]$
$\frac{1}{2}\rho = V_o^2/2g$
$P_{n_{MAX.}}$ = PRESSURE AT ITS MAXIMUM FOR 1 IN. DIA. CAVITY
10,000
1000
100
100,000
10,000
1000
100
CRUSHING STRENGTH OF SPHERE, σ_o, PSI.

D. ARNOLD

Intra-Company Communication

LC(b)-420
11/15/62

To: W. W. Hawley

From: D. Arnold

Title: Derivation of Elasticity Relations Required for the Design of a Mercury Filled Omni-Directional Accelerometer which is Insensitive to Temperature Changes

Object: The primary objective of this report was to derive certain equations of elasticity to be employed in the design of the omni-accelerometer. The actual use of these relations will be presented in a later report of the design.

Statement of Problem: The design of the accelerometer dictates that mercury be used as the pressure inducing filler medium. However, due to its extremely large thermal expansion coefficient, high pressure would be induced in the system if the sphere were completely filled with mercury. *The initial design study of this problem, which showed the feasibility of using an Invar inner sphere as the thermal compensator, has been used as a guide in the present report.

Results Obtained: Equation (16), Page (5) is the final expression obtained. This relation can be used to determine the effects of cavities in the structure and temperature changes on pressures induced in the accelerometer. Furthermore, it is seen that a careful selection of materials and geometrical dimensions can be used to keep the pressure sensitivity of the instrument low.

D. Arnold
D. Arnold

cc: C. F. Husen
R. S. Kraemer
W. D. Longyear
W. F. Mac Innes

* Reference Aeronutronic Report U-1775, Appendix B

NOMENCLATURE

SYMBOL	DESCRIPTION	USUAL UNITS
a	INNER RADIUS OF SPHERE	IN.
b	OUTER RADIUS OF SPHERE	IN.
C_1, C_2	INTEGRATION CONSTANTS	
E	MODULUS OF ELASTICITY	PSI
K_2	COEFFICIENT OF COMPRESSION OF MERCURY	$IN.^3/IN.^3/PSI.$
p	PRESSURE	PSI.
r	RADIAL DISTANCE FROM CENTER OF SPHERE	IN.
T	TEMPERATURE RISE ABOVE 80 °F	°F
u	RADIAL DISPLACEMENT	IN
V	VOLUME	$IN.^3$
$\bar{V}_2$	INITIAL VOLUME OF VOID	$IN.^3$
V'	FINAL VOLUME	$IN.^3$
α	COEFF. OF THERMAL EXPANSION, LINEAR	$IN./IN./°F$
β_2	CUBICAL EXPANSION COEFFICIENT OF MERCURY	$IN.^3/IN.^3/°F$
μ	POISSON'S RATIO	
σ_r, σ_t	RADIAL AND TANGENTIAL NORMAL STRESSES	PSI.

SUBSCRIPTS 1, 2, AND 3 REFER TO OUTER SPHERE, MERCURY, AND INNER SPHERE, RESPECTIVELY

SUPERSCRIPTS p AND T REFER TO PRESSURE AND TEMPERATURE, RESPECTIVELY

THERMAL EXPANSION EQUATIONS - FORMULATION OF

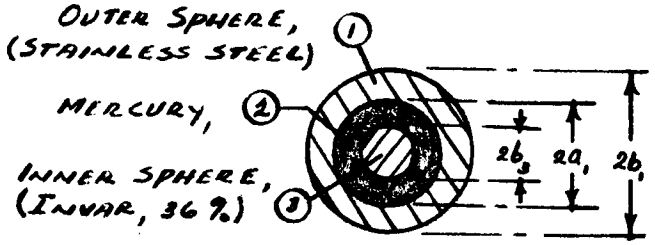

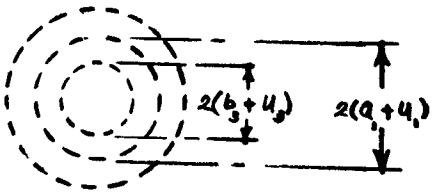

INITIAL GEOMETRY

AFTER THERMAL EXPANSION

INITIAL VOL., ALL CAVITIES; $V_2 = \frac{4}{3}\pi(a_1^3 - b_3^3) + \sum \bar{V}_2$ (1)

WHERE $\sum \bar{V}_2$ IS THE TOTAL INITIAL VOLUME OF ALL VOIDS, FILLED BY MERCURY, OTHER THAN THAT GIVEN BY THE TERM $\frac{4}{3}\pi(a_1^3 - b_3^3)$. IT SHOULD BE NOTED THAT PROTRUSIONS WHICH DISPLACE MERCURY ARE TAKEN AS NEGATIVE VOIDS.

FINAL VOL., ALL CAVITIES; $V_2' = \frac{4}{3}\pi\left[(a_1+u_1)^3 - (b_3+u_3)^3\right] + \sum(\bar{V}_2 + \Delta\bar{V}_2)$ (2)

VOL. CHANGE, ALL CAVITIES; $\Delta V_2 = V_2' - V_2 = 4\pi(a_1^2 u_1 - b_3^2 u_3) + \sum \Delta\bar{V}_2$ (3)

THE DISPLACEMENTS OF THE SPHERES, u_1 AND u_3, ARE ASSUMED TO BE DUE TO BOTH PRESSURE AND TEMPERATURE. OR IN EQUATION FORM,

$$u_1 = u_1^P + u_1^T \quad (4)$$

$$u_3 = u_3^P + u_3^T \quad (5)$$

FROM TABLE 1, PAGE 9 ONE OBTAINS,

$$u_1^p = \frac{[2(1-2\mu_1)a_1^3 + (1+\mu_1)b_1^3]a_1}{2E_1(b_1^3 - a_1^3)}\, p \qquad (6)$$

$$u_1^T = \frac{3\alpha_1 a_1}{b_1^3 - a_1^3}\int_{a_1}^{b_1} T_1 r^2\, dr \qquad (7)$$

$$u_3^p = -\frac{(1-2\mu_3)b_3}{E_3}\, p \qquad (8)$$

$$u_3^T = \frac{3\alpha_3}{b_3^3}\int_0^{b_3} T_3 r^2\, dr \qquad (9)$$

THE VOLUME CHANGE OF MERCURY, DUE TO PRESSURE AND TEMPERATURE, MAY ALSO BE EXPRESSED AS,

$$\Delta V_{Hg.} = \iiint_V \left(-K_2 p + \beta_2 T_2\right) dV_2 \qquad (10)$$

$$= -K_2 p V_2 + \beta_2 \iiint_V T_2\, dV_2 \qquad \text{FOR } K_2, p, \text{ AND } \beta_2 = \text{CONSTANT} \qquad (11)$$

IF THE VOIDS ARE INITIALLY FILLED WITH MERCURY AT ZERO PRESSURE THEN THE NET VOLUME CHANGE IS ZERO. ONE THEN OBTAINS,

$$\Delta V_2 - \Delta V_{Hg.} = 0 \qquad (12)$$

MAKING USE OF EQS. (3) THRU (5) AND EQ. 11 GIVES,

$$4\pi\left[a_1^2(u_1^p + u_1^T) - b_3^2(u_3^p + u_3^T)\right] + \sum \Delta \bar{V}_2 + K_2 p V_2 - \beta_2 \iiint T_2\, dV_2 = 0 \qquad (13)$$

* NOTE; $K_2 = \frac{1}{V}\frac{\partial V}{\partial p}$ B-4

IF USE IS MADE OF Eqs. (6) THRU (9), Eq. (13) REDUCES TO,

$$p = \frac{-\frac{3\alpha_1 a_1^3}{b_1^3 - a_1^3}\int_{a_1}^{b_1} T_1 r^2\,dr + \frac{\beta_2}{4\pi}\iiint_{V_2} T_2\,dV_2 + 3\alpha_3\int_0^{b_3} T_3 r^2\,dr - \frac{1}{4\pi}\sum \Delta\bar{V}_2}{\frac{[2(1-2\mu_1)a_1^3 + (1+\mu_1)b_1^3]a_1^3}{2E_1(b_1^3 - a_1^3)} + \frac{K_2 V_2}{4\pi} + \frac{(1-2\mu_3)b_3^3}{E_3}} \qquad (14)$$

FOR THE SPECIFIC CASE OF A CONSTANT TEMPERATURE RISE ΔT_0 EQUATION (14) REDUCES TO,

$$p = \frac{\left[-\alpha_1 a_1^3 + \frac{\beta_2}{4\pi} V_2 + \alpha_3 b_3^3\right]\Delta T_0 - \frac{1}{4\pi}\sum \Delta\bar{V}_2}{\frac{[2(1-2\mu_1)a_1^3 + (1+\mu_1)b_1^3]a_1^3}{2E_1(b_1^3 - a_1^3)} + \frac{K_2 V_2}{4\pi} + \frac{(1-2\mu_3)b_3^3}{E_3}} \qquad (15)$$

BUT, PER Eq. (11); $V_2 = \frac{4}{3}\pi(a_1^3 - b_3^3) + \sum \bar{V}_2$

THEN Eq. (15) REDUCES TO,

$$p = \frac{\left\{-\alpha_1 a_1^3 + \beta_2\left[\frac{1}{3}(a_1^3 - b_3^3) + \frac{1}{4\pi}\sum \bar{V}_2\right] + \alpha_3 b_3^3\right\}\Delta T_0 - \frac{1}{4\pi}\sum \Delta\bar{V}_2}{\frac{[2(1-2\mu_1)a_1^3 + (1+\mu_1)b_1^3]a_1^3}{2E_1(b_1^3 - a_1^3)} + K_2\left[\frac{1}{3}(a_1^3 - b_3^3) + \frac{1}{4\pi}\sum \bar{V}_2\right] + \frac{(1-2\mu_3)b_3^3}{E_3}} \qquad (16)$$

Eq. 16 WILL BE USED IN A LATER REPORT FOR THE ANALYSIS OF THE OMNI-ACCELEROMETER.

ELASTICITY EQUATIONS FOR SPHERES SUBJECTED TO MECHANICAL (PRESSURE) AND THERMAL FORCES

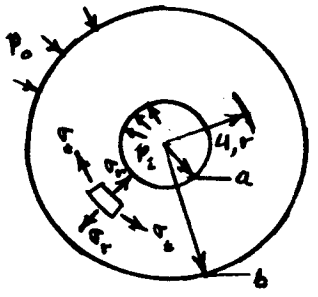

* THE ELASTICITY RELATIONS WHICH GOVERN THE RADIAL STRESS σ_r, TANGENTIAL STRESS σ_t, AND RADIAL DISPLACEMENT u OF A SPHERE WITH THE TEMPERATURE AND MATERIAL PROPERTIES SYMMETRICAL WITH RESPECT TO THE CENTER ARE,

$$\sigma_r = -\frac{2E\alpha}{1-\mu}\frac{1}{r^3}\int_a^r Tr^2\,dr + \frac{E}{1-2\mu}C_1 - \frac{2E}{(1+\mu)r^3}C_2 \qquad (17)$$

$$\sigma_t = \frac{E\alpha}{1-\mu}\frac{1}{r^3}\int_a^r Tr^2\,dr + \frac{E}{1-2\mu}C_1 + \frac{E}{(1+\mu)r^3}C_2 - \frac{E\alpha T}{1-\mu} \qquad (18)$$

$$u = \frac{1+\mu}{1-\mu}\frac{\alpha}{r^2}\int_a^r Tr^2\,dr + C_1 r + \frac{C_2}{r^2} \qquad (19)$$

WHERE C_1 AND C_2 ARE INTEGRATION CONSTANTS AND a IS ANY CONVENIENT LOWER LIMIT FOR THE INTEGRAL, SUCH AS THE INNER RADIUS OF A HOLLOW SPHERE,

---

* REF. TIMOSHENKO AND GOODIER, THEORY OF ELASTICITY, MC GRAW HILL BOOK CO., PP. 416-419

SOLID SPHERE

FOR THIS CASE THE LOWER LIMIT a OF THE INTEGRALS IS TAKEN AS ZERO. SINCE $u = 0$ AT $r = 0$, FROM Eq. (19) THIS REQUIRES THAT $C_2 = 0$. AT $r = b$, $\sigma_r = -p_o$, THEREFORE FROM Eq. (17)

$$C_1 = -\frac{1-2\mu}{E} p_o + \frac{2(1-2\mu)\alpha}{(1-\mu) b^3} \int_0^b T r^2 \, dr \qquad (20)$$

EQUATIONS (17) THRU (19) BECOME,

$$\sigma_r = \frac{2E\alpha}{1-\mu}\left(\frac{1}{b^3}\int_0^b T r^2 \, dr - \frac{1}{r^3}\int_0^r T r^2 \, dr\right) - p_o \qquad (21)$$

$$\sigma_t = \frac{E\alpha}{1-\mu}\left(\frac{2}{b^3}\int_0^b T r^2 \, dr + \frac{1}{r^3}\int_0^r T r^2 \, dr - T\right) - p_o \qquad (22)$$

$$u = \frac{\alpha r}{1-\mu}\left[\frac{2(1-2\mu)}{b^3}\int_0^b T r^2 \, dr + \frac{1+\mu}{r^3}\int_0^r T r^2 \, dr\right] - \frac{(1-2\mu) r}{E} p_o \qquad (23)$$

HOLLOW SPHERE

IN THIS PROBLEM THE TWO BOUNDARY CONDITIONS ARE TAKEN AS;

$r = a$	$r = b$
$\sigma_r = -p_i$	$\sigma_r = -p_o$

THEREFORE, FROM Eq. (17) ONE OBTAINS,

$$\frac{E}{1-2\mu} C_1 - \frac{2E}{(1+\mu) a^3} C_2 = -p_i \qquad (24)$$

$$\frac{E}{1-2\mu} C_1 - \frac{2E}{(1+\mu) b^3} C_2 = -p_o + \frac{2E\alpha}{1-\mu} \frac{1}{b^3} \int_a^b T r^2 \, dr \qquad (25)$$

HOLLOW SPHERE - CONT'D.

IF EQUATIONS (24) AND (25) ARE SOLVED SIMULTANEOUSLY THE FOLLOWING RELATIONS FOR C_1 AND C_2 ARE OBTAINED,

$$C_1 = \frac{2(1-2\mu)}{1-\mu}\frac{\alpha}{b^3-a^3}\int_a^b Tr^2\,dr + \left(\frac{1-2\mu}{E}\right)\left(\frac{-b^3p_o + a^3p_i}{b^3-a^3}\right) \tag{26}$$

$$C_2 = \left(\frac{1+\mu}{1-\mu}\right)\left(\frac{a^3}{b^3-a^3}\right)\alpha\int_a^b Tr^2\,dr - \left(\frac{1+\mu}{2E}\right)\frac{a^3b^3}{b^3-a^3}(p_o - p_i) \tag{27}$$

EQUATIONS (17) THRU (19), FOR THE STRESSES AND RADIAL DISPLACEMENT, THEN BECOME;

$$\sigma_r = \frac{2E\alpha}{1-\mu}\left[\frac{(r^3-a^3)}{r^3(b^3-a^3)}\int_a^b Tr^2\,dr - \frac{1}{r^3}\int_a^r Tr^2\,dr\right] + \frac{(-r^3+a^3)b^3p_o + (r^3-b^3)a^3p_i}{r^3(b^3-a^3)} \tag{28}$$

$$\sigma_t = \frac{E\alpha}{1-\mu}\left[\frac{(2r^3+a^3)}{r^3(b^3-a^3)}\int_a^b Tr^2\,dr + \frac{1}{r^3}\int_a^r Tr^2\,dr - T\right] \tag{29}$$

$$\frac{-(2r^3+a^3)b^3p_o + (2r^3+b^3)a^3p_i}{2r^3(b^3-a^3)}$$

$$u = \frac{r\alpha}{1-\mu}\left\{\frac{[2(1-2\mu)r^3 + (1+\mu)a^3]}{r^3(b^3-a^3)}\int_a^b Tr^2\,dr + \frac{1+\mu}{r^3}\int_a^r Tr^2\,dr\right\} \tag{30}$$

$$+ \frac{-[2(1-2\mu)r^3 + (1+\mu)a^3]b^3p_o + [2(1-2\mu)r^3 + (1+\mu)b^3]a^3p_i}{2Er^2(b^3-a^3)}$$

AERONUTRONIC DIVISION
Ford Motor Company,
LC(b)-420

OPERATION:
DEPARTMENT:
DATE: 11-15-62
ANALYSIS: STRESS
PAGE: 9
BY: D. ARNOLD
MODEL:
CHECKED:
REPT. NO:

TABLE I ; FORMULAE FOR THE EXTENSIONAL ANALYSIS OF ELASTIC SPHERES

	Loading	Radial Stress, σ_r — General	Radial Stress, σ_r — At Inner Radius $r=a$	Radial Stress, σ_r — At Outer Radius $r=b$	Tangential Stress, σ_θ — General	Tangential Stress, σ_θ — At Inner Radius $r=a$	Tangential Stress, σ_θ — At Outer Radius $r=b$
Solid Sphere	External Pressure, p_o	$-p_o$	$-p_o$	$-p_o$	$-p_o$	$-p_o$	$-p_o$
	Temperature, $T=T(r)$	$\frac{2E\alpha}{1-\mu}\left(\frac{1}{b^3}\int_0^b Tr^2dr - \frac{1}{r^3}\int_0^r Tr^2dr\right)$	$\frac{2E\alpha}{1-\mu}\left(\frac{1}{b^3}\int_0^b Tr^2dr - \frac{T_a}{3}\right)$	0	$\frac{E\alpha}{1-\mu}\left(\frac{2}{b^3}\int_0^b Tr^2dr + \frac{1}{r^3}\int_0^r Tr^2dr - T\right)$	$\frac{2E\alpha}{1-\mu}\left(\frac{1}{b^3}\int_0^b Tr^2dr - \frac{T_a}{3}\right)$	$\frac{E\alpha}{1-\mu}\left(\frac{2}{b^3}\int_0^b Tr^2dr - T_b\right)$
Hollow Sphere	Internal Pressure, p_i	$\frac{(r^3-b^3)a^3}{r^3(b^3-a^3)}p_i$	$-p_i$	0	$\frac{(2r^3+b^3)a^3}{2r^3(b^3-a^3)}p_i$	$\frac{2a^3+b^3}{2(b^3-a^3)}p_i$	$\frac{3a^3}{2(b^3-a^3)}p_i$
	External Pressure, p_o	$\frac{(-r^3+a^3)b^3}{r^3(b^3-a^3)}p_o$	0	$-p_o$	$-\frac{(2r^3+a^3)b^3}{2r^3(b^3-a^3)}p_o$	$-\frac{3b^3}{2(b^3-a^3)}p_o$	$-\frac{(2b^3+a^3)}{2(b^3-a^3)}p_o$
	Temperature, $T=T(r)$	$\frac{2E\alpha}{1-\mu}\left[\frac{(r^3-a^3)}{r^3(b^3-a^3)}\int_a^b Tr^2dr - \frac{1}{r^3}\int_a^r Tr^2dr\right]$	0	0	$\frac{E\alpha}{1-\mu}\left[\frac{2r^3+a^3}{r^3(b^3-a^3)}\int_a^b Tr^2dr + \frac{1}{r^3}\int_a^r Tr^2dr - T\right]$	$\frac{E\alpha}{1-\mu}\left[\frac{3}{b^3-a^3}\int_a^b Tr^2dr - T_a\right]$	$\frac{E\alpha}{1-\mu}\left[\frac{3}{b^3-a^3}\int_a^b Tr^2dr - T_b\right]$

	Loading	Radial Displacement, u — General	Radial Displacement, u — At Inner Radius, $r=a$	Radial Displacement, u — At Outer Radius, $r=b$
Solid Sphere	External Pressure, p_o	$-\frac{(1-2\mu)}{E}rp_o$	0	$-\frac{(1-2\mu)}{E}bp_o$
	Temperature, $T=T(r)$	$\frac{\alpha r}{1-\mu}\left[\frac{2(1-2\mu)}{b^3}\int_0^b Tr^2dr + \frac{1+\mu}{r^3}\int_0^r Tr^2dr\right]$	0	$\frac{3\alpha}{b^2}\int_0^b Tr^2dr$
Hollow Sphere	Internal Pressure, p_i	$\frac{[2(1-2\mu)r^3+(1+\mu)b^3]a^3}{2Er^2(b^3-a^3)}p_i$	$\frac{[2(1-2\mu)a^3+(1+\mu)b^3]a}{2E(b^3-a^3)}p_i$	$\frac{3(1-\mu)a^3b}{2E(b^3-a^3)}p_i$
	External Pressure, p_o	$-\frac{[2(1-2\mu)r^3+(1+\mu)a^3]b^3}{2Er^2(b^3-a^3)}p_o$	$-\frac{3(1-\mu)a^3b^3}{2E(b^3-a^3)}p_o$	$-\frac{[2(1-2\mu)b^3+(1+\mu)a^3]b}{2E(b^3-a^3)}p_o$
	Temperature, $T=T(r)$	$\frac{\alpha r}{1-\mu}\left\{\frac{[2(1-2\mu)r^3+(1+\mu)a^3]}{r^3(b^3-a^3)}\int_a^b Tr^2dr + \frac{1+\mu}{r^3}\int_a^r Tr^2dr\right\}$	$\frac{3\alpha a}{b^3-a^3}\int_a^b Tr^2dr$	$\frac{3\alpha b}{b^3-a^3}\int_a^b Tr^2dr$

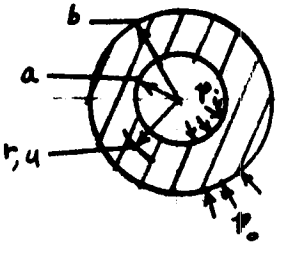

Intra-Company Communication

LC(b)-421
11/21/62

To: W. W. Hawley

From: C. F. Husen

Subject: Invar Thermal Compensator to be Used in Omni-Directional Accelerometer

Reference: LC(b)-420, Derivation of Elasticity Relations Required for the Design of a Mercury Filled Omni-Directional Accelerometer which is Insensitive to Temperature Changes, D. Arnold, 11/15/62

Summary

In order to compensate for the differential rates of expansion between the mercury fluid and the case of the accelerometer an Invar mass is to be rigidly suspended in the chamber of the accelerometer. For proper compensation the expansion in volume of the mercury and Invar sphere should exactly equal the expansion of the outer case. The required diameter of the Invar sphere has been determined and is equal to 0.9248 inches.

Discussion

Elasticity relations required for the design of a thermally compensated omni-directional accelerometer have been derived and were presented in memorandum LC(b)-420. Using these relationships the thermal expansion equations were obtained. For the specific case of a constant temperature rise an equation for pressure as a function of temperature was presented as Eq. 16 in the above reference from which is obtained the following expression:

For a unit Δ T the pressure rise is

$$P = \frac{-\alpha_1 a_1^3 + \beta_2\left[\frac{1}{3}(a_1^3 - b_3^3) + \frac{1}{4\pi}(V_v - V_s - V_c)\right] + \alpha_3\left[b_3^3 + \frac{1}{4\pi}(V_s - V_v)\right] + \alpha_1\left(\frac{1}{4\pi}V_c\right)}{\frac{\left[2(1-2\mu_1)a_1^3 + (1+\mu_1)b_1^3\right]a_1^3}{2E_1(b_1^3 - a_1^3)} + k_2\left[\frac{1}{3}(a_1^3 - b_3^3) + \frac{1}{4\pi}(V_v - V_s - V_c)\right] + \frac{(1-2\mu_3)}{E_3}\left[b_3^3 + \frac{1}{4\pi}(V_s - V_v)\right] + \frac{(1-2\mu_1)}{E_1 4\pi}V_c}$$

177V

where for the stainless steel case

a_1 = inner radius of case = 0.5 inches

b_1 = outer " " " = 0.9 inches

μ_1 = Poisson's ratio = 0.25

α_1 = Linear coefficient of thermal expansion = 9.3×10^{-6} in/in/°F

E_1 = Modulus of elasticity = 29×10^6 psi

and for the mercury

β_2 = Cubical expansion coefficient of mercury = 101×10^{-6} $in^3/in^3/°F$

K_2 = Coefficient of compression of mercury = 0.259×10^{-6} $in^3/in^3/psi$

and for the Invar sphere

α_3 = Linear coefficient of thermal expansion = 0.7×10^{-6}

μ_3 = Poisson's ratio = 0.29

E_3 = Modulus of elasticity = 21×10^6 psi

b_3 = Radius of invar sphere

also

V_v = Volume of voids in the Invar sphere filled with mercury

V_s = Volume of supporting stem on Invar sphere

V_c = Volume of three stainless steel columns supporting Invar sphere

Substitution of the above values yields

$$P = \left[\frac{3.045833 - 32.966667\, b_3^3 + 7.981620(V_v - V_s) - 7.297253\, V_c}{1.448918 - 6.633333\, b_3^3 + 1.901901(V_v - V_s) - 1.923854\, V_c} \right] \times 10^2 \quad PSI/°F$$

This equation may then be solved for b_3 where P = 0 for perfect thermal compensation. However, since the various volumes are involved functions of b_3, a solution was obtained by selecting values of b_3 and solving for the pressure. The required radius of the Invar sphere for perfect thermal compensation was computed to be 0.4624 inches. The variation of pressure in psi/^{o}F with sphere radius is presented in Figure 1.

Using the slope of the curve given in Fig. 1 near P = 0, an estimate can be made of the maximum permissible error in differential volume between case, mercury, and Invar compensator in order to meet the specifications. The slope of the curve near P = 0 is $\frac{C}{+}$ = 2347.072 psi/^{o}/in.$_{+}$ The maximum error in accuracy permitted at 5g is $\pm$ 2.5g + 10% of 5g or $\pm$ 3g's. This corresponds to a maximum allowable ΔP of approximately 0.75 psi. For a $\Delta T = 105^{o}$ the change in radius of the Invar compensator may be computed.

$$\Delta r = \left(\frac{\Delta P}{\Delta T}\right)/C = \left(\frac{.75}{105}\right)/2347.072 = 3.04\times10^{-6} \text{ IN.}$$

The volume change due to the change in radius is approximately equal to that of a shell of radius r and thickness Δr minus cutouts due to slots and holes in the Invar sphere. The radius r is the radius of an Invar sphere for a perfectly thermally compensated accelerometer.

The volume was computed as

$$V = 7.405\times10^{-6} \text{ IN}^3$$

This is equivalent to a solid sphere of diameter d where

$$d^3 = \frac{6V}{\pi} = \frac{6\times7.405\times10^{-6}}{\pi} = 14.1\times10^{-6}$$

and d = .0242 inches.

Provision has been made for fine adjustments in volume of mercury by changing the length of an 0-80 set screw in the Invar compensator. To compensate for the volume above a change in length of about 0.003 inches would be required.

C. F. Husen

CFH:pod

cc: D. Arnold
R. S. Kraemer
W. D. Longyear
W. F. Mac Innes

C.F.H. 11/15/62

FIGURE 1

RADIUS OF INVAR SPHERE

REQUIRED FOR PERFECT TEMPERATURE

COMPENSATION

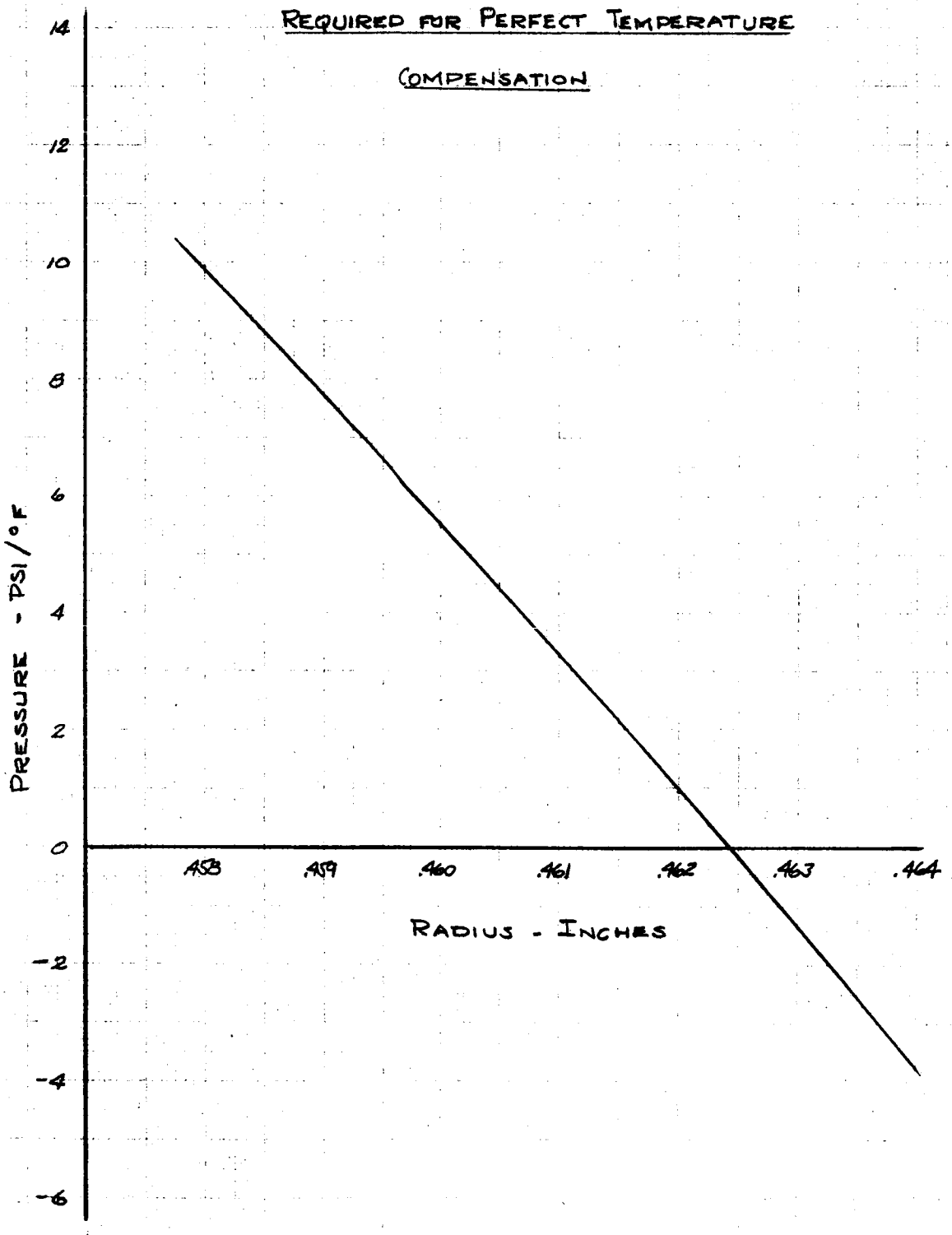

Intra-Company Communication

LC(b)-422
19 December 1962

TO: W. W. Hawley

cc: R. S. Kraemer
W. F. Mac Innes
G. J. Thomas

FROM: G. F. Husen

SUBJECT: Analysis of Volume Changes Due to Deflections and Error in Acceleration Measurement Due To Volume and Pressure Changes Caused by Deflections and Thermal Expansions

SUMMARY

An analysis of the approximate maximum error due to volume and pressure changes caused by deflections and thermal expansions has been completed. The approximate volume change due to deflection of the pressure transducer, elongation of the screws joining the hemispherical case shells, and case distortion was determined as 89.57×10^{-6} in.^{3} for a 2000 g impact. The error in acceleration measurement due to translation of the center of gravity caused by volumetric changes resulting from deflections and thermal expansions was estimated to be negligible for a 5 g impact and was approximately 0.17% for a 2000 g impact. The error due to pressure changes caused by deflections and thermal expansion was estimated to be 1.97% at 2000 g's. These error computations were based on a maximum allowable error in acceleration of 60% for a 5 g impact as required by the accelerometer specifications. As a result of the analysis the pressure change due to temperature must be less than 6.94×10^{-3} psi/$^\circ$F for proper temperature compensation for a temperature change of 105°F.

DISCUSSION

An analysis of the approximate maximum error in acceleration measurement due to volume and pressure changes has been performed. The volume changes were assumed to be a result of deflection of the pressure transducer and elongation of the screws joining the two hemispherical case shells due to internal pressure caused by an impact, and from case distortion due to an external load. The approximate volume change due to these deflections was computed as 89.57×10^{-6} in.^{3} for a 2000 g impact and 0.224×10^{-6} in.^{3} for a 5 g impact. In these calculations it was assumed that the effect on the deflections from pressure due to change in volume was of second order.

If it is assumed that the change in volume will create a void in the volume of mercury then an estimate of the error in measured acceleration due to the volume changes may be made as indicated in Aeronutronic Report No. U-1775, Appendix D. Assuming that, for the worst case, the void travels one diameter of the cavity then the translation of the center of gravity is approximately 1.33×10^{-6} inches due to the deflections considered. The translation of the cg due to thermal expansions may be considered in the same manner and the translation is 0.1415×10^{-4} inches. Comparison of the cg travel with the displacement corresponding to a

177

30 ft/sec velocity shock for a 2000 g impact yields an approximate error of 0.17% in acceleration measurement. For a 5 g impact the error from the effect of volume change on cg location is negligible.

The error due to pressure changes caused by the above deflections and by thermal expansion was also estimated. In memo LC(b)-421 it was shown that the maximum allowable change in pressure was 0.75 psi in order to meet the accuracy specified at an impact of 5 g's. Assuming the accelerometer has been thermally compensated for a maximum $\Delta P = 0.75$ psi for a temperature change of 105°F then the error in acceleration measured at 2000 g's is about 0.15% and is about 60% at 5 g's. An approximation of the change in pressure due to volume change for the deflection considered above was made. For a temperature change of 105°F the error in acceleration at 2000 g's and at 5 g's is about 1.8%.

If it is assumed that all errors are additive for an estimate of maximum error then the error in measured acceleration is about 2.1% at 2000 g's and 61.8% at 5 g's. Therefore, the largest error in acceleration measurement from deflection and thermal expansion may be expected at the low end of the range and may be due primarily to pressure change if the accelerometer is not properly compensated for thermal expansion. In addition it should be noted that the maximum allowable error permitted by the design specifications is 60% at 5 g's. Therefore, the maximum change in pressure from thermal expansion assumed above should be reduced from 0.75 psi to about 0.728 psi for a 105°F temperature change in order to reduce the computed total error from 61.8% to the allowable maximum of 60%. For proper temperature compensation, then, the pressure change due to temperature must be less than 6.94×10^{-3} psi/°F for a possible 105°F temperature change.

The analysis is presented as an Appendix in pages 3 to 11.

/cyl

Attachment

Volume Change Due to Deflection

I. Uniformly loaded circular diaphragm deflection

For a uniformly loaded circular plate with fixed edges

$$\delta = \frac{3W(1-\mu^2)r^2}{16\pi E t^3} \quad \text{and} \quad S = \frac{3W(1+\mu)}{8\pi t^2}$$

where δ = deflection of plate at center
W = load
μ = Poisson's ratio
E = modulus of elasticity
t = thickness of plate
r = radius of plate
S = stress in plate at center

From the equation for stress $t^2 = \frac{3W(1+\mu)}{8\pi S}$

and $t = \left[\frac{3W(1+\mu)}{8\pi S}\right]^{\frac{1}{2}}$

Since $S = E\epsilon$ where ϵ is the strain

then $t = \left[\frac{3W(1+\mu)}{8\pi E\epsilon}\right]^{\frac{1}{2}}$

substituting in equation for deflection

$$\delta = \frac{3W(1-\mu^2)r^2}{16\pi E\left[\frac{3W(1+\mu)}{8\pi E\epsilon}\right]^{\frac{3}{2}}} = \frac{3W(1-\mu^2)r^2}{\left[\frac{13.5W^3(1+\mu)^3}{\pi E\epsilon^3}\right]^{\frac{1}{2}}} = \left[\frac{9r^4\pi E\epsilon^3(1+\mu)^2}{13.5(1+\mu)W}\right]^{\frac{1}{2}}$$

PREPARED BY	DATE	PREPARING ACTIVITY	Ford Motor Company, AERONUTRONIC DIVISION
C.F. HAUEN			
CHECKED BY	DATE	TITLE OR SUBJECT	PROJECT OR MODEL: Aerothermodynamic Accelerometer
APPROVED BY	DATE	APPENDIX	SHEET 3 of 11 — DOCUMENT OR REPORT NO.

now the load $W = P\pi r^2$ where P is the pressure on the diaphragm

then $\delta = \left[\frac{9r^2 E\epsilon^3 (1-\mu)^2}{13.5(1+\mu)P}\right]^{\frac{1}{2}} = .816\, r(1-\mu)\sqrt{\frac{E\epsilon^3}{(1+\mu)P}}$

for $\mu = .3$ $(1+\mu) = 1.3$ $(1-\mu) = .7$

$\delta = .5015\, r\sqrt{\frac{E\epsilon^3}{P}}$

the diaphragm surface strain was estimated by the manufacturer to be on the order of 10^{-6} in/in/psi

then for $\epsilon = 10^{-6}P$ in/in/psi $r = .125$ in. $E = 29\times10^6$ psi

$\delta = .5015 \times .125\sqrt{\frac{29\times10^6 \times 10^{-18} P^3}{P}} = .06044 \times 5.38\times10^{-6} P$

$\delta = .325\times10^{-6} P$ in.

Assuming the diaphragm deflects as a sine curve

$\Delta V = .297\pi r^2 h = .297\pi(.125)^2(.325\times10^{-6}P)$

$\Delta V = 4.74\times10^{-9} P$ cu in.

at 2000 g impact $P = 500$ psi

and $\Delta V = 4.74\times10^{-9}\times500 = 2.37\times10^{-6}$ cu in

PREPARED BY C.F. Hisen	DATE	PREPARING ACTIVITY	Ford Motor Company AERONUTRONIC DIVISION
CHECKED BY	DATE	TITLE OR SUBJECT	PROJECT OR MODEL Accelerometer
APPROVED BY	DATE	APPENDIX	SHEET 4 of 11 / DOCUMENT OR REPORT NO.

II ΔV due to elongation of screws joining hemispherical shells

The highest force due to impact forcing the shells apart is for an impact parallel to the axes of the joint.

For the condition of 2000 g's

$$F = \pi r^2 g = \pi \times 1.5 \times (.5)^2 \times 2000 = 393 \text{ lbs}$$

then the average deflection is

$$\delta_{av} = \frac{FL}{AE} = \frac{393 \times .25 \times 4}{6 \times \pi (.188)^2 \times 29 \times 10^6} = 46.3 \times 10^{-6} \text{ in}$$

assuming the change in volume may be approximated by a cylinder

$$\Delta V = \pi r^2 h = \pi (.5)^2 \times 46.3 \times 10^{-6} = 35.6 \times 10^{-6} \text{ cu. in.}$$

III ΔV due to case distortion

In Appendix C of Aeronutronic Pub. No. U-1775 the effect of case distortion due to an external load was approximated by loading an accelerometer in a compressive testing machine. It was concluded that the case volume variation with load was a linear function and was

$$\Delta V = 1.58 \times 10^{-8} \text{ cu. in./lb.}$$

then assuming the external force = wg where w is the weight of the accelerometer

$$F = 1 \times 2000 = 2000 \text{ lbs for an impact of 2000 g's}$$

and $\Delta V = 1.58 \times 10^{-8} \times 2000 = 31.6 \times 10^{-6}$ cu. in.

PREPARED BY	DATE	PREPARING ACTIVITY	Ford Motor Company, AERONUTRONIC DIVISION
C.F. HUSEN			
CHECKED BY	DATE	TITLE OR SUBJECT	PROJECT OR MODEL
		APPENDIX	Accelerometer
APPROVED BY	DATE		SHEET 5 OF 11 — DOCUMENT OR REPORT NO.

Effect Due To Volume Changes Caused By Deflections and Thermal Expansion

I. Examination of Case Due to Deflections

Before we discuss the changes in volume due to deflection of the case, screws, and pressure diaphragm are equivalent to errors in the total volume of mercury. Assuming that, for the worst case, these errors travel one diameter of the cavity in the accelerometer, it was shown in Memorandum No. [illegible] Appendix D that the translation of the mass center of the mercury was approximately

$$X = 1.91\,V$$

where X is the translation of the mass center in inches and V is the void volume

Then for the various void volumes the translation of the mercury due to ... [illegible]

a) Void due to diaphragm deflection

$$V = 2.37 \times 10^{-6}\ in^3$$

and

$$X = 1.91 \times 2.37 \times 10^{-6} = 4.535 \times 10^{-6}\ in$$

b) Void due to deflection of screws joining hemispherical shells:

$$V = 31.6 \times 10^{-6}\ cu\ in$$

$$X = 1.91 \times 31.6 \times 10^{-6} = 60.0 \times 10^{-6}\ in$$

c) Void due to case distortion

$$V = 31.6 \times 10^{-6}\ cu\ in$$

$$X = 1.91 \times 31.6 \times 10^{-6} = 60.3 \times 10^{-6}\ in$$

PREPARED BY	DATE	PREPARING ACTIVITY	Ford Motor Company, AERONUTRONIC DIVISION
C.F. Hiisen			
CHECKED BY	DATE	TITLE OR SUBJECT	PROJECT OR MODEL
			Omnidirectional Accelerometer
APPROVED BY	DATE	Appendix	SHEET 6 of 11 — DOCUMENT OR REPORT NO.

[illegible] of the cg due [illegible]

[illegible]

$= 1.3283 \times 10^{-4}$ in.

II. [illegible] THERMAL EXPANSIONS

[illegible] due to thermal expansion [illegible] when [illegible] are shown in [illegible]. L(b) [illegible] permissible error in [illegible] for [illegible] of 305 °F was approximately

$$V = 7.405 \times 10^{-6} \text{ in}^3$$

and the [illegible] of the CG is

$$x = 1.91 \times 7.405 \times 10^{-6} = .1415 \times 10^{-4} \text{ in}$$

III. [illegible] TRAVEL

(a) for a [illegible] g impact

for a velocity shock where $\Delta V = 30$ ft/sec and $g = 2000$

$$x = \frac{V^2}{2g} = \frac{(30 \times 12)^2}{2 \times 386 \times 2000} = 840 \times 10^{-4} \text{ in}$$

the error caused by the various deflections is then approximately

$$\frac{1.3283 \times 10^{-4}}{840 \times 10^{-4}} = .00157 = .157\% \text{ for } 2000g \text{ impact}$$

and error due to thermal expansion is approximately

$$\frac{.1415 \times 10^{-4}}{840 \times 10^{-4}} = .0001685 = .01685\% \text{ for } 2000g \text{ impact}$$

The total error at 2000 g's due to CG movement is 0.1759 %

PREPARED BY	DATE	PREPARING ACTIVITY	Ford Motor Company AERONUTRONIC DIVISION
C.F. Hansen			
CHECKED BY	DATE	TITLE OR SUBJECT	PROJECT OR MODEL: Omnidirectional Accelerometer
APPROVED BY	DATE	APPENDIX	SHEET: 8 of 11 / DOCUMENT OR REPORT NO.

[illegible] 5g impact

For a velocity shock above $\Delta V = 30$ ft/sec and $g = 5$.

$$h = \frac{(30)^2}{2 \times 32 \times 5} = .336 \text{ in.}$$

The error due to deflections at 5g is approximately

[illegible] = $.9875 \times 10^{-8}$ or $.9875 \times 10^{-6}$ % which is negligible

The error due to thermal expansion is approximately

[illegible] = $.421 \times 10^{-6}$ or $.421 \times 10^{-4}$ %

Therefore, the error due to effect of deflections and thermal expansion under the 5g impact are negligible.

Error Due to Pressure Sensor

Error due to Deflections and Thermal Expansions

I Thermal Expansions

It was shown in Memo LC(6)-421 that the maximum permissible change in pressure without 0.75 PSI in order to meet the specified accuracy requirement at an impact of 5g's. The error from $\Delta P = 0.75$ psi is

for a 2000 g impact $P = 500$ psi and error = $\frac{.75}{500} = .15\%$

for a 5g impact $P = 1.25$ psi and error = $\frac{.75}{1.25} = 60\%$

PREPARED BY	DATE	PREPARING ACTIVITY
C.F. Hansen		
CHECKED BY	DATE	TITLE OR SUBJECT
		Appendix
APPROVED BY	DATE	

Ford Motor Company
AERONUTRONIC DIVISION

PROJECT OR MODEL: Omnidirectional Accelerometer

SHEET: 8 of 11

DOCUMENT OR REPORT NO.:

V. [illegible]

The [illegible] volume change due to deflection of ~~[illegible]~~ during the case shock is:

$$V_{def.} = (51.6 + 2.37 + 35.6) \times 10^{-6}$$
$$= 89.57 \times 10^{-6} \text{ cu in} \quad \text{for a 2000 g impact}$$

and [illegible] $= .224 \times 10^{-6}$ cu in for a 5 g impact

If it is assumed that the volume change is due to a change in radius of the [illegible] compensator [illegible] cutout [illegible] and holes then

$$\Delta V \cong 4\pi R^2 \Delta R - \frac{\pi R \alpha h \Delta R}{180} - \pi r^2 \Delta R$$

$$\Delta V \cong 4\pi(\text{[illegible]})^2 \Delta R - \frac{3 \times \pi \times .434 \times 95 \times .07 \Delta R}{180} - \frac{3\pi(.2)^2}{4} \Delta R$$

$$\Delta V \cong (\text{[illegible]} \times 3 - .0342 \times 3)\Delta R = 2.4346 \Delta R$$

then $\Delta R \cong \frac{\Delta V}{2.4346} = \frac{89.57 \times 10^{-6}}{2.4346} = 36.8 \times 10^{-6}$ in. for a 2000 g impact

$$\Delta R \cong \frac{.224 \times 10^{-6}}{2.4346} = 9.2 \times 10^{-8} \text{ in. for a 5 g impact}$$

In Memo. LC(b)-421 a curve of Pressure in PSI/°F vs. Radius of the sphere was presented. The slope of the curve near 0 PSI/°F is
$C = 2347.07$ PSI/°/in.

For a temperature change of 105 °F the change in pressure is:

$$\Delta P = C \cdot \Delta R \cdot \Delta T = 2347.07 \times 36.8 \times 10^{-6} \times 105 = 9.075 \text{ PSI for a 2000 g impact}$$

$$\Delta P = 2347.07 \times 9.2 \times 10^{-8} \times 105 = .0227 \text{ PSI for a 5 g impact}$$

Ford Motor Company, AERONUTRONIC DIVISION

PREPARED BY	DATE	PREPARING ACTIVITY
C. F. Husen		
CHECKED BY	**DATE**	**TITLE OR SUBJECT**
APPROVED BY	**DATE**	
		Appendix

PROJECT OR MODEL: Omnidirectional Accelerometer

SHEET	DOCUMENT OR REPORT NO.
9 , 11	

III Combined Thermal and Deflection Pressure Error

The combined error in pressure reading due to thermal expansion or contraction and from deflections is then:

for a 2000 g input

$\Delta P = .075 + 9.075 = 9.825$ psi

and error $= \frac{9.825}{500} = .0965$ or 1.965 %

for a 5 g input

$\Delta P = .075 + .0227 = .7727$ psi

error $= \frac{.7727}{1.25} = .618$ or 61.8 %

For Combined Errors For Volumetric (CE Travel) and Pressure Changes

It is assumed that all errors are additive for an estimate of maximum error then:

for a 2000 g input

$Error_{TOT} = (.0965 + .174)\% = 2.139\%$

for a 5 g input

$Error_{TOT} = (61.8 + NEG.) = 61.8\%$

PREPARED BY	DATE	PREPARING ACTIVITY	Ford Motor Company, AERONUTRONIC DIVISION
C.F. Hulsen			
CHECKED BY	DATE	TITLE OR SUBJECT	PROJECT OR MODEL
			Accelerometer
APPROVED BY	DATE	APPENDIX	SHEET 10 of 11 / DOCUMENT OR REPORT NO.

Therefore the greatest error may be expected at the lowest of the required acceleration measurement ranges and may primarily be due to pressure changes if the accelerometer is not properly compensated for thermal expansion. In addition, it should be noted that a maximum error of 60% at 5 g's is permitted by the design specification, and therefore, the maximum change in pressure from thermal expansion assumed in Sec Par above should be reduced to approximately

$$\Delta P = \frac{42}{668} \times 0.75 = 0.128 \text{ PSI for } 105°F \text{ temperature change}$$

or $\Delta P = 6.94 \times 10^{-3}$ PSI/°

For proper temperature compensation the pressure change due to temperature must be less than the amount shown above.

PREPARED BY	DATE	PREPARING ACTIVITY	Ford Motor Company AERONUTRONIC DIVISION
C.F. HUSEN			
CHECKED BY	DATE	TITLE OR SUBJECT	PROJECT OR MODEL
		APPENDIX	Accelerometer
APPROVED BY	DATE		SHEET 11 OF 11 / DOCUMENT OR REPORT NO.

Intra-Company Communication

LC(b)-423
27 December 1962

To: W. W. Hawley
From: C. F. Husen
cc: W. F. Mac Innes
R. S. Kraemer
G. J. Thomas

Subject: Determination of Torque to be Applied when Tightening Nut on Invar Compensator Stem

Summary

In order to prevent movement of the invar compensator from its supports under shock loading a preload in tension in the attachment stem of the compensator is required. For an impact of 3000 g's the preload required was found to be 237 pounds. The torque required must overcome friction in the threads on the stem and between the bottom surface of the nut and outer accelerometer shell in addition to providing the desired tensile load. For clean dry surfaces the coefficient of friction appears to vary between 0.4 and 0.57 while for a lubricated surface the variation in coefficient is from 0.07 to 0.15. The amount of torque to be applied to the nut during assembly was computed to be 43 inch pounds for the dry friction case and 12 inch pounds for the lubricated, or greasy friction, case. Because of the wide variation in coefficient of friction possible it would be desirable to obtain an experimental value for the friction coefficient. This will permit a more accurate determination of the proper amount of torque to be applied to the unit during assembly of the invar compensator and outer case of the accelerometer.

Discussion

Since any movement of the invar compensator and pressure transducer assembly will cause an error in measured acceleration due to a change in pressure head it is necessary to prevent movement of the compensator from its supports. An impact parallel to the axis of the spherical compensator and the compensator attachment stem, on the side of the accelerometer to which the compensator is attached, will produce the highest forces tending to lift the compensator from its supports. This force is due to

1777

buoyancy of the invar compensator in mercury. For an impact of 3000 g's the force is approximately 237 pounds in tension on the attachment stem. To prevent displacement of the compensator a tensile preload in the stem equal to or greater than 237 pounds is required.

The torque required to turn a screw against a load and friction in the threads may be obtained from

$$T = \frac{WD_m}{2} \left[\frac{\cos \phi \tan \lambda + f}{\cos \phi - f \tan \lambda} \right] \quad \text{inch pounds} \qquad (1)$$

where W = load

D_m = Mean diameter of screw thread

ϕ = ½ thread angle

λ = Lead angle

f = coefficient of friction

The stem corresponds to a 10-32 screw with a central hole 0.063 inches in diameter. Substituting the parameters for a 10-32 screw into Equation (1) yields

$$T = 0.08485 \; W \left[\frac{0.0508 + f}{0.866 - 0.0586 f} \right] \quad \text{inch pounds} \qquad (2)$$

The torque required to overcome friction between the nut and the outer shell of the accelerometer, with the assumption of uniform pressure, may be obtained approximately from:

$$T = \frac{2}{3} f W \frac{(r_o^3 - r_i^3)}{(r_o^2 - r_i^2)} \text{ inch pounds} \qquad (3)$$

where r_o is the outer radius of the nut and r_i is the inner radius.

For the nut used on the compensator stem

$$T = 0.1996 \; fW \quad \text{inch pounds} \qquad (4)$$

The total torque required for a load W may be obtained from the sum of Equations (2) and (4). The torque required to produce the minimum tensile preload of 237 pounds is given in Figure 1 for a range of values of friction coefficient.

The maximum torque that may be applied will depend on the ultimate tensile stress of the stem material. The tensile load that will produce a given stress may be determined from

$$S = \frac{S_t}{2} + \left[S_t^2 + \frac{S_s^2}{4} \right]^{\frac{1}{2}} \qquad (5)$$

where S is the total combined stress in tension,

S_t is the tensile stress due to a load W or

$$S_t = \frac{W}{a} = 69.5\ W \text{ psi} \qquad (6)$$

and S_s is the shear stress due to torsion caused by friction in the screw threads

$$\text{or } S_s = \frac{16\ T\ D_o}{\pi (D_o^4 - D_i^4)} = 1578T$$

on substitution of Equation (2) for T

$$S_s = 134\ W \left[\frac{0.0508 + f}{0.866 - 0.0586\ f} \right] \qquad (7)$$

Substituion of Equations (6) and (7) into Equation (5) yields

$$S = \left\{ 34.75 + \left[4830 + \left(\frac{0.0508 + f}{0.866 - 0.0586\ f} \right)^2 \right]^{\frac{1}{2}} \right\} W \qquad (8)$$

For a given value of tensile stress, S, Equation (8) may be solved for the load, W, which will produce the stress level. The total torque required for the computed load W is obtained from the sum of Equations (2) and (4). The torque required for an ultimate tensile stress of 70,000 psi has been

determined for a range of friction coefficients and is given in Figure 1. The torque required for a yield stress of 40,000 psi is also given in Figure 1.

The coefficient of friction will depend on surface condition and whether the stem and nut have been lubricated or are dry and clean. For clean dry surfaces several sources give values of friction coefficient, f, which range from about 0.4 to 0.56. The torque to be applied to the nut during assembly of the compensator and outer case for this range of f can be obtained from Figure 1. A value of 43 inch pounds will produce a tensile load greater than the required 237 pounds and a tensile stress less than yield for the extremes of the dry friction coefficient range.

If the threads and nut are lubricated before assembly, coefficients of friction ranging from 0.07 to 0.15 appear to be common. For this range, a torque of 12 inch pounds will provide a slightly higher tensile load than the required 237 pounds at the upper end of the range but will exceed the yield stress for the lower end of the range. This will result in a somewhat lowered margin of safety for friction coefficients at the low end of the range.

It can be seen that a single value of torque cannot be obtained that will be satisfactory for the full range of possible friction coefficients. Therefore, an experimental determination of the approximate coefficient of friction before assembly is desirable. This would permit a closer approximation of the required torque with a corresponding improvement in margin between the value of torque selected and the torques corresponding to the minimum and maximum boundary conditions of required tensile preload and maximum tensile stress.

C. F. Husen

CFH:pod

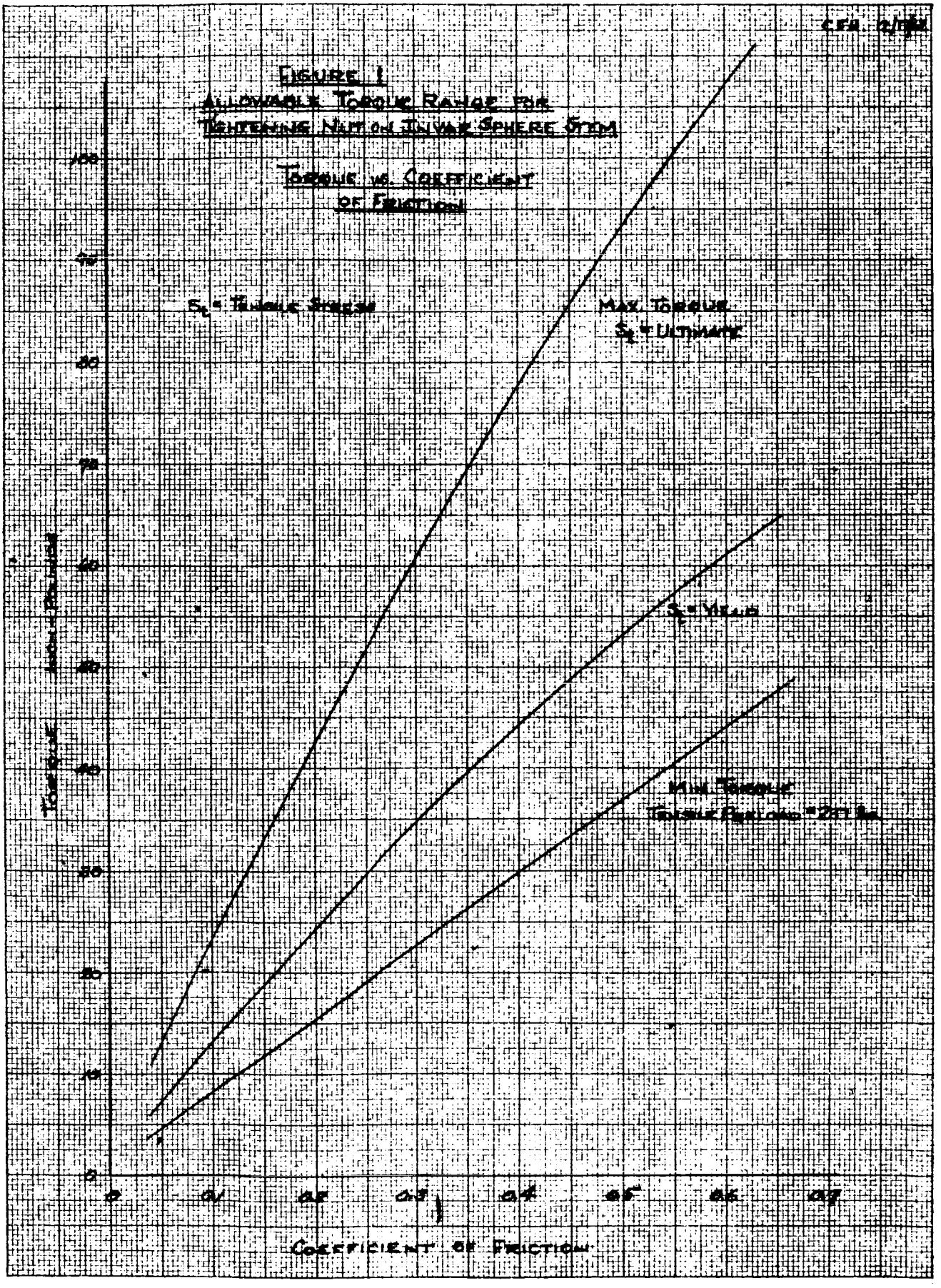

Intra-Company Communication

LFC-ME-015
1/11/63

To: W. W. Hawley

From: C. F. Husen

Subject: Impact Tests of Plastics Considered for Use as an Accelerometer Coating

Reference: (1) Memo #LFC-ME-011 by I. F. Sobczak

(2) Memo #LC(b)-418 by D. Arnold

(3) Intra-Company Communication to W. W. Hawley from N. E. Quackenbush, Subject: Impact Limiter for Omnidirectional Accelerometer dated 11/26/62

Summary:

Impact tests of a simulated accelerometer against 1/8 inch thick sheets of nine plastic materials were conducted. The purpose of the tests was to determine the properties of the materials under shock loading for possible use as an impact limiter for the omnidirectional accelerometer. The acceleration-time history and the rebound height were obtained for four drop heights for each plastic sample.

Polypropylene appeared to exhibit the desired qualities. The acceleration on impact was limited to about 4600 g. The modulus of elasticity for this material, computed from the impact data, is about 125,000 psi. High density polyethylene could also be used if the modulus of elasticity was increased to between 75,000 psi and 100,000 psi. The sample tested limited accelerations to 2300 g which is too low for the desired operating range of the accelerometer. The modulus of elasticity for the sample tested, based on the impact data, was about 32,000 psi.

Methods of forming the covering and bonding it to the case of the accelerometer are under investigation.

Discussion:

In Reference 3 above it was pointed out that the compressive properties of plastics may be expected to be a function of the loading rate, and in addition, information on dynamic loading on plastics is limited. For these reasons impact tests of a simulated accelerometer against 1/8 inch thick sheets of plastic were performed.

177v

Nine different plastic samples were tested in order to cover a range of values of modulus of elasticity. A mass was dropped from four different heights onto each sample and the acceleration was measured.

The test apparatus consisted of a drop weight guided by two parallel strands of music wire. The impact surface of the weight was a hemisphere of the same radius as the outer surface of the omni-directional accelerometer. In addition the weight had approximately the same mass as the accelerometer. An Endevco accelerometer mounted to the top of the weight was used to measure the acceleration. Acceleration-time histories of each impact were obtained by use of an oscilloscope and a Polaroid-Land camera. The horizontal sweep circuit of the oscilloscope was set to trigger when the voltage output of the Endevco accelerometer exceeded approximately 25 mv. The rebound height was determined visually with the aid of a meter stick.

The velocity determined by integration of the area under the acceleration-time curve agreed to within 5% of the velocity change obtained from the drop and rebound heights. In addition excellent repeatability was obtained. Therefore, it is felt that the oscilloscope data are good reproductions of the acceleration-time histories of the impacts.

The acceleration as a function of drop height for each plastic sample is presented in Figure 1. In order to protect the pressure transducer in the omnidirectional accelerometer from an overpressure that would rupture the diaphragm the acceleration must be limited to less than 5000 g. From Figure 1 it can be seen that the polypropylene sample tested appears to meet this requirement with a limit of about 4600 g. High density polyethylene also showed very good limiting characteristics. The sample of polyethylene tested limited at 2300 g. However, it is desirable to be able to measure 3000 g with the omnidirectional accelerometer, and therefore, the coating should not limit the acceleration to a value less than 3000 g's.

If a polyethylene plastic with a modulus of elasticity between 75,000 psi and 100,000 psi could be obtained this material would also be suitable as a coating.

It was found that most of the acceleration-time curves could be represented by a triangular pulse shape. Assuming a triangular wave form and with the aid of Equation 22 from Reference 1 the expressions for maximum deflection, stress, and modulus of elasticity were derived. The modulus of elasticity for polypropylene computed from the test data is presented in Figure 2. The average of the values of modulus corresponding to the lowest three drop heights is approximately 125,000 psi. The slightly lower value for the modulus of elasticity corresponding to the highest drop height is due to yielding of the material and operation in the

non-linear range of the stress-strain curve. A value of 32,000 psi was obtained for the modulus for the high density polyethylene sample. A trapezoidal shock pulse in place of a triangular shape was used as a better approximation of the acceleration time history for computation of the maximum deflection and modulus of elasticity of the polyethylene sample. For the two plastics selected as suitable coating material, good agreement was obtained between test data for modulus of elasticity corresponding to a maximum acceleration load factor and theoretical results presented in Figure 2, Page 9 of Reference 2.

Several items are still under consideration. These are the method of forming the material and the method of bonding the formed plastic to the case of the accelerometer. While both materials are moldable the heat required for molding is close to or above the maximum the accelerometer can withstand without damage. A special mold to form the plastic may be necessary.

The test data and the analysis have been included as an appendix.

C. F. Husen

CFH:pod

Attachment

cc: R. S. Kraemer
W. F. Mac Innes
I. F. Sobczak
G. J. Thomas
N. Quackenbush

FIGURE 1

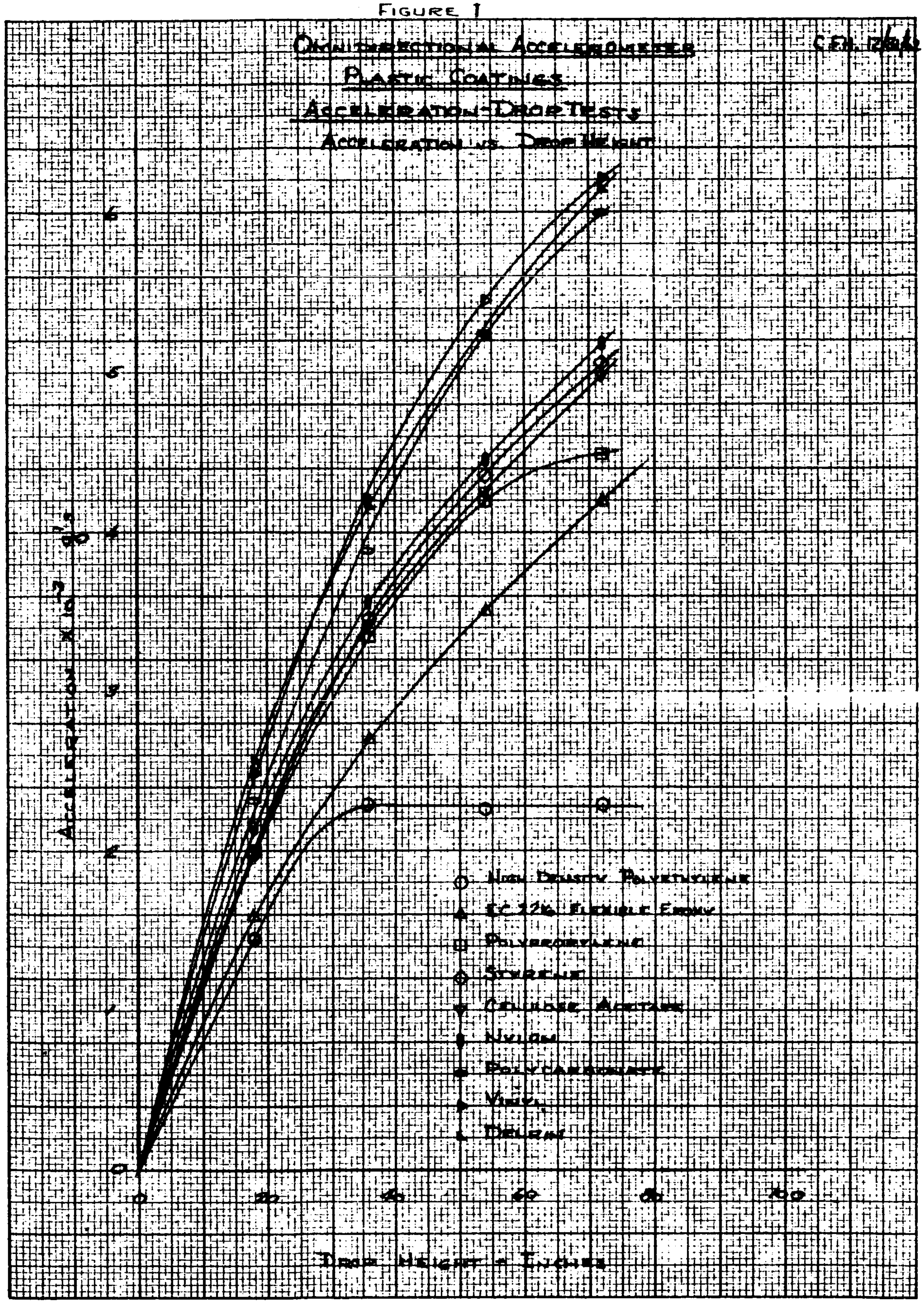
OMNIDIRECTIONAL ACCELEROMETER
PLASTIC COATINGS
ACCELERATION-DROP TESTS
ACCELERATION VS DROP HEIGHT
ACCELERATION X 10^3 g's
DROP HEIGHT - INCHES
0
20
40
60
80
100
HIGH DENSITY POLYETHYLENE
EC 1216 FLEXIBLE EPOXY
POLYPROPYLENE
STYRENE
CELLULOSE ACETATE
NYLON
POLYCARBONATE
VINYL
DELRIN

4

FIGURE 2

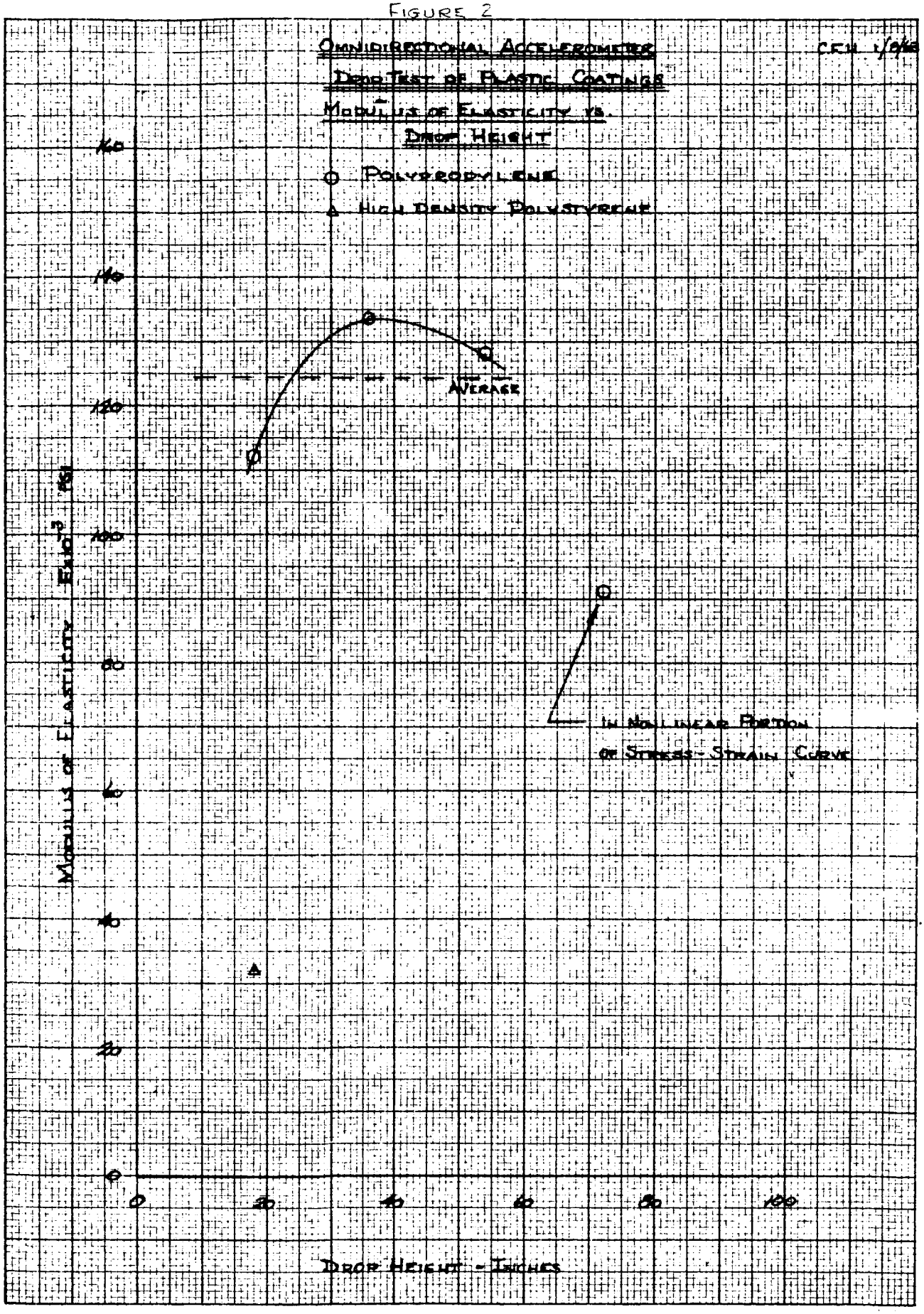
OMNIDIRECTIONAL ACCELEROMETER
DROP TEST OF PLASTIC COATINGS
MODULUS OF ELASTICITY VS.
DROP HEIGHT
CFH 1/64
○ POLYPROPYLENE
△ HIGH DENSITY POLYSTYRENE
AVERAGE
IN NON-LINEAR PORTION
OF STRESS-STRAIN CURVE
MODULUS OF ELASTICITY E x 10^3 PSI
DROP HEIGHT - INCHES

1. Accelerometer

Endevco Model 2225
Serial No. RAN45
Sensitivity = 8.25 RMS mV / Peak G
Corrected Sensitivity = E · 8.25 · $\frac{5363+300}{5363+93}$ · 8.45 $\frac{\text{RMS mV}}{\text{Peak G}}$

2. Calibration

input · 12 V RMS = 1420 g's peak
peak to peak g's = 2840 g's

3. Experimental Acceleration Table

Material	Drop Height			
	18"	36"	54"	72"
High Density Polyethylene	1450	2290	2250	2280
EC 2216 Flexible Epoxy	1590	2700	3500	4200
Polypropylene	2000	3340	4200	4490
Styrene	1980	3460	4360	5060 *
Cellulose Acetate	2000	3430	4260	4990
Nylon	2150	3570	4450	5190
Polycarbonate	2320	3990	5250	6000
Vinyl	2480	4220	5450	6210
Delrin	2570	4170	5220	6150

* Failure of Sample on Impact

PREPARED BY	DATE	PREPARING ACTIVITY	Ford Motor Company AERONUTRONIC DIVISION
C.F. Hayes	12/31/62		
CHECKED BY	DATE	TITLE OR SUBJECT: Acceleration Drop Tests of Plastic Coatings Appendix	PROJECT OR MODEL: Communications / Accelerometer
APPROVED BY	DATE		SHEET: 6 of ∞ DOCUMENT OR REPORT NO.

4. Experimental Velocity Change

$$V = \sqrt{2gh_1} + \sqrt{2gh_2} = 27.73\left(\sqrt{h_1} + \sqrt{h_2}\right)$$

MATERIAL	DROP HEIGHT							
	18"		36"		54"		72"	
	Average Rebound in.	ΔV in/sec	Average Rebound in.	ΔV in/sec	Average Rebound in.	ΔV in/sec	Average Rebound in.	ΔV in/sec
High Density Polyethylene	3.75	171.3	6.00	234.0	6.75	276.1	7.25	309.9
EC 226 Flexible Epoxy	3.25	167.5	6.00	236.0	7.25	278.7	9.25	319.5
Polypropylene	4.50	176.4	9.25	260.6	10.50	293.8	11.25	328.9
Styrene	4.75	178.1	8.75	264.5	11.75	299.0	2.50*	279.0
Cellulose Acetate	6.50	188.3	12.50	284.5	16.00	314.9	18.25	353.9
Nylon	6.75	189.7	11.25	259.5	14.75	310.7	17.25	350.5
Polycarbonate	7.00	191.0	13.25	267.2	17.75	321.0	23.00	368.2
Vinyl	8.25	197.4	13.50	268.3	18.25	322.7	22.75	367.6
Delrin	9.00	200.8	15.0	273.5	18.00	321.8	24.50	372.4

* FAILURE OF SAMPLE ON IMPACT

Integration of the area under the acceleration-time curves with a planimeter yielded values of velocity which agreed to within 5% of the data above. Therefore it is felt that the oscilloscope data are reasonably good reproductions of the acceleration-time history of the impacts. Most curves generated may be represented by a triangular pulse shape. The acceleration-time curves for high density polyethylene are more accurately represented by a trapezoidal pulse shape due to limiting of the acceleration by yielding of the material. The accelerations measured are presented in figure 1 as a function of drop height. Polypropylene appears to exhibit the desired qualities for an accelerometer coating since it tends to limit the acceleration to a value greater than 3000 g's but less than 5000 g's.

PREPARED BY	DATE	PREPARING ACTIVITY	Ford Motor Company, AERONUTRONIC DIVISION
C.K.H.			
CHECKED BY	DATE	TITLE OR SUBJECT: ACCELERATION DROP TESTS OF PLASTIC COATING & APPENDIX	PROJECT OR MODEL: CANNON ELECTRONIC ACCELEROMETER
APPROVED BY	DATE		SHEET 7 OF; DOCUMENT OR REPORT NO.

5. Determination of Modulus of Elasticity

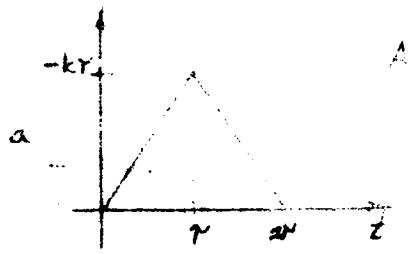

Assuming the pulse shape may be represented by a triangular pulse where $a = -kt \quad 0<t<\tau$ ①

$a = -2k\tau + kt \quad \tau<t<2\tau$

The velocity may be obtained from

$V = \int a\,dt$

therefore for $(0<t<\tau) \quad V_1 = -\int_0^t kt\,dt = -\frac{kt^2}{2} + C$

when $t=0 \quad V = V_0 \quad$ and $\quad C = V_0$

$V_1 = -\frac{kt^2}{2} + V_0 \qquad (0<t<\tau)$ ③

for $(\tau<t<2\tau) \quad V_2 = \int_\tau^t (-2k\tau + kt)\,dt = \left(-2k\tau t + \frac{kt^2}{2}\right)\Big|_\tau^t + C$

$V_2 = -2k\tau t + \frac{kt^2}{2} + 2k\tau^2 - \frac{k\tau^2}{2} + C$

$V_2 = k\left(\frac{3}{2}\tau^2 - 2\tau t + \frac{1}{2}t^2\right) + C$

when $t=\tau \quad V_2 = V_1 = -\frac{k}{2}\tau^2 + V_0 = C$

$V_2 = k\left(\tau^2 - 2\tau t + \frac{1}{2}t^2\right) + V_0 \qquad (\tau<t<2\tau)$ ④

The displacement may be obtained from $\delta = \int V\,dt$

and for $(0<t<\tau)$

$\delta_1 = \int_0^t \left(-\frac{kt^2}{2} + V_0\right)dt = -\frac{kt^3}{6} + V_0 t + C$

when $t=0 \quad \delta = 0 \quad$ and $\quad C = 0$

PREPARED BY	DATE	PREPARING ACTIVITY	Ford Motor Company, AERONUTRONIC DIVISION
CHECKED BY	DATE	TITLE OR SUBJECT: ACCELERATION LOAD TESTS OF PLASTIC COATINGS	PROJECT OR MODEL
APPROVED BY	DATE		SHEET / OF — DOCUMENT OR REPORT NO.

then $\delta_1 = -\frac{kt^3}{6} + V_0 t \qquad (0 < t < \tau)$ ⑤

for $(\tau < t < 2\tau) \quad \delta_2 = \int_\tau^t \left[k(\tau^2 - 2\tau t + t t^2) + V_0\right] dt$

$\delta_2 = \left[k\left(\tau^2 t - \tau t^2 + \frac{t^3}{3}\right) + V_0 t\right]_\tau^t + C$

$\delta_2 = k\left(\frac{t^3}{3} - \tau t^2 + \tau^2 t - \frac{\tau^3}{3}\right) + V_0(t - \tau) + C$

when $t = \tau \quad \delta_2 = \delta_1 = -\frac{k\tau^3}{6} + V_0\tau + C$

$\delta_2 = k\left(\frac{t^3}{6} - \tau t^2 + \tau^2 t - \frac{\tau^3}{3}\right) + V_0 t$ ⑥

when $V = 0$ δ = maximum and the time at which the maximum deflection occurs is:

for $(0 < t < \tau) \qquad t = \sqrt{\frac{2V_0}{k}}$ ⑦

and for $(\tau < t < 2\tau)$

$k(\tau^2 - 2\tau t + \frac{1}{2}t^2) + V_0 = 0$

$t^2 - 4\tau t + 2\left(\tau^2 + \frac{V_0}{k}\right) = 0$

$t = 2\tau \pm \sqrt{2}\sqrt{\tau^2 - \frac{V_0}{k}}$ ⑧

if $\sqrt{\frac{2V_0}{k}} \geq \tau$ the maximum deflection will occur in $(\tau < t < 2\tau)$ ⑨

with the time computed by equations ⑦ or ⑧ the maximum deflection may be obtained from equations ③ or ⑥ depending on the time period.

PREPARED BY	DATE	PREPARING ACTIVITY	Ford Motor Company, AERONUTRONIC DIVISION
C.F. HUSES			
CHECKED BY	DATE	TITLE OR SUBJECT	PROJECT OR MODEL
		ACCELERATION DROP TESTS OF PLASTIC COATINGS APPENDIX	COMMUNICATIONAL ACCELEROMETER
APPROVED BY	DATE		SHEET 9 OF / DOCUMENT OR REPORT NO.

from memo LFC-ME-011, 12/27/62 Page 5 Equation (12)

$$n = -2\pi F_{cy} \frac{R_g^2}{W}(y^2 \ln y) \qquad (10)$$

where n = number of earth g's
F_{cy} = stress (yield)
R_g = radius of hunter
W = weight of payload
y = parameter $\frac{r}{R_g}$ where r is distance from center to plane of contact

This equation may be used to determine the stress produced by impact of the weight on the plastic samples.

$$F_{cy} = \frac{-nW}{2\pi R_g^2 (y^2 \ln y)} \qquad (11)$$

where W = 1.1 pounds
R_g = .9 inches

$$\text{or } F_{cy} = \frac{-.216\, n}{(y^2 \ln y)} \qquad (13)$$

where $y = \frac{R_g - \delta}{R_g}$ (13)

δ is the maximum deflection then F_{cy} is the maximum stress.
The modulus of elasticity may be obtained from

PREPARED BY	DATE	PREPARING ACTIVITY	Ford Motor Company, AERONUTRONIC DIVISION
CHECKED BY	DATE	TITLE OR SUBJECT: ACCELERATION DROP TEST OF PLASTIC COATINGS APPENDIX	PROJECT OR MODEL: OMNIDIRECTIONAL ACCELEROMETER
APPROVED BY	DATE		SHEET: 10 OF; DOCUMENT OR REPORT NO.

$$S = E\epsilon \qquad (2)$$

$$\text{or} \quad E = \frac{S}{\epsilon} = \frac{K_g \times .125}{g} \qquad (3)$$

The effect of drop height, ie rate of loading, on modulus of elasticity may be determined from the data obtained for each plastic from drop test data and the above equations. Restricting the investigation to polypropylene since this plastic appears to exhibit the desired bonding properties, the analysis is as follows:

6. Modulus of elasticity Computations

Polypropylene - 48" drop height

$w = 2000$ g's

Pulse period $T = 2\tau = 4.58 \times 10^{-4}$ sec

$\tau = 2.29 \times 10^{-4}$ sec

$V_0 = \sqrt{2gh}$

$= 118$ in/sec

$K = \frac{2000 \times 386}{2.29 \times 10^{-4}} = 338 \times 10^9$

time for maximum deflection

$$t = \sqrt{\frac{2V_0}{K}} = \sqrt{\frac{2 \times 118}{3.38 \times 10^9}} = \sqrt{69.9 \times 10^{-9}} = 264 \times 10^{-4} \text{ sec} > \tau$$

therefore from eq (3)

$$t = 2 \times 2.29 \times 10^{-4} \pm \sqrt{2}\sqrt{(2.29 \times 10^{-4})^2 - \frac{118}{3.38 \times 10^9}}$$

$$t = 4.58 \times 10^{-4} \pm 1.414 \sqrt{5.25 \times 10^{-8} - 3.49 \times 10^{-8}}$$

$$t = 4.58 \times 10^{-4} \pm 1.414 \times 1.328 \times 10^{-4}$$

$$t = 4.58 \times 10^{-4} \pm 1.876 \times 10^{-4}$$

$$t = 2.704 \times 10^{-4} \text{ sec}$$

PREPARED BY	DATE	PREPARING ACTIVITY	Ford Motor Company, AERONUTRONIC DIVISION
C.F. HUSEN			
CHECKED BY	DATE	TITLE OR SUBJECT: ACCELERATION DROP TEST OF PLASTIC COATINGS APPENDIX	PROJECT OR MODEL: OMNIDIRECTIONAL ACCELEROMETER
APPROVED BY	DATE		SHEET: 11 OF — DOCUMENT OR REPORT NO.

$$\delta = K\left(\frac{t^3}{6} - \frac{\tau t^2}{2} + \tau^2 t - \frac{\tau^3}{3}\right) + \dot{u}_0 t$$

$$\delta = 2.38\times10^{9}\left[\frac{(2.704\times10^{-4})^3}{6} - \frac{2.29\times10^{-4}(2.704\times10^{-4})^2}{2} + (2.29\times10^{-4})^2 2.704\times10^{-4} - \frac{(2.29\times10^{-4})^3}{3}\right] + 118\times 2.704\times10^{-4}$$

$$\delta = 2.38\times10^{9}\left[3.3\times10^{-12} - 16.78\times10^{-12} + 14.2\times10^{-12} - 4.0\times10^{-12}\right] + 319\times10^{-4}$$

$$\delta = -.0111 + .0319 = .0208 \text{ in}$$

$$y = \frac{R-\delta}{R} = \frac{0.9 - .0208}{0.9} = .976$$

$$f_y = \frac{-.216\, n}{y^2 A_y} = \frac{-.216\times 2000}{(.976)^2 A_y .976}$$

$$f_y = \frac{432}{.953\times(-.0243)} = 18{,}660 \text{ PSI}$$

and $E = \frac{S}{\epsilon} = \frac{18660\times.125}{.0208}$

$$E = 112{,}000 \text{ PSI}$$

Polypropylene

For a drop height = 36 inches

$n = 3340$ $\qquad T = 2\tau = 3.9\times10^{-4}$ sec

$\tau = 1.95\times10^{-4}$ sec

$V_0 = \sqrt{2gh} = 167$ in/sec $\qquad K = \frac{3340\times36}{1.95\times10^{-4}} = 6.62\times10^{9}$

PREPARED BY	DATE	PREPARING ACTIVITY	Ford Motor Company AERONUTRONIC DIVISION
C.A. Hewson			
CHECKED BY	DATE	TITLE OR SUBJECT: Acceleration Drop Test of Plastic Coatings Appendix	PROJECT OR MODEL: Communications Satellite
APPROVED BY	DATE		SHEET 12 of — DOCUMENT OR REPORT NO.

time for maximum deflection

$$t = 3.495\times10^{-4} \pm \sqrt{(1.95\times10^{-4})^2 - \frac{167}{6.62\times10^{9}}}$$

$$t = 3.90\times10^{-4} \pm 1.914\sqrt{3.8\times10^{-8} - 2.52\times10^{-8}}$$

$$t = 3.9\times10^{-4} \pm 1.914\times1.131\times10^{-4}$$

$$t = 3.9\times10^{-4} \pm 1.6\times10^{-4}$$

$$t = 2.3\times10^{-4} \text{ sec.}$$

$$\delta = 6.62\times10^{9}\left[\frac{(2.3\times10^{-4})^3}{6} - 1.95\times10^{-4}(2.3\times10^{-4})^2 + (1.95\times10^{-4})^2 2.3\times10^{-4} - \frac{(1.95\times10^{-4})^3}{3}\right] + 167\times2.3\times10^{-4}$$

$$\delta = 6.62\times10^{9}\left[2.023\times10^{-12} - 10.31\times10^{-12} + 8.75\times10^{-12} - 2.47\times10^{-12}\right] + .0384$$

$$\delta = .00325 + .0384 = .02515 \text{ inches}$$

$$y = \frac{0.9 - .02515}{0.9} = .972$$

$$F_{cy} = \frac{-.316\times3340}{(.972)^2 \ln .972} = 26,050 \text{ PSI}$$

$$\text{and } E = \frac{26850\times.125}{.02515} = 133,600 \text{ PSI}$$

Polypropylene

For a drop height = 54 inches

$n = 4200$ $\qquad T = 2\pi = 3.6\times10^{-4}$ sec

$\tau = 1.8\times10^{-4}$ sec

$V_0 = \sqrt{2gh} = 204.5$ in/sec $\qquad k = \frac{4200\times386}{18\times10^{-4}} = 9.02\times10^{9}$

PREPARED BY	DATE	PREPARING ACTIVITY	Ford Motor Company, AERONUTRONIC DIVISION
C.F. Hussey			
CHECKED BY	DATE	TITLE OR SUBJECT: Acceleration Drop Height of Plastic Coatings Appendix	PROJECT OR MODEL: Optical Aberration Accelerometer
APPROVED BY	DATE		SHEET: 13 of — DOCUMENT OR REPORT NO. —

time for maximum deflection

$$t = 3.8\times10^{-4} \pm \sqrt{3.61\times10^{-8} - \frac{2.25\times10^{-8}}{9.125\times10^{9}}}$$

$$t = 3.8\times10^{-4} \pm 1.414\sqrt{3.61\times10^{-8} - 2.467\times10^{-8}}$$

$$t = 3.8\times10^{-4} \pm 1.414 \times 1.144\times10^{-4}$$

$$t = 3.8\times10^{-4} \pm 1.43\times10^{-4}$$

$$t = 2.37\times10^{-4} \text{ sec}$$

$$\delta = 9.125\times10^{9}\left[\frac{(2.57\times10^{-4})^3}{6} - 1.9\times10^{4}(2.37\times10^{-4})^2 + (1.9\times10^{4})^2 2.37\times10^{-4} - \frac{(1.9\times10^{4})^3}{3}\right] + .236\times2.37\times10^{-4}$$

$$\delta = 9.125\times10^{9}\left[2.22\times10^{-12} - 10.68\times10^{-12} + 8.55\times10^{-12} - 2.286\times10^{-12}\right] + .05595$$

$$\delta = -.03003 + .05595 = .03592 \text{ inches}$$

$$y = \frac{0.9 - .03592}{0.9} = .960$$

$$F_{cy} = \frac{-.216\times4490}{(.960)^2 h_n .960} = 25{,}800 \text{ PSI}$$

and $E = \frac{25{,}800\times.125}{.03592} = 91{,}000$ PSI

Summarizing

Polypropylene

DROP HEIGHT	E (PSI)
18 inches	112,000
36 "	133,600
54 "	128,000
72 "	91,000

For a 72 inch drop the lower value of E is probably due to yielding of the material and operation in the nonlinear range of the stress-strain curve.

PREPARED BY	DATE	PREPARING ACTIVITY	Ford Motor Company, AERONUTRONIC DIVISION
C.F. Nuzen			
CHECKED BY	DATE	TITLE OR SUBJECT: Acceleration Drop Test of Plastic Coatings Appendix	PROJECT OR MODEL: Omnidirectional Accelerometer
APPROVED BY	DATE		SHEET 15 OF; DOCUMENT OR REPORT NO.

time for maximum deflection

$$t = 2.48\times10^{-4} \pm \sqrt{2}\sqrt{(1.8\times10^{-4})^2 - \frac{204.5}{9.02\times10^9}}$$

$$t = 3.6\times10^{-4} \pm 1.414\sqrt{3.24\times10^{-8} - 2.266\times10^{-8}}$$

$$t = 3.6\times10^{-4} \pm 1.414\times.977\times10^{-4}$$

$$t = 3.6\times10^{-4} \pm 1.398\times10^{-4}$$

$$t = 2.202\times10^{-4} \text{ sec}$$

$$\delta = 9.02\times10^9\left[\frac{(2.202\times10^{-4})^3}{6} - 1.8\times10^{-4}(2.202\times10^{-4})^2 + (1.8\times10^{-4})^2 2.202\times10^{-4} - \frac{(1.8\times10^{-4})^3}{3}\right] + 204.5\times2.202\times10^{-4}$$

$$\delta = 9.02\times10^9\left[1.783\times10^{-12} - 8.74\times10^{-12} + 7.14\times10^{-12} - 1.946\times10^{-12}\right] + .0450$$

$$\delta = -.0159 + .0450 = .0291 \text{ inches}$$

$$y = \frac{0.9 - .0291}{0.9} = .968$$

$$F_{zy} = \frac{-.216\times4200}{(.968)^2 \ln .968} = 29{,}800 \text{ PSI}$$

and $$E = \frac{29800\times.125}{.0291} = 128{,}000 \text{ PSI}$$

Polypropylene

For a drop height = 72 inches

$n = 4490$ $\qquad T = 2\gamma = 3.8\times10^{-4}$ sec

$T = 1.9\times10^{-4}$ sec

$V = \sqrt{2gh} = 236$ in/sec $\qquad k = \frac{4490\times386}{1.9\times10^{-4}} = 9.125\times10^9$

PREPARED BY	DATE	PREPARING ACTIVITY	Ford Motor Company, AERONUTRONIC DIVISION
C.F. HUSEN			
CHECKED BY	DATE	TITLE OR SUBJECT: ACCELERATION DROP TEST OF PLASTIC COATINGS APPENDIX	PROJECT OR MODEL: OMNIDIRECTIONAL ACCELEROMETER
APPROVED BY	DATE		SHEET: 14 OF — DOCUMENT OR REPORT NO

high shock pulse time - 48" drop height

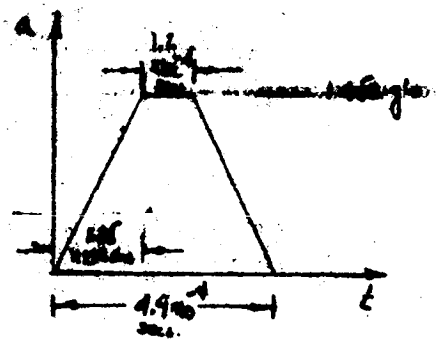

$V = \int a\,dt$

$V_1 = \int -k_1 t\,dt = -\frac{k_1 t^2}{2} + C$

when $t = 0$ $V = V_0$ $\therefore C = V_0$

$V_1 = -\frac{k_1 t^2}{2} + V_0 \qquad (0 < t < \tau_1)$

$V_2 = \int_{\tau_1}^{t} -k_2\,dt = -k_2 t \Big|_{\tau_1}^{t} + C = -k_2 t + k_2\tau_1 + C$

when $t = \tau_1$ $\quad V_2 = V_1 = -\frac{k_1\tau_1^2}{2} + V_0$ $\quad \therefore C = -\frac{k_1\tau_1^2}{2} + V_0$

and $V_2 = -k_2(t-\tau_1) - \frac{k_1\tau_1^2}{2} + V_0 \qquad (\tau_1 < t < \tau_2)$

deflection is a maximum when $V = 0$

or

$$-k_2(t-\tau_1) - \frac{k_1\tau_1^2}{2} + V_0 = 0$$

$$-k_2 t + k_2\tau_1 - \frac{k_1\tau_1^2}{2} + V_0 = 0$$

$$t = \tau_1 - \frac{k_1\tau_1^2}{2k_2} + \frac{V_0}{k_2}$$

for the above case $\quad \tau_1 = 1.85 \times 10^{-4}$ sec $\quad k_1 = 3.03 \times 10^9$

$V_0 = 118$ in/sec $\quad k_2 = 5.6 \times 10^5$

and $t = 1.85 \times 10^{-4} - \frac{3.03 \times 10^9 (1.85 \times 10^{-4})^2}{2 \times 5.6 \times 10^5} + \frac{118}{5.6 \times 10^5} = 1.85 \times 10^{-4} - .925 \times 10^{-4} + 2.105 \times 10^{-4} = 3.03 \times 10^{-4}$ sec.

PREPARED BY	DATE	PREPARING ACTIVITY	Ford Motor Company AERONUTRONIC DIVISION
C.F. Husen			
CHECKED BY	DATE	TITLE OR SUBJECT: Acceleration Drop Test of Plastic Coatings Appendix	PROJECT OR MODEL: Omnidirectional Accelerometer
APPROVED BY	DATE		SHEET: 16 of — DOCUMENT OR REPORT NO.

$$\delta_2 = \int \ddot{\delta}\,dt = \int_{T_1}^{t} \left[-k_2(t-T_1) - k_1\frac{T_1^2}{2} + V_0 \right] dt$$

$$\delta_2 = \left[-\frac{k_2 t^2}{2} + k_2 T_1 t - \frac{k_1 T_1^2 t}{2} + V_0 t \right]_{T_1}^{t} + C$$

$$\delta_2 = -\frac{k_2 t^2}{2} + k_2 T_1 t - \frac{k_1 T_1^2 t}{2} + V_0 t + \frac{k_2 T_1^2}{2} + \frac{k_2 T_1^2}{2} + \frac{k_1 T_1^3}{2} - V_0 T_1 + C$$

when $t = T_1$ $\quad \delta_2 = \delta_1 = -\frac{k_2 T_1^3}{6} + V_0 T_1$

$$\delta_2 = -\frac{k_2 T_1^2}{2} + k_2 T_1^2 - \frac{k_1 T_1^3}{2} + V_0 T_1 - \frac{k_2 T_1^2}{2} + \frac{k_1 T_1^3}{2} - V_0 T_1 + C = -\frac{k_2 t^3}{6} + V_0 T_1$$

$$\therefore C = -\frac{k_2 T_1^3}{6} + V_0 T_1$$

and $$\delta_2 = -\frac{k_2 t^2}{2} + k_2 T_1 t - \frac{k_1 T_1^2 t}{2} - \frac{k_2 T_1^2}{2} + \frac{k_1 T_1^3}{3} + V_0 t$$

$$\delta_2 = k_1 T_1^2 \left(\frac{T_1}{3} - \frac{t}{2} \right) - \frac{k_2}{2}\left(t^2 - 2T_1 t + T_1^2 \right) + V_0 t$$

$$\delta_2 = k_1 T_1^2 \left(\frac{T_1}{3} - \frac{t}{2} \right) - \frac{k_2}{2}(t - T_1)^2 + V_0 t$$

for $t = 3.03 \times 10^{-4}$

$$\delta_{max} = 3.03\times10^{9}(1.85\times10^{-4})^2\left(.6167\times10^{-4} - 1.515\times10^{-4}\right) - 2.8\times10^{5}(3.03-1.85)^2\times10^{-8} + 118\times 3.03\times10^{-4}$$

$$= -703.5 \times .8983 \times 10^{-4} - 3.9\times10^{-3} + .03572$$

$$= -.0093 - .0035 + .03572$$

$$\delta_{max} = .0344 \text{ inches}$$

$$y = \frac{0.9 - .0344}{0.9} = .9625$$

PREPARED BY	DATE	PREPARING ACTIVITY
C. F. Hussey		
CHECKED BY	DATE	TITLE OR SUBJECT
		Acceleration Drop Test of Plastic Coatings
APPROVED BY	DATE	Appendix

Ford Motor Company
AERONUTRONIC DIVISION

PROJECT OR MODEL: Omnidirectional Accelerometer

SHEET: 17 of

DOCUMENT OR REPORT NO.: -

$F_{cy} = \frac{-.210 \times 1450}{(.9625)^2 \ln .9625}$ = 8840 PSI

and $E = \frac{8840 \times .125}{.0344}$ = 32,100 PSI

For remaining drop heights the plastic yielded limiting acceleration to 2300 g. Operation is, therefore, in the non linear range of stress-strain curve. The modulus of elasticity which is the slope of the stress-strain curve may, therefore, be expected to be less than the above value.

PREPARED BY	DATE	PREPARING ACTIVITY	Ford Motor Company, AERONUTRONIC DIVISION
C.F. HUSEN			
CHECKED BY	DATE	TITLE OR SUBJECT: ACCELERATION DROP TEST OF PLASTIC COATINGS APPENDIX	PROJECT OR MODEL: CANDIDATE TRANSIT ACCELEROMETER
APPROVED BY	DATE		SHEET 18 OF; ISSUE OR REPORT NO.

Intra-Company Communication

LFC-ME-069
5/9/63

To: W. F. Mac Innes

CC: R. S. Kraemer
D. L. Elder
H. M. Marshall

From: C. F. Husen

Subject: Voids in the Mercury Filling the Omni-Directional Accelerometer

---

Summary:

Since acceleration data obtained with the omni-directional accelerometers during vibration and shock tests are characteristic of voids in the mercury filling the accelerometer, a series of experiments to improve the fill were instituted. Several variations in fill procedure were tried with no apparent reduction in void size.

A series of tests using a 1 mm diameter manometer tube were conducted in order to determine the approximate void size. The results of these experiments indicated a void of between 5.5×10^{-4} and 10.5×10^{-4} cubic inches with an average size of about 8×10^{-4} cubic inches. Since approximately the same results were obtained on three different accelerometer units it would appear that this size void can be expected in all units.

In order to determine if the void was due to trapped gas or to mercury surface tension one unit was filled with silicone oil. No change in oil level in the manometer tube was observed with changes in pressure which indicated that a complete fill of the sphere was obtained. Because oil will adhere to the cavity walls, and therefore, will flow into small channels and sharp corners, it is felt that the voids are primarily caused by the high surface tension of the mercury which does not permit the mercury to completely fill these same channels and corners.

Discussion:

Acceleration-time data have been obtained with several omni-directional accelerometer units during vibration and shock tests. The data recorded appears to be characteristic of large voids in the mercury when compared with similar time history data obtained on a two transducer model. Because the presence of a void in the mercury has a very significant effect on the distortion, phase lag, and damping of the accelerometer output, considerable effort has been expended in an attempt to eliminate the void.

Initial efforts were to improve filling methods. Several variations in a vacuum filling procedure were tried. These included pouring the mercury in and out numerous times, striking the outside of the ball, and exciting the accelerometer case with ultrasonic vibration and with a vibratool. In addition the sphere was heated in order to help drive off trapped gases. All these methods were unsuccessful in that no apparent change in the output of the accelerometer with vibration and shock excitation were noted.

In order to determine if the poor acceleration-time data obtained during vibration and shock tests were due to a void and not characteristic of the design a 1 mm diameter glass manometer was inserted into the fill hole of the accelerometer. The accelerometer was then vacuum filled with mercury and a column of mercury was allowed to stand in the tube. The change in mercury level in the tube was determined for a change in pressure from vacuum to atmospheric.

The data obtained and the void volume determined from the data are presented in an appendix. These data were obtained from three different accelerometer units and therefore are felt to be characteristic of the present design. The void volume was computed to be between 5.5×10^{-4} and 10.5×10^{-4} cu. in. with an average value of about 8×10^{-4} cu. in. for an internal pressure of approximately 2 inches of mercury.

Two possible causes of the mercury void exist. These are trapped gas, and the high surface tension of the mercury. The high surface tension does not permit the mercury to wet the cavity walls which may prevent the mercury from completely filling small channels and sharp corners. To determine the difference in void size when the accelerometer is filled with a material which wets the metal, the accelerometer was vacuum filled with silicone oil.

A similar arrangement to that used to determine the change in mercury level was employed for the silicone oil. However, oil viscosity forced the use of a 2 mm diameter tube in place of the 1 mm diameter tube. No change in height of the oil was noted for a change in pressure from vacuum to atmospheric. This indicated that a complete fill with no void was obtained. It would appear, therefore, that the voids in the mercury are primarily due to surface tension effects.

In view of the surface tension effect one additional variation of the filling procedure was tried. This was to apply pressure up to 500 psi several times on a partially filled sphere in an attempt to force mercury into small channels and spaces. This procedure was also unsuccessful with a void measured of about the same size as that previously determined.

Two new methods of improving the fill are to be tried. These methods will consist of modifications to the accelerometer rather than an additional modification of fill procedure. The first is an attempt to reduce the mercury surface tension by plating the interior cavity surfaces with a very fine layer of gold. The second method will be to fill small and relatively inaccesible voids around the transducer and in sharp corners with RTV silicone rubber.

C. F. Husen

DETERMINATION OF VOID VOLUME WITH MERCURY FILL

USING A 1 mm MANOMETER TUBE INSERTED IN THE FILL HOLE THE FOLLOWING DATA WAS OBTAINED

HEIGHT OF Hg IN TUBE		PRESSURE
5.0	IN.	VAC.
4.75	IN.	ATM.
4.79	IN	VAC
4.56	IN.	ATM.
3.91	IN.	VAC
3.67	IN.	ATM
3.93	IN.	VAC
3.67	IN.	ATM

WITH AN IMPROVEMENT IN THE VACUUM SYSTEM AND APPROXIMATELY 1 ORDER OF MAGNITUDE BETTER VACUUM. THE FOLLOWING DATA WAS OBTAINED

4.65	IN.	VAC
4.33	IN	ATM
4.64	IN.	VAC
4.33	IN	ATM
4.64	IN.	VAC USING ROUGHING PUMP ONLY

IN AN ATTEMPT TO IMPROVE THE FILL WITH THE USE OF AN ULTRASONIC CLEANER AS A VIBRATION EXCITATION SOURCE THE MERCURY HEIGHT WAS DETERMINED BEFORE AND AFTER EXCITATION WITH THE SYSTEM AT 4×10^{-6} mm PRESSURE. NO CHANGE IN MERCURY HEIGHT WAS NOTED. WHEN FILLED USING THE ULTRASONIC CLEANER THE FOLLOWING DATA WAS OBTAINED SIMILAR TO THAT ABOVE:

PREPARED BY	DATE	PREPARING ACTIVITY	Ford Motor Company, AERONUTRONIC DIVISION
C.F. Hussey	4/23/63		
CHECKED BY	DATE	TITLE OR SUBJECT	PROJECT OR MODEL
		APPENDIX	OMNIDIRECTIONAL ACCELEROMETER
APPROVED BY	DATE	SHEET 3 OF 6	DOCUMENT OR REPORT NO.

1.72	in Hg.	Atm.
2.13	in Hg	Vac.
1.72	in Hg	Atm.

Converting the above data to void volume where

P_1 = Pressure head on accelerometer in vacuum

P_2 = " " " " at atmospheric pressure

V_1 = Void volume in vacuum with head P_1

V_2 = " " at atmospheric pressure

$$\frac{P_2}{P_2} = \frac{V_2}{V_1} = \frac{V_1 - \Delta V}{V_1}$$

$$\text{or } V_1 = \frac{\Delta V}{1 - \frac{P_1}{P_2}}$$

P_1 in. Hg	P_2 in. Hg	P_1/P_2	$1 - P_1/P_2$	ΔV cu. in.	V_1 cu. in.
5.0	34.75	0.144	0.856	3.045×10^{-4}	3.56×10^{-4}
4.79	34.56	0.1388	0.8612	2.802×10^{-4}	3.255×10^{-4}
3.91	33.67	0.1161	0.8839	2.923×10^{-4}	3.31×10^{-4}
3.93	33.67	0.1167	0.8833	3.167×10^{-4}	3.59×10^{-4}
4.65	34.33	0.1355	0.8645	3.90×10^{-4}	4.515×10^{-4}
4.64	34.33	0.1351	0.8649	3.777×10^{-4}	4.37×10^{-4}
2.13	31.72	0.0672	0.9328	4.995×10^{-4}	5.35×10^{-4}

Prepared by	Date	Preparing activity
C. F. Husel	4/23/63	
Checked by	Date	Title or subject
		Appendix
Approved by	Date	

Ford Motor Company
Aeronutronic Division

Project or model: Omnidirectional Accelerometer

Sheet: 4 of 6

Document or report no.:

SINCE THE ACCELEROMETER IS NORMALLY SEALED WITH A PRESSURE OF APPROXIMATELY 2 IN. OF MERCURY

$$V_{VOID} = \frac{P_i V_i}{2}$$

P_i	V_i	V_{VOID}
5.0	3.56×10^{-4}	8.9×10^{-4}
4.79	3.255×10^{-4}	7.8×10^{-4}
3.91	3.31×10^{-4}	6.47×10^{-4}
3.93	3.59×10^{-4}	7.05×10^{-4}
4.65	4.515×10^{-4}	10.5×10^{-4}
4.64	4.37×10^{-4}	10.12×10^{-4}
2.13	5.35×10^{-4}	5.65×10^{-4}

THEN WHEN FILLED WITH MERCURY AT A PRESSURE OF 2 IN. Hg. AVERAGE VOID VOLUME FROM MEASUREMENTS = 8.07×10^{-4} cuin

DETERMINATION OF VOID VOLUME WITH SILICONE OIL FILL

TO DETERMINE THE DIFFERENCE IN VOID SIZE WHEN THE ACCELEROMETER IS FILLED WITH A MATERIAL WHICH WETS THE METAL THE ACCELEROMETER WAS VACUUM FILLED WITH SILICONE OIL. NO CHANGE IN HEIGHT OF THE OIL IN A MANOMETER TUBE WAS NOTED FOR A CHANGE IN PRESSURE FROM VACUUM TO ATMOSPHERIC. THIS INDICATES A COMPLETE FILL WITH NO VOID. AS A SEPARATE CHECK OF THE FILL:

WT WITH OIL = 474 gms

WT CLEANED = 471.4 gms WT OIL = 2.6 gms

PREPARED BY	DATE	PREPARING ACTIVITY	Ford Motor Company, AERONUTRONIC DIVISION
C.F. Hused	4/30/63		
CHECKED BY	DATE	TITLE OR SUBJECT	PROJECT OR MODEL
		APPENDIX	OMNIDIRECTIONAL ACCELEROMETER
APPROVED BY	DATE		SHEET 5 OF 6 / DOCUMENT OR REPORT NO.

SPECIFIC GRAVITY OF OIL $\simeq$ .96

$V = \frac{2.6}{.96} = 2.71$ CC

$V = 2.71 \times .061 = .165$ CU IN.

VOLUME OF CAVITY COMPUTED TO BE $\simeq$ .14 CU IN.

VOLUME OF MANOMETER TUBE $= \frac{\pi}{4}\left(\frac{2.02}{254}\right)^2 \times 3.5 = .0174$ CU IN.

TOTAL VOLUME $\simeq .14 + .0174 = .1574$ CU IN.

THEREFORE A COMPLETE FILL WITH OIL WAS OBTAINED VERIFYING THE DATA AND EFFECT OF PRESSURE NOTED.

PREPARED BY	DATE	PREPARING ACTIVITY	Ford Motor Company, AERONUTRONIC DIVISION
C. F. HUSEN	4/30/63		
CHECKED BY	DATE	TITLE OR SUBJECT	PROJECT OR MODEL
		APPENDIX	OMNIDIRECTIONAL ACCELEROMETER
APPROVED BY	DATE		SHEET 6 OF 6 / DOCUMENT OR REPORT NO.